Development and Characterization of a Novel Model of Ibrutinib Resistance in Chronic Lymphocytic Leukemia (CLL) that Displays Sensitivity to PI3K inhibition

By

Godsent Ehiremen

A Thesis submitted to the Faculty of Graduate Studies of

The University of Manitoba

in partial fulfillment of the requirements of the degree of

MASTER OF SCIENCE

Department of Pharmacology and Therapeutics

University of Manitoba

Winnipeg, Manitoba

Copyright © 2021 by Godsent Ehiremen

ABSTRACT

BACKGROUND: Chronic Lymphocytic Leukemia (CLL) is a B-cell malignancy driven by a hyperactive B-cell receptor pathway (BCR-P). BCR signalling includes Bruton's tyrosine kinase (BTK) activation of extracellular signal-regulated kinase 1 and 2 (ERK1/2)-mediated proliferation via phospholipase C gamma 2 (PLCγ2), and phosphatidylinositol-3-Kinaseδ-Protein Kinase B (PI3Kδ-AKT) signalling promoting cell survival. The BTK inhibitor ibrutinib revolutionized CLL treatment; unfortunately, resistance is now on the rise, creating the need for a better understanding of the effects of long-term ibrutinib use. This project aims to establish and characterize a cell line model of ibrutinib resistance in order to identify cell signalling events and other changes induced by long-term ibrutinib use.

METHODS: The BJAB cell line known to partly mimic CLL cell responses *in vitro,* was used for all investigations. Ibrutinib-resistant BJAB ($IBR10^2$) cells were created via a chronic dose-escalation approach. BJAB and $IBR10^2$ cells were treated with the BCR-P inhibitors ibrutinib (BTK), idelalisib (PI3Kδ), copanlisib (PI3Kα/β/δ/γ) and ravoxertinib (ERK1/2) alone and in combinations for 72 hours. Combinations were assessed for synergistic/additive/antagonistic cell death via flow cytometry and western blot was used for protein expression analyses.

RESULTS: $IBR10^2$ cells were resistant to all BCR-P inhibitors used. Synergism in cell viability reduction was observed in ibrutinib-idelalisib/copanlisib combinations. Ravoxertinib displayed antagonism in both BJAB and $IBR10^2$ cells (to a lesser extent) when combined with all inhibitors used. Protein analysis showed PI3K-AKT-mediated ERK activation and 45% less baseline activity of ERK in $IBR10^2$ relative to BJABs; BTK activation was abolished in $IBR10^2$ cells. Ibrutinib-idelalisib combination resulted in a statistically significant synergistic reduction in ERK activation in both cell lines, but also AKT activation in BJAB cells. Notably, ibrutinib-

idelalisib was shown to be synergistic in patient-derived CLL cells, and transcriptomic analysis showed that IBR10^2 cells expressed reduced levels of BCR, PI3K-AKT and MAPK pathway targets.

CONCLUSION: Our work on IBR10^2 cells shows a new mechanism of ibrutinib resistance characterized by BCR pathway rewiring. We also provide evidence for an additional benefit on combining ibrutinib and a PI3K inhibitor in primary CLL cells. In summary, we propose a novel mechanism of ibrutinib resistance and define combination therapies against this resistance.

ACKNOWLEDGMENTS

First and foremost, I thank God for giving me the grace, wisdom and perseverance to succeed in this endeavour. I would also like to acknowledge the Katyal laboratory and my supervisor Dr. Sachin Katyal, along with close collaborator Dr. James Johnston for their never-ending support and help in discussing results, formulating ideas and designing the experiments needed to achieve the contents of this thesis. In like manner, I acknowledge the funding agencies including CancerCare Manitoba Foundation (CCMF), The Canadian Institutes of Health Research (CIHR), The Terry Fox Research Institute (TFRI) and Research Manitoba, that provided the funds needed to conduct the research. Finally, the contributions of my family, friends and Katyal laboratory members (Haynes, Ali, Asha, Bozena, Odile, Mariam, Alvin, etc.) to my scientific, physical and mental well-being when conducting this research cannot go unmentioned as it was paramount to my success.

DEDICATION

I would like to dedicate this thesis first to my family, but also everyone who listened, contributed, criticized and supported in any and every way, during my journey. Names will not be mentioned because it truly took a village to get me to the finish line. Everyone knows who they are and what they did, so as you read this, I want to say from the bottom of my heart: THANK YOU.

TABLE OF CONTENTS

Abstract ii
Acknowledgments iv
Dedication v
List of Tables viii
List of Figures ix
Table of abbreviations x
Introduction 1
Chronic Lymphocytic Leukemia (CLL) overview 1
Clinical classification/staging 2
CLL pathogenesis 3
Prognostic markers and risk factors 6
The B-cell Receptor (BCR) pathway 7
BCR Activation 7
BCR signal propagation 8
Cellular signalling pathways activated by the BCR 10
Regulation of BCR pathway activation 11
BCR pathway signalling and interactions with integrins 12
The BCR pathway in CLL 13
The CLL tumour microenvironment 16
Other pathways important to CLL pathogenesis and survival 19
Apoptotic pathways 20
DNA damage repair 21
CLL Treatment 23
Chemoimmunotherapy 23
Small molecule inhibitors 25
Ibrutinib resistance in CLL 31
Project aims and rationale 34
Hypotheses 34
Materials and Methods 35
Cell culture 35
B-cell receptor pathway inhibitors 35
Flow cytometry 35
Synergy-antagonism studies 36

Development of an ibrutinib-resistant BJAB cell line (IBR10^2 cells) 37
Protein expression studies 38
Analysis of western blot results 39
Microarray studies....40
Data and Statistical analyses....41
Inhibitor single dose-response curves 41
Cell viability/death experiments. 41
Protein expression analyses. 41
Microarray data analysis. 41
Results 43
IBR10^2 cells have the best resistance profile out of three ibrutinib-resistant BJAB cell lines..43
IBR10^2 cells are resistant to B-cell receptor pathway inhibition....45
The PI3K-AKT pathway is crucial to IBR10^2 and BJAB cell survival 46
BJAB cells. 48
IBR10^2 cells. 51
PI3K inhibitors sensitize IBR10^2 cells to ibrutinib treatment 53
Synergy-antagonism analyses....53
Protein expression analyses of BCR signalling 55
BTK and PI3K-AKT signalling terminate with ERK activation in BJAB cells....58
Synergy-antagonism analyses....58
Protein expression analyses 59
Idelalisib-ibrutinib/copanlisib combination leads to cooperative cell death in CLL cells 60
Ibrutinib-idelalisib combination leads to synergistic cell death in CLL cells 62
The PI3K-AKT and MAPK-ERK pathways are altered at the RNA level in IBR10^2 cells....65
Discussion 74
Identification of a novel cell line model of ibrutinib resistance 74
Limitations and applicability of findings 81
Summary of Findings....87
Significance....88
Future directions....89
References....91
Appendix 111

LIST OF TABLES

Table i…… x

Table 1…… 3

Table 2…… 38

Table 3…… 40

Table 4…… 64

Table 5…… 67

Table 6…… 70

Table 7…… 72

Supplementary table 1…… 111

Supplementary table 2…… 112

Supplementary table 3…… 113

Supplementary table 4…… 114

Supplementary table 5…… 115

Supplementary table 6…… 116

Supplementary table 7…… 117

Supplementary table 8…… 119

Supplementary table 9…… 121

LIST OF FIGURES

Figure i……... 5

Figure ii…….…….. 13

Figure iii…….……. 22

Figure iv…….. 26

Figure v……... 37

Figure vi…….. 39

Figure vii……. 42

Figure 1…….…….. 44

Figure 2…….…….. 46

Figure 3…….…….. 47

Figure 4…….…….. 50

Figure 5…….…….. 54

Figure 6…….…….. 56

Figure 7…….…….. 59

Figure 8…….…….. 61

Figure 9…….…….. 62

Figure 10……. 66

TABLE OF ABBREVIATIONS

Table i: Important abbreviations are listed in the table below.

CLL – Chronic lymphocytic leukemia	BMSC – Bone marrow-derived stromal cell
CD – Cluster of differentiation	FCR – Fludaraine-Cyclophosphamide-Rituximab (chemoimmunotherapy regimen)
SLL – Small lymphocytic leukemia	OS – Overall survival
MBL – Monoclonal B-lymphocytosis	PFS – Progression-free survival
MCL – Mantle cell lymphoma	C481S – Cysteine to Serine amino acid substitution at position 481 (this is mutation)
IGHV – Immunoglobulin heavy chain variable region	R665W – Arginine to tryptophan amino acid substitution at position 665 (a mutation)
M-CLL – *IGHV*-Mutated CLL	ITK – IL-2-inducible T-cell kinase
U-CLL – *IGHV*-Unmutated CLL	BLK – B-lymphocyte kinase
BCR – B-cell receptor	EGFR – Epidermal growth factor receptor
PCs – Proliferation centers	BJAB – A Burkitt's lymphoma cell line
FISH – Fluorescent in situ hybridization	EC_{50} – Effective concentration to achieve 50% of response (cell death response was assessed here)
ATM – Ataxia telangiectasia mutated	p-BTK/AKT/ERK – Phosphorylated BTK/AKT/ERK
BCL-2 – B-cell lymphoma 2	TAC – Transcription Analysis Console
ZAP-70 – Zeta-chain-associated protein kinase 70	**IBR10^2** – BJAB cells treated with 10μM ibrutinib twice before exposure to 20μM ibrutinib (at 1x10^6 cells/mL)
SYK – Spleen tyrosine kinase	IBR5$^{1/2}$ – BJAB cells treated with 5μM ibrutinib before exposure to 20μM ibrutinib (at 5x10^5 cells/mL, ½ of 1x^6 cells/ mL)
BTK – Bruton's tyrosine kinase	IBR5^1 – BJAB cells treated with 5μM ibrutinib once before exposure to 20μM ibrutinib (at 1x^6 cells/ mL)
PI3K – Phosphatidyl-inositol-3-kinase	DMSO – Dimethyl sulfoxide
PM – Plasma membrane	IQR – Interquartile range
PLCγ2 – Phospholipase C gamma-2	SEM – Standard error of the mean
MAPK – Mitogen-associated protein kinase	CI – Combination index
ERK – Extracellular signal regulated kinase	NS – Not significant (re: results)
PIP3 – Phosphatidylinositol-3,4,5-triphosphate	SHP-1 – SH2 domain-containing phosphatase-1

PIP2 – Phosphatidylinositol 4,5-biphosphate	SHIP – SH2 domain containing inositol 5'-phoshpate (SHIP)
AKT/PKB – Protein kinase B (same protein)	IL4R – IL-4 receptor
PKC – Protein Kinase C	CCL3 – C-C motif ligand 3
IKK – IκB kinase	PC – Proliferation center
SDF-1/CXCL12 – Stromal derived factor 1/ C-X-C motif chemokine 12 (same protein)	ABC-DLBCL – Activated B-cell Diffuse Large B-cell lymphoma
CD40L – Cluster of differentiation 40 Ligand	BL – Burkitt's lymphoma
IL – Interleukin	
TF – Transcription factor	
NLC – Nurse-like cells	
BAFF – B-cell activating factor	
APRIL – A proliferation-inducing ligand	
TNF – Tumour necrosis factor	
JAK-STAT – Janus Kinase-Signal transducer and activator of transcription	
CXCR – C-X-C chemokine receptor	

INTRODUCTION

Chronic Lymphocytic Leukemia (CLL) overview

Chronic lymphocytic leukemia (CLL) is B-cell malignancy characterized by monoclonal leukemic cells, with a prevalence of 5.0 and 7.9 per 100,000 in the United States and Manitoba, Canada respectively[1,2]. The median age at diagnosis for CLL is 72 years and it is typically diagnosed during routine bloodwork[2]. CLL cells are small, mature-looking lymphocytes, with a dense nucleus, narrow cytoplasm and indiscernible nucleoi, mixed with other immature lymphocytes with abundant cytoplasm and discernible nucleoli, called prolymphocytes, which can make up to 55% of the lymphocytes in a patient's blood[3]. In order for a CLL diagnosis to be made, there has to be greater than $5x10^9$ B-cells per litre in the blood for at least three months and these cells have to be monoclonal (kappa or lambda positive), be cluster of differentiation 5 (CD5), CD19 and CD23 positive, while expressing low levels of CD20 and no CD10[4–7]. Also, CLL cells are CD200 positive and this helps rule out Mantle Cell Lymphoma (MCL)[8]. At diagnosis, CLL patients range from asymptomatic to having disease-related symptoms like fatigue, night sweats and increased frequency of infections, with possibly enlarged lymph nodes (lymphadenopathy) and/or spleen (splenomegaly)[9].

Other related/similar conditions ruled out in the diagnosis of CLL include monoclonal B-lymphocytosis (MBL), prolymphocytic B-leukemia (B-PLL) and small lymphocytic lymphoma (SLL). MBL is defined as having less than $5x10^9$ monoclonal B-cells per litre in the blood, in addition to an absence of clinical lymphadenopathy, splenomegaly or disease-related symptoms[10]. However, MBL patients may go on to develop CLL, SLL or other lymphomas. B-PLL is diagnosed if the percentage of prolymphocytes in the blood exceeds 55%; a B-PLL diagnosis comes with a poor prognosis because it is a more aggressive leukemia than CLL[3].

Finally, SLL is a disease biologically identical to CLL that prominently involves the lymph node and spleen, but with a peripheral B-cell count less than $5x10^9$ cells per litre[11].

Clinical classification/staging

CLL patients are classified into different disease stages/risk groups using two systems: The Rai and Binet systems, predominantly used in North America and Europe respectively[12,13]. The Rai system has been modified to include only three prognostic groups instead of five and both systems categorize patients into different disease stages, based on results from physical examination and basic laboratory tests. For the modified Rai stratification, the low-risk group (Rai stage 0) of patients will present with lymphocytosis in the blood and/or bone marrow[9]. Patients with lymphocytosis, lymphadenopathy and/or splenomegaly, with or without hepatomegaly (enlarged liver), are classified as having intermediate-risk disease (Rai stages I and II). Finally, patients who present with lymphocytosis, enlarged nodes and anemia (low red blood cell count) or thrombocytopenia (low platelet count), have high-risk disease (Rai stages III and IV)[9]. Median survival decreases with increased Rai stage, with low-risk patients projected to have a much better prognosis than intermediate and high risk disease patients. For reference, Rai stage 0 patients have a median survival >10 years and stage III and IV patients, 1.5 to 5 years (Table 1).

The Binet system stratifies patients into three groups (A, B and C) based on the number of involved areas (i.e. splenomegaly, hepatomegaly and lymphadenopathy in the cervical, axillary and inguinal regions), platelet count and hemoglobin levels[13]. Stage A patients present with less than three involved areas (out of the five outlined above) with hemoglobin greater than or equal to (≥) 100 g/L and platelets counts ≥ $100x10^9$ per litre (Hgb ≥ 100 g/L, platelets ≥ $100x10^9$ /L). Stage B patients have three or more involved areas with Hgb ≥ 100 g/L and

platelets ≥ $100x10^9$ /L. Lastly, Binet Stage C patients have Hgb < 100 g/L and/or platelets < $100x10^9$ /L, with any number of involved areas. For the Binet system, Stage A patients have the longest median survival and Stage C patients, the shortest median survival[13]. Table 1 shows both Rai and Binet staging systems.

Table 1: CLL disease classification and projected prognosis.

Rai Staging System			Prognosis	Binet Staging System		
Rai Stage	**Description**	**Modified Rai Risk Level**	**Median Survival (years)**	**Stage**	**Laboratory results**	**Number of involved areas**
0	Lymphocytosis (>$5x10^9$ B-cells/L)	Low risk; Best prognosis	**> 10**	A	Hemoglobin ≥ 100 g/L Platelets ≥$100x10^9$ /L	Less than 3
I and II	Lymphocytosis with lymphadenopathy and/or splenomegaly	Intermediate risk; moderate prognosis	**7-9**	B	Hemoglobin ≥ 100 g/L Platelets ≥$100x10^9$ /L	Greater than or equal to 3
III and IV	Lymphocytosis with lymphadenopathy and/or splenomegaly with anemia or thrombocytopenia	High risk; worst prognosis	**1.5 - 5**	C	Hemoglobin < 100 g/L Platelets <$100x10^9$ /L	Any number

CLL pathogenesis

There are two currently accepted ways CLL may arise: from a hematopoietic stem cell (HSC) precursor, or from B-cells with different immunoglobulin heavy chain variable region (*IGHV*) gene mutation status (Figure i). CLL may arise from a HSC precursor which gets mutated into a CLL HSC, because xenografts of HSC from CLL patients result in B-cells with a CLL-like phenotype[14]. Nonetheless, these cells harbour different chromosomal abnormalities and express a unique *IGHV*, different from that of the original clone. As a result, it is suspected that these B-cells arise from precursors that underwent an independent *IGHV* re-arrangement. In normal B-cell development, naïve B-cells ($CD5^+$, $CD27^-$) may undergo T-cell dependent

germinal center (GC) differentiation with *IGHV* hypermutation ($CD5^+$, $CD27^+$), or may become mature B-cells in a GC-independent fashion without *IGHV* somatic hypermutation ($CD5^+$, $CD27^-$)[15–17]. Alternatively, a $CD5^+CD27^-$ memory-like B-cell could arise from a CLL HSC or other non-naïve B-progenitor cells; all three paths lead to antigen-experienced B-cells, which undergo multiple cell divisions and acquire genetic mutations that make them malignant. Clonal expansion of these cells leads to MBL, which may progress to CLL[15–17] (Figure i). Given the possibilities above, whether a patient develops *IGHV* mutated (M-CLL) or *IGHV* unmutated (U-CLL) depends on the cell of origin. CLL that originates from B-cells that underwent GC maturation ($CD5^+$, $CD27^+$) become M-CLL and those that arise from pre-GC B-cells ($CD5^+$, $CD27^-$), U-CLL. Studies have shown that patients with M-CLL have predominantly anergic (inactive) B-cell receptor (BCR) signalling and a better prognosis, while patients with U-CLL are more likely to have active BCR signalling, a more aggressive disease and worse prognosis[18].

CLL is typically called an indolent leukemia because only about 0.39% of CLL cells divide daily[19]. Nevertheless, so-called "proliferation centers" (PCs) exist in patients' lymph nodes, bone marrow and spleen, and are known to drive disease progression and affect how patients respond to treatment[20]. CLL cells cycle through PCs, where they come into contact with a host of other cell types and cellular signals, that promote proliferation, survival and inhibit apoptosis[20–22]. The sustenance supplied by the tumour microenvironment formed in the PCs allow CLL cells to survive. Additionally, CLL cells in these PCs are protected from traditional CLL treatments by some of these cell types, and it is likely that resistant clones to all types of CLL treatments arise and expand in the PCs, while other cells in the peripheral blood not receiving these survival signals, perish. Peripheral blood CLL cells are not as resilient as those in the PCs because they are simply not protected by the plethora of survival-promoting signals and

the physical protection provided by the PCs. The PC microenvironment in CLL is discussed in greater detail in an upcoming section on the CLL tumour microenvironment.

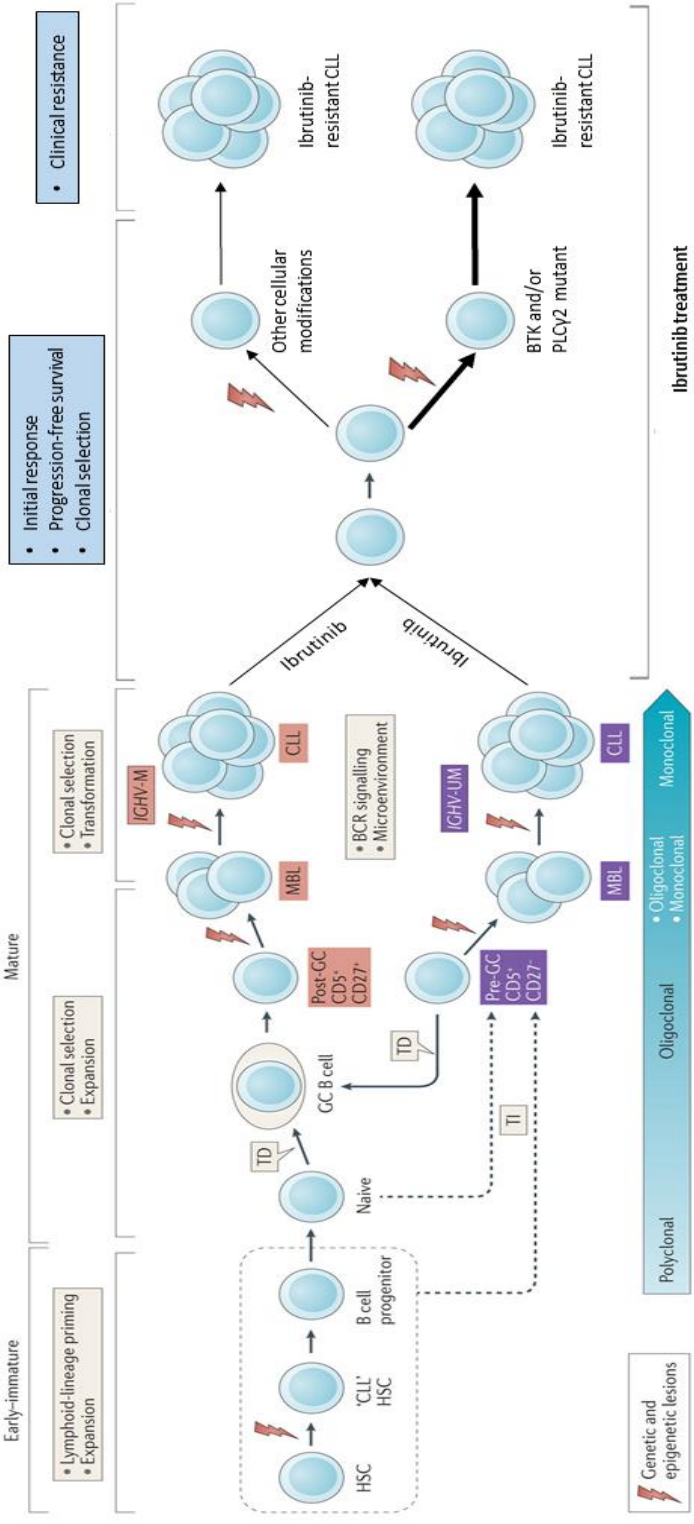


Figure i. The cellular origin of chronic lymphocytic leukemia and development of clinical ibrutinib resistance. Chronic lymphocytic leukaemia (CLL) may originate at the stem cell stage, as suggested by the capacity of CLL-derived haematopoietic stem cells (HSCs) to engraft after xenotransplantation into immunodeficient mice, giving rise to an increased proportion of polyclonal pro-B cells, and, eventually, to monoclonal or oligoclonal $CD5^+$ B cell populations with features resembling monoclonal B cell lymphocytosis (MBL). Immunoglobulin heavy chain variable region-mutated (*IGHV*-M) CLLs seem to originate from post-germinal centre (GC) $CD5^+CD27^+$ B cells, which are transcriptionally similar to memory B cells and are most likely to be derived from $CD5^+CD27^-$ B cells that have undergone the GC reaction. *IGHV*-UM CLL seem to arise from pre-GC $CD5^+CD27^-$ B cells, which may derive from naive B cells or from a separate lineage of precursor B cells. Additional genetic and epigenetic abnormalities, B cell receptor (BCR) stimulation and microenvironmental factors will contribute to give rise to the precursor of CLL, MBL, and, ultimately, to frank monoclonal CLL. Upon treatment with ibrutinib, patients respond with a reduction in palpable nodes concomitant with lymphocytosis. Over time, with clonal expansion, ibrutinib resistance ultimately occurs, mainly via *BTK* and/or *PLCG2* mutations (85%). TD, T cell-dependent antigen; TI, T cell-independent antigen. Illustration and caption modified from: *Fabbri, G., Dalla-Favera, R. The molecular pathogenesis of chronic lymphocytic leukaemia. Nat Rev Cancer* 16, 145–162 (2016).

Prognostic markers and risk factors

Although the Rai and Binet staging systems help stratify patients into general risk groups, with increasing diagnostic and treatment technologies, today, much more is known about CLL and the risk factors/markers that can better predict a patient's disease course and their response to specific treatments. Information can be obtained from cytogenetic tests, which determine chromosomal abnormalities (if any) possessed by CLL patients. Typically, Fluorescence in situ Hybridization (FISH) tests provide cytogenetic data on CLL patients, which can be used to infer vital prognostic information. Important chromosomal abnormalities in CLL include a deletion in the p-arm of chromosome 17 (del(17p13)), deletion in the q-arm of chromosome 11 (del(11q22; 23)), a deletion in the q-arm of chromosome 13 (del(13q)) and trisomy of chromosome 12[23]. Approximately 80% of CLL patients harbor at least one of the four cytogenetic abnormalities above[24]. Del(17p) is associated with a deletion of the tumour suppression gene *TP53*, which encodes the p53 protein important to DNA repair and genomic stability[25]. Unfortunately, in about 80% of patients with del(17p), there is a mutation in the second allele of the *TP53* gene[26]. Patients with del(17p) have a terrible prognosis, with genomic complexities and a more aggressive disease leading to earlier relapse/resistance to therapy than the other abnormalities[9].

Del(11q) is associated with a deletion of the gene encoding the Ataxia Telangiectasia Mutated (ATM) protein, which is important for DNA double-strand break repair (DSBR)[27,28]. Del(11q) is seen in 25% of advanced-stage patients and 10% of patients with early stage CLL[29]. *ATM* deletion is associated with reduced overall survival with chemotherapy, rapid disease progression and patients are often middle-aged men with bulky lymphadenopathy[27]. About 40% of del(11q) patients also have a mutation in the other ATM allele[27,30,31]. Trisomy 12 is observed in 10-20% of CLL patients but the specific genes and prognostic impact of the chromosomal

alteration are unclear[26]. Del(13q) is the most common chromosomal abnormality in CLL, present in about 55% of all patients[24]. Del(13q14) is of prognostic importance because the micro-ribonucleic acids (mi-RNAs) 15a (miR-15a) and 16-1 (miR-16-1) were found to be in the chromosomal region of the deletion[32]. MiR-15a and 16-1 function to repress expression of the B-cell lymphoma 2 (BCL-2) and Zeta-chain-associated protein kinase 70 (ZAP-70) proteins, which are involved in cell death and BCR signalling, respectively[33,34]. In about 70% of CLL patients, these mi-RNAs are altered; when deleted or expressed at lower levels, they allow the expression of genes that confer resistance to cell death (BCL-2) and increased BCR signalling (ZAP-70).

The BCR pathway is an important signalling cascade that leads to increased cell proliferation and survival in CLL. Thus, patients who have 20% of cells positive for ZAP-70 were shown to experience worse disease outcome compared to patients who are ZAP-70 negative (<20%)[35]. However, ZAP-70 is no longer used as a prognostic marker because it is hard to reproducibly measure. In addition to disease stage, FISH results/mutation status and *IGHV* mutation status, CLL severity has been shown to progress with age and sex, with men having worse prognosis than women[23]. Patients aged 65 and younger have a better prognosis than patients older than 65 years. Moreover, the 10-year overall survival of CLL patients have also been shown to be favourably influenced by unmutated *NOTCH1* and *SF3B1*, serum β_2-microglobulin $\leq$3.5mg/L and negative CD38 expression.

The B-cell Receptor (BCR) pathway

BCR Activation

B-cells can possess a receptor called the B-cell receptor (BCR), which is a surface immunoglobulin (Ig), typically IgM. Igs are proteins made up of two heavy chains and two light chains; the heavy chains are connected by a disulfide bond and each associate with a light chain

on their extracellular N-terminus to form the ligand (called antigen for the BCR)-binding site[36]. On the cytoplasmic end, each Ig heavy chain contains ITAM (Immunoreceptor Tyrosine-based Activation Motif) segment with which they non-covalently bind to a heterodimer consisting of Igα and Igβ (also called CD79a and b)[37]. Upon antigen binding to the BCR, spleen tyrosine kinase (SYK) and LYN (both Src family kinases) phosphorylate Igα and Igβ on their ITAM segments to initiate BCR signalling[38,39]. SYK and LYN phosphorylation of Igα and Igβ results in the recruitment of important signalling players consisting of kinases (SYK, LYN and BTK – Bruton's Tyrosine Kinase), adaptor proteins (BLNK – B-cell linker and GRB2-growth factor receptor-bound protein 2) and VAV, a guanine exchange factor[37]. The kinases listed above are responsible for amplifying the BCR signal; SYK phosphorylates Igα and Igβ and LYN recruits tyrosine kinases and forms a complex with CD19 and other co-stimulatory molecules that promote BCR activation via threshold reduction[38,40].

CD19 and BTK promote BCR aggregation and microcluster formation in lipid rafts[41,42]. Microclusters are multiple BCRs coming together, possibly on lipid rafts, in order to amplify the signalling effect induced by an antigen[43]. Lipid rafts are special parts of the plasma membrane (PM) rich in glycosphingolipids that are organized and floating in the plasma membrane, allowing protein complexes of pathways to dock and be in close proximity for optimal signalling[44]. Upon promotion of signal activation, the BCR signal is propagated and phospholipase C γ2 (PLCγ2), Phosphatidylinositol-3-Kinase (PI3K) and BTK play very important roles (Figure ii).

BCR signal propagation

After recruitment of SYK and LYN to the phosphorylated ITAM of the BCR, BLNK is recruited to the non-ITAM portion of CD79a, binds to CD79a via its Src homology 2 (SH2)

domain and gets phosphorylated by SYK[45,46]. Upon SYK phosphorylation, BLNK functions as a scaffold protein, binding to BTK and PLCγ2 via its SH2 domain[47,48]. BLNK's scaffolding function brings BTK and PLCγ2 closer to SYK, allowing PLCγ2 to be phosphorylated by both BTK and SYK[49]. Once phosphorylated, PLCγ2 converts phosphatidylinositol 4,5-biphosphate (PIP2) from the plasma membrane (PM) to inositol 1,4,5-triphosphate (IP3) and Diacylglycerol (DAG): **PIP2 + PLCγ2 → IP3 + DAG**. DAG activates protein kinase C (PKC) which goes on to induce the Mitogen-Activated Protein Kinase-Extracellular signal-regulated kinases 1/2 (MAPK-ERK) pathway [49]. IP3 binds to its receptor on the endoplasmic reticulum (ER), IP3R, leading to calcium (Ca^{2+}) release from ER stores.

The BTK protein is a tec family kinase important to BCR signal amplification[37]. Upon BCR activation, BTK gets phosphorylated by SYK and LYN at the tyrosine 551 (Y551) site of its kinase domain and afterwards, autophosphorylates at the tyrosine 223 (Y223) site in its SH3 domain to increase its own activation[50]. BTK activation is further augmented via its connection to the PI3K pathway. By acting as a scaffold protein, BTK recruits phosphatidylinositol-4-phosphate 5 (PIP5) kinases (PIP5Ks), which synthesize PIP2; PIP2 gets phosphorylated by PI3K to generate PIP3 (phosphatidylinositol-3,4,5-triphosphate), which recruits more BTK for activation[51]. IκB kinase (IKK) has been shown to be activated by BTK, enabling it to phosphorylate I-κBα, an inhibitor of NF-κB[52]. I-κBα phosphorylation frees NF-κB to translocate to the nucleus and activate genes involved in inflammation, proliferation and B-cell survival[52]. BTK role as an important protein in intermediate BCR signal transduction is highlighted in a condition called X-linked agammaglobulinemia (XLA). The *BTK* gene is on the X chromosome and BTK loss of function results in XLA, a condition characterized by significant BCR

signalling defects[53]. In XLA, a mutation in BTK's pleckstrin domain prevents membrane recruitment by PIP3 and blunts Ca^{2+} flux induced by the BCR pathway[37] (Figure ii).

Antigen binding to the BCR also activates the PI3K pathway. The PI3Ks have different classes with different functions; the class most relevant to BCR signalling are the class I PI3Ks[54]. Class I PI3Ks have a catalytic and regulatory subunit. Normally, the p85 protein (a regulatory PI3K subunit) complexes with the p110 catalytic subunit, inactivating it[55]. Upon antigen binding to the BCR, LYN phosphorylates CD19 and p85 gets recruited to the PM, where it associates with CD19[49,56]. CD19-p85 co-association results in the activation of the p110 catalytic subunit[57]. P110 has four isoforms: p110α, p110β, p110δ and p110γ[54]. The p110α (PI3Kα) isoform has been shown to be partially redundant with PI3Kδ in B-cell development and tonic (low-level, constitutive) BCR pathway signalling, while PI3Kδ is primarily responsible for antigen-dependent activation of B-cells[58]. PI3Kγ has been shown to be important in CLL cell migration and microenvironment interactions, while PI3Kβ has not been implicated in B-cell development, BCR signalling or CLL[58,59]. Once activated, PI3K (p110) phosphorylates PIP2 to PIP3[37]. The presence of PIP3 in the PM leads to the recruitment of BTK and other pleckstrin homology domain-containing kinases like BTK and AKT (also called protein kinase B – PKB), further activating the BCR[60] (Figure ii).

Cellular signalling pathways activated by the BCR

Depending on the bound antigen, maturation stage of the cell and other factors, multiple downstream pathways are activated by the BCR[37]. The AKT pathway is important for B-cell survival via the BCR. After PI3K phosphorylates PIP2 to produce PIP3, PIP3 phosphorylates and activates AKT and recruits it to the PM[61]. Once activated, AKT promotes survival by phosphorylating (in activation or inhibitory manner) multiple downstream targets. AKT inhibits

the pro-apoptotic proteins Bad and FOX03a (Forkhead box O3), and inhibits glycogen synthase kinase 3-alpha and beta (GSK-3α and β) to promote nuclear translocation of nuclear factor of activated T-cells (NFAT), a transcription factor (TF)[62,63]. Classical NF-kB signalling is important for B-cell survival via the BCR; in this pathway, NF-κB is inactive in the cytoplasm as a dimer, typically of the p50/p65 and p50/p50 proteins, bound to IκB[64]. Upon BCR-mediated stimulation by BTK, PI3K and AKT, the IKK complex phosphorylates IκB. IκB phosphorylation eventually leads to its proteasomal degradation, freeing NF-κB to translocated to the nucleus and induce gene transcription. NF-κB activates genes responsible for survival, inflammation and proliferation of B-cells, but requires upstream BTK, Ca^{2+} and VAV protein activity[65–67].

The MAPK-ERK pathway is activated after antigen binding to BCR via DAG signalling through PKC, but also by VAV and GRB2[68]. MAPK regulates TFs including Elk1 and c-Myc (via ERK1/2), ATF2 (via p38 MAPK) and c-Jun (via JNK – c-Jun N-terminal Kinase)[69]. These TFs can induce B-cell survival, proliferation or apoptosis, depending on cell maturation stage and activation status. After BCR-mediated activation, Ca^{2+} can activate TFs like NF-kB, Jun and NFAT, depending the potency and duration[70] (Figure ii).

Regulation of BCR pathway activation

If the BCR pathway is not regulated, it can be activated uncontrollably, leading to autoimmune disorders and malignancies. Inhibitory regulators like FcγRIIB, SH2 domain-containing inositol 5'-phosphatase (SHIP), SH2 domain-containing phosphatase (SHP-1) and kinases with differential activation and inhibitory properties like LYN, are responsible for BCR regulation[37,49]. FcγRIIB is a transmembrane receptor that transmits signals via an Immunoreceptor Tyrosine-based Inhibitory Motif (ITIM) on its cytoplasmic tail. FcγRIIB inhibits BCR pathway activation by co-ligating with the BCR then recruiting SHIP to the PM;

SHIP hydrolyses PIP3, eliminating membrane binding of BTK, AKT and PLCγ2 [71–74]. By inhibiting BTK's PM-binding ability, SHIP inhibits the formation of BCR microclusters on lipid rafts. This is because BTK's activating signal is important to the actin remodelling required for microcluster formation[42]. The above roles implicate SHIP in initial BCR activation regulation and the regulation of Ca^{2+} flux required for downstream protein activation. SHP-1 can associate with ITIM-containing molecules and BCR-FcγRIIB co-ligation leads to the stoppage of SHP-1 autoinhibition. This allows an activated SHP-1 to dephosphorylate multiple substrates like BTK and SYK[75]. Finally, LYN has been shown to be required for FcγRIIB and SHIP phosphorylation, making it crucial to BCR regulation[76,77]. LYN's dual role in activating and inhibiting the BCR is an example of why understanding and targeting the BCR pathway in disease can be difficult, resulting in unexpected effects.

BCR pathway signalling and interactions with integrins

Integrins are transmembrane receptors that can transfer signalling information across the PM in either direction. There are two types of integrin-mediated signalling: outside-in and inside-out signalling[78]. Outside-in signalling involves a ligand binding to an integrin on its extracellular domain, activating a signalling cascade in the cell leading to differentiation, apoptosis, survival or growth [78]. The chemokine SDF-1 (stromal cell-derived factor 1), also called CXCL12 (C-X-C motif chemokine 12), has been shown to activate BTK and PLCγ2 via outside-in signalling, leading to an integrin-mediated migration towards SDF-1[79]. Alternatively, inside-out signalling involves activation from the cytoplasmic side of integrins (mediated by BTK and PLCγ2 in the BCR pathway), leading to a conformational change in the integrin into the active form, which promotes a higher affinity binding of ligand[80]. BTK and PLCγ2-mediated inside-out integrin signalling promotes cell adhesion and migration in B-cells. Specifically, PLCγ2 produces IP3

and DAG, which go on to activate integrins via inside-out signalling. This BCR-mediated inside-out integrin adhesion signalling requires the activation of LYN, PI3K, BTK and PLCγ2.

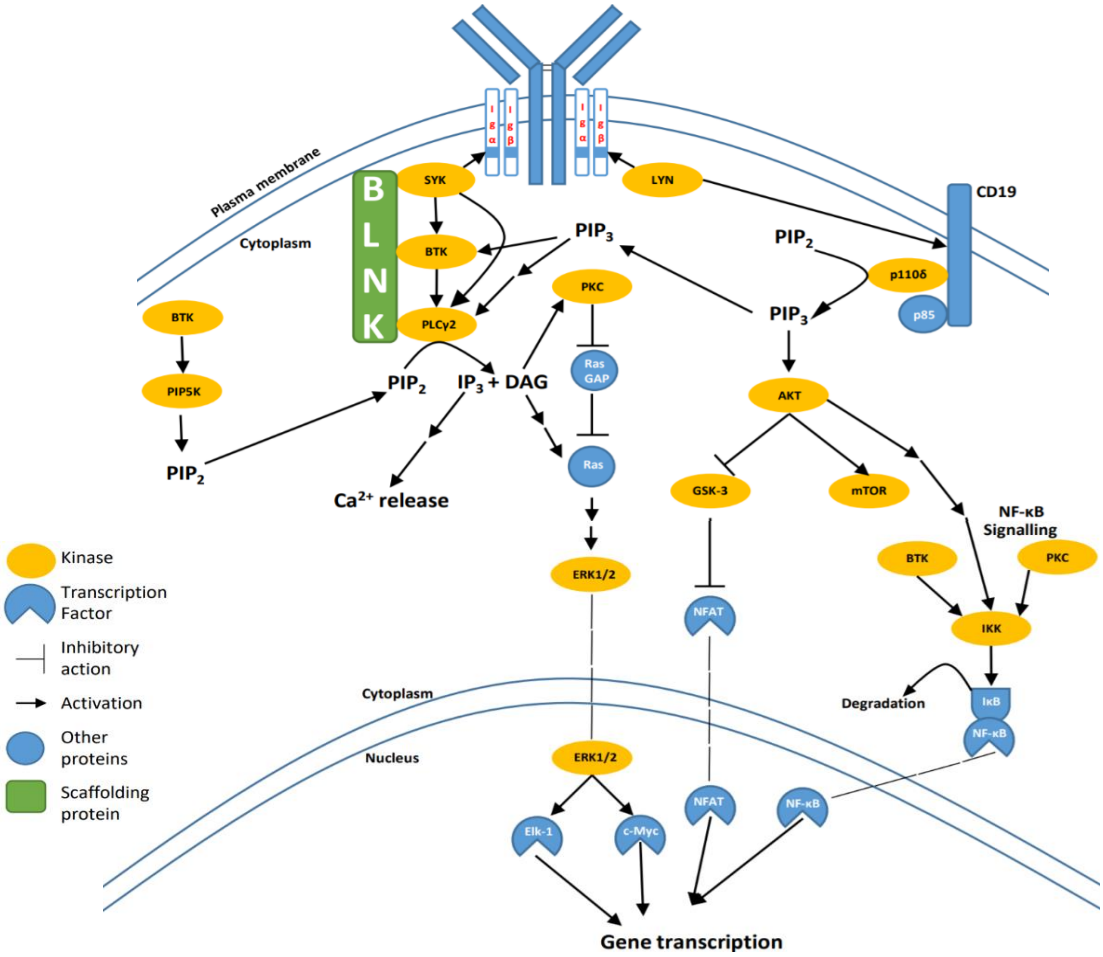


Figure ii. The B-cell receptor pathway. A schematic and legend for a simplified outline of the B-cell receptor pathway, highlighting some signalling cascades important to B-cells and CLL cells.

The BCR pathway in CLL

LYN and SYK, important factors in BCR activation, are dysregulated in CLL. SYK has been shown to be overexpressed in CLL at the transcription and protein levels; LYN has been shown to be overexpressed at the protein, but not transcription level[81,82]. Both LYN and SYK kinase

activity have been shown to be hyperactive in CLL. *In vitro*, LYN is constitutively active in CLL and baseline SYK phosphorylation is higher in CLL compared to normal B-cells. Like its activation pathways, BCR amplification and propagation are altered in CLL at the BTK and PI3K levels. BTK signalling is amplified in CLL, promoting survival via PLCγ2, NF-kB and PI3K interactions; also, BTK gene expression is elevated in CLL[83]. Using the BTK inhibitor ibrutinib in CLL leads to caspase-dependent apoptosis and the inhibition of BTK phosphorylation and its downstream activation targets (ERK, NF-kB and AKT)[83]. Ibrutinib also inhibits CLL cell proliferation via CpG and microenvironment stimulation[84]. Another difference between normal B-cells and CLL cells, is that CLL cells express high nuclear levels of NF-kB and have exaggerated responses to CD40 ligand (CD40L) stimulation, which promotes prolonged cell survival via the PI3K-AKT pathway[85]. Furthermore, high NF-kB levels result in the overexpression of anti-apoptotic proteins. Expectedly, the MAPK pathway is also dysregulated in CLL. Some CLL patients exhibit constitutive ERK1/2 phosphorylation, associated with decreased responsiveness to BCR stimulation; these cells are similar to anergic/inactive B-cells[86]. Expression of the TF Myc has been shown to be dependent on ERK1/2 activation after BCR stimulation, providing evidence that this pathway is important to CLL cell proliferation and survival[87].

PI3Kδ protein expression is similar in normal B-cells and CLL cells, but PI3K is constitutively active in CLL cells, increasing their survival[88]. For this reason, PI3Kδ inhibitors induce apoptosis in CLL cells in a caspase-dependent manner; also, PI3Kα inhibitor use leads to a decrease in stromal cell protection of CLL cells, ultimately leading to apoptosis[89,90]. Downstream of PI3K, the AKT pathway is constitutively active in CLL. Therefore, using a PI3Kδ inhibitor results in a reduction in AKT activation, MCL-1 (induced myeloid leukemia cell

differentiation protein) expression and inhibition of BAX (BCL-2-associated X protein) and XIAP (X-linked inhibitor of apoptosis protein; an anti-apoptotic protein) protein expression[88,90]. BAX and MCL-1 are both members of the BCL-2 family of apoptotic proteins.

The BCR signalling pathways described above are altered in CLL, leading to disease progression, second malignancies and death. Overall, there is an upregulation of BCR-related genes in CLL cells in the bone marrow and lymph nodes compared to peripheral blood, independent of ZAP-70 and *IGHV* mutation status[22]. In practice, patients' CLL cells can either have a somatic hypermutated or unmutated *IGHV* gene as described above. *IGHV* mutation is strongly associated with an overexpression of ZAP-70[37]. ZAP-70 promotes CLL cell migration towards chemokines, amplifies cell response to survival stimuli in the tumour microenvironment and enhances BCR signalling in blood-derived CLL cells[91,92]. In contrast, some other B-cell malignancies are defined by the presence of a translocation involving the immunoglobulin gene, seen in the majority of cases, such as in MCL, Burkitt's lymphoma and Follicular lymphoma[93,94]. Although, for some of these lymphomas, BCR signalling still plays an important role, especially in activated B-cell diffuse large B-cell lymphoma (ABC DLBCL)[95].

BCR signalling, integrins and adhesion molecules in CLL

The CLL tumour microenvironment in the peripheral blood, lymph nodes, spleen and bone marrow) has been shown to promote cell proliferation and survival, partially via augmentation of BCR signalling[96]. In the bone marrow and lymph nodes, CLL cells encounter T-cells, nurse-like cells (NLCs) and bone marrow stromal cells (BMSCs), all of which are accessory cells that promote CLL cell survival and proliferation[96]. Gene expression analysis identified genes associated with the BCR as being the most differentially expressed when comparing CLL cells from the lymph node to peripheral blood-derived CLL cells (genes upregulated in the lymph

nodes)[22]. CLL cell co-culture with stromal cells showed activation of SYK and AKT, providing evidence of tumour microenvironment cell-cell interactions upregulating the BCR pathway[21,97]. Inhibitor work *in vitro* showed the general effects of the following BCR pathway inhibitors: In CLL-stromal cell co-culture, the SYK inhibitor R406 induced a block in AKT activation, a reduction in CXCL12-mediated homing signals and lower stromal cell-induced MCL-1 expression[97]. Using the PI3Kδ inhibitor idelalisib resulted in lower CLL cell viability and a reduction of amplified chemokines and cytokines in CLL-NLC co-culture[98]. Finally, the BTK inhibitor ibrutinib blocked cell survival induced by stromal cell co-culture with CLL cells and the protective effects of pro-survival microenvironment signals induced by tumour necrosis factor α (TNFα) and BAFF (B-cell activating factor), both members of the TNF superfamily of cytokines[83].

The CLL tumour microenvironment

Since CLL cells do not exist in a vacuum, their interactions with other cell types and molecules found in the peripheral blood, lymph nodes, spleen and bone marrow have various effects on their survival and viability[21,22]. Although cell-cell interactions may occur at any of the aforementioned sites, the lymph node, spleen and marrow comprise the proliferation centers (PCs) because the interactions engaged in by CLL cells in these environments have been shown to induce significant survival and proliferation effects, compared to the peripheral blood[21,22]. The following sections will separate CLL cell interactions based on cell types and provide information based on *in vitro* and *in vivo* studies.

CLL cells. CLL cells communicate with each other and this cell-cell interaction is very important in CLL. CLL cells express CD40L and CD40 (TNF superfamily member)[99,100]. CD40L binds to normal B-cells and promotes proliferation and survival and has the same effect on CLL cells[101–

[103]. In addition, CD40L stimulates cytokine release in CLL and prevents chemotherapy-induced apoptosis[102]. CLL cells also express BAFF and APRIL (A Proliferation-Inducing Ligand) and their respective receptors BAFF-R (BAFF-receptor), TACI (transmembrane activator and CAML interactor) and BMCA (B-cell maturation antigen)[104]. Like CD40L and CD40, BAFF and APRIL on CLL can bind to their receptors on other CLL cells, potentiating survival. Other survival-promoting activities of CLL cells include interleukin-7 (IL-7) and TNF-α production and VEGFR (vascular endothelial growth factor-receptor) expression[105–108]. IL-7 is a lymphoid stem cell growth factor which can prevent apoptosis via the JAK-STAT (Janus Kinase – Signal transducer and activator of transcription) pathway signalling through β2 integrin[105]. CLL cells can produce TNF-α *in vitro* and it decreases apoptosis by generating BCL-2; furthermore, serum TNF-α levels are higher in CLL patients and increase with advanced disease[106,109]. VEGF is secreted by CLL cells, which also express the VEGF receptors, VEGF1R and VEGF2R; high protein levels of VEGF2R have been associated with advanced disease and elevated lymphocyte counts [110,111]. VEGF also activates the JAK-STAT pathway to promote CLL cell survival[110]. In addition to the above receptors, CLL cells express higher levels of IL-4 receptor (IL-4R) compared to normal B-cells and IL-4R signalling increases CLL cell survival[112]. IL-4 signalling through the IL-4R in CLL cells has been shown to increase CLL cells' expression of CD79b at the RNA and protein levels and also increase sIgM expression and subsequently, BCR signalling through BTK and PI3K, resulting in ERK and NF-κB activation[113–115]. Nonetheless, IL-4 can also result in ERK activation independent of the BCR signalosome (BTK, PI3K, etc.) in CLL[116]. IL-4-mediated increase in sIgM expression was observed to be greater in patients with U-CLL than in those with M-CLL, and IL-4 stimulation of CLL cells reduced their expression of

CXCR4 and CXCR5[113,114]. In the PCs, T-cells secrete IL-4, which induces the above effects via the JAK3/STAT6 pathway.

Nurse-like cells (NLCs). NLCs are large, adherent tumour-associated macrophages that mostly interact with CLL cells by directly binding to them in the peripheral blood, but these cells can also be found in secondary lymphoid tissues and the spleen[117]. NLC-CLL co-culture has been found to reduce CLL cell spontaneous apoptosis and promotes drug resistance and proliferation, via cell-to-cell contact[117]. NLCs exert their effects on CLL cells by expressing factors and cell surface markers which interact with receptors expressed on CLL cells to promote or induce proliferation and/or survival. These factors and markers include CD40L, BAFF, APRIL, plexin B1, CXCL12 and CXCL13[118].

Stromal cells (SCs). Like NLCs, CLL-stromal cell interactions result in a reduction in spontaneous apoptosis, survival and drug-resistance promotion[117]. SCs produce CD54 and CD106 which bind to β_1 and β_2 integrins on CLL cells, promoting survival[119]. BCR pathway activation leads to CLL secretion of chemokine C-C motif ligand 3 (CCL3), which attracts SCs and T-cells to the CLL cells[120]. SCs also secrete the chemokines CXCL12 and CXCL13 which bind to CXCR4 and CXCR5 (C-X-C chemokine receptor 4 and 5) on CLL cells to promote cell migration towards SCs[121]. Once in contact with SCs, CLL cells can produce IL-6 and IL-8, which enhance CLL-SC adhesion, promoting survival[122]. CLL cells also interact with BMSC by releasing microvesicles that can activate the AKT pathway in CLL-BMSC[123]. BMSCs play an important role in normal B-cell development by providing a safe haven for B-cells to attach to and receive survival and growth signals[121,124]. Like NLC-CLL and CLL-CLL cell interactions, SCs also support CLL cells through CD40-CD40L mediated pathways[125]. Finally, all NOTCH

receptors and ligands are upregulated in CLL and BMSCs; NOTCH signalling terminates in various cellular functions including proliferation, differentiation and survival[126].

T-cells. CLL patients with early disease have increased number of circulating T-cells; however, this number decreases with disease progression[127]. This is because the T-cells can either promote or prevent CLL cell proliferation. Evidence exists for the former because T-cells have been found to co-localize with CLL cells; hence, they presumably support CLL cell proliferation[20]. T-cells may interact with CLL cells in the bone or lymphoid tissues, but also in the peripheral blood[121]. With respect to IL-4 signalling, CLL patients with more aggressive disease have been observed to express higher levels of T-cells that spontaneously produce IL-4 and IL-2, compared to patients with steady disease and age-and-sex-matched controls[128]. This highlights the importance of IL-4 signalling in the CLL tumour microenvironment to disease progression and/or severity, via mechanisms outlined above. Finally, T-cells are attracted to CLL cells and SCs by the cytokine CCL3 as described above.

It is important to state that there is a plethora of other interactions and factors influencing CLL cell survival and disease course, in addition to the cell-cell and ligand-receptor interactions listed above. The complexity and importance of the proliferation center tumour microenvironment to CLL progression and pathogenesis is evident when agents targeting pathways in this niche are utilized[129].

Other pathways important to CLL pathogenesis and survival

In addition to the BCR pathway, interactions in the CLL tumour environment stimulate or inhibit other pathways that are important to CLL cell survival. Two such pathways are highlighted below.

Apoptotic pathways

Apoptosis is a type of programmed cell death and is a normal process used to eliminate sick cells or during development, typically cells that are no longer needed[130]. Apoptotic cell death is characterized by cell shrinkage and disintegration of the cell into smaller membrane-bound components called apoptotic bodies, which are phagocytosed typically by macrophages[130]. There are two major pathways by which apoptosis may occur; the intrinsic or caspase-dependent pathway, and the extrinsic pathway. The intrinsic pathway involves mitochondrial outer membrane permeabilization (MOMP) that is induced by cellular stressors like DNA damage or endoplasmic reticulum stress, leading to the release of proteins like cytochrome c, Smac (also known Diablo) and Omi into the outer mitochondrial membrane from the intermembrane space[130]. Normally, XIAP binds to and inhibits the caspase proteins (caspase 3, 7 and 9) to prevent apoptosis; however, once released, Smac and Omi bind to XIAP and antagonize it, allowing potentiation of caspase-dependent apoptosis. Importantly, MOMP is tightly controlled by the BCL-2 family of proteins which are responsible for inducing MOMP in response to cellular stressors[130]. Important members of the Bcl-2 family include the pro-apoptotic proteins Bax and Bak, anti-apoptotic proteins Bcl-2, Bcl-XL and Mcl-1, and the BH3 (Bcl-2 homology 3) proteins Bad, Bim, Bid and Noxa. Bax and Bak induce MOMP, Bcl-2 and Mcl-1 block MOMP (by inhibiting Bad, Bax, Bim and Bid), and Bid/Bim activate Bax/Bad and/or inhibit Bcl-2/Mcl-1[130]. The delicate balance between the activities of the different members of the Bcl-2 family of proteins regulates MOMP and therefore intrinsic apoptosis.

The extrinsic apoptosis pathway involves the activation of death receptors, which are a subset of TNFR (TNF receptor) family of receptors. The death receptors share a common domain of approximately 80 amino acids called the death domain (DD), located in the

cytoplasmic region of these receptors[131]. In the extrinsic pathway, death ligands like TNF or TRAIL (TNF-related Apoptosis inducing ligand) bind to their receptors (TNFR/TRAIL-R) leading to the formation of complexes that activate caspase-8 via different mechanisms, leading to caspase-dependent cell death signalling. However, the different subdivisions of the extrinsic pathway are also suspected to induce cell death via other mechanisms[131].

In CLL, intrinsic apoptotic signalling is dysregulated. This is because CLL cells are known to express high levels of Bcl-2 and Mcl-1, giving them a survival advantage as these proteins inhibit apoptosis in these cells with high genomic instability[121,132,133]. Specifically, Mcl-1 levels are upregulated in CLL cells via BCR signalling in the tumour microenvironment, as described above[134]. It is important to state that the expression and regulation of the Bcl-2 family proteins are altered by CLL cell interactions in the microenvironment but also in response to treatment regimens employed to treat the disease[121]. Also, the extrinsic apoptotic pathway is important to CLL, but will not be discussed in this thesis.

DNA damage repair

DNA damage occurs constantly in normal cells and CLL cells are no different. Various mechanisms exist to repair damaged DNA, depending on the type of DNA damage incurred and the phase of the cell cycle a cell is in (Figure iii). To list a few, different types of DNA repair include base excision repair, single-strand break repair and double-strand break repair[135]. The following section will focus on DNA double-strand break repair due to the importance of certain proteins involved in this process and their relevance to CLL. DNA double-strand break repair (DSBR) is further subdivided into two major types of repair: non-homologous end-joining (NHEJ) and homologous recombination repair (HRR)[25,135]. NHEJ is a quick, error-prone method of DSBR in which the cell induces single-strand excisions in each direction from the DNA break

site and uses these excised strands to search for regions of homology to mediate strand annealing[136]. NHEJ can be used by cells in any phase of the cell cycle, though it is typically used in the G1 phase[135,136]. On the other hand, HRR is only active during the late S and G2 phases of the cell cycle, because it is reliant on the presence of sister chromatids (Figure iii). Unlike NHEJ, HRR is slower and error-free because the DSB is cut out and a 3' overhang is used to invade the sister chromatid to identify an intact copy, which is used to repair the break[136].

NHEJ is used mostly for simple DSBR whereas HRR is typically employed for more complex DSBs (Figure iii)[136]. ATM is important in sensing DSBs, initiating the recruitment of important repair factors (dependent on type of break) but also specifically, HRR resection[25]. Likewise, p53 is important in DNA DSBR as it is involved in the fate of the cell after the break; cell cycle arrest for repair, senescence or apoptosis. P53 is phosphorylated and activated by ATM in response to DNA DSBs[137]. In CLL, the frequencies of mutations and deletions in P53 and ATM have been addressed above with regards to their effect on patient prognosis[9]. P53 deletion

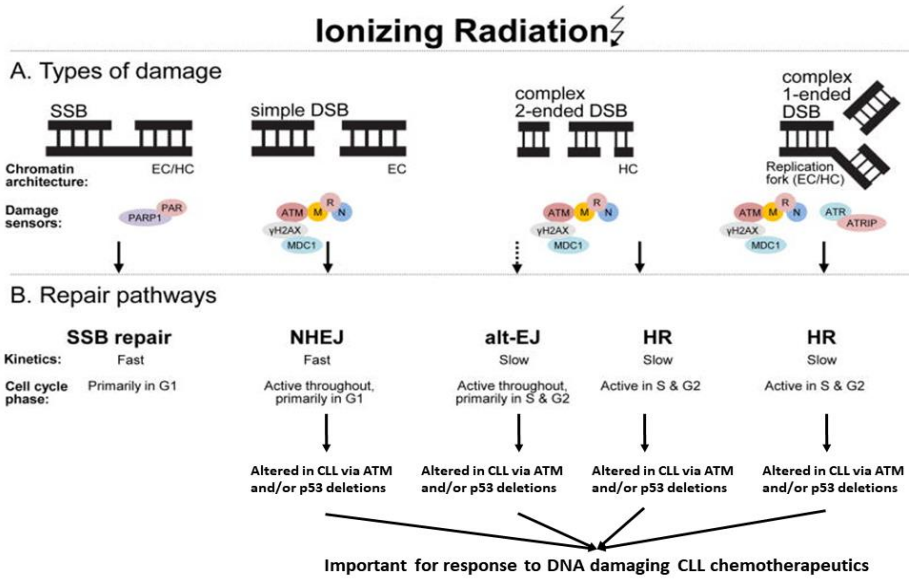


Figure iii. DNA damage repair pathways and relevance to CLL. A schematic of DNA damage repair pathways highlighting important proteins. Illustration modified from: Morgan MA, Lawrence TS. Molecular Pathways: Overcoming Radiation Resistance by Targeting DNA Damage Response Pathways. *Clin Cancer Res*.

or mutation is associated with chemoresistance due to a lack of p53-mediated apoptosis[9,138]. This is because p53 is required for most CLL-relevant chemotherapeutics (fludarabine, chlorambucil) to induce cell death[121,138,139]. Given the reliance of chemotherapy on DNA damage and ATM's role as a DNA damage repair initiator, it is easy to see why ATM deletion and/or mutations in CLL might confer a poor response to chemoimmunotherapy.

CLL Treatment

Like most cancers, CLL was traditionally treated with chemotherapeutic agents including DNA alkylating agents like cyclophosphamide or chlorambucil, and nucleoside analogs like fludarabine (Figure iv) [25,121,140]. Other single-agent treatments for CLL in the past also included the use of antibodies (immunotherapy) targeting CLL cell surface markers. Recently, there have been significant advances in CLL treatment with combinations of chemotherapy and immunotherapy (chemoimmunotherapy), but most importantly, the introduction of targeted therapies using small molecule inhibitors of kinases and other factors important to CLL pathogenesis and progression[9]. Analysis of response to treatment in clinical trials is typically assessed using the following parameters: overall response (OR) rate, complete response (CR), partial response (PR), overall survival (OS) and progression free survival (PFS) [9,141]. However, recent studies have customized these responses to better fit the CLL treatment response landscape, including PR with lymphocytosis (for ibrutinib) and investigating minimal residual disease (MRD) in the blood and/or bone marrow, a predictor of long-term prognosis and relapse (for Venetoclax) [142,143]. For an outline of CLL treatment paradigms, see Figure iv below.

Chemoimmunotherapy

For younger, fit CLL patients with M-CLL and no del(11q)/del(17p), the current recommended treatment is combination chemoimmunotherapy with fludarabine,

cyclophosphamide and rituximab (FCR)[140]. Fludarabine is a nucleoside analog that induces CLL apoptosis by inhibiting DNA synthesis, but also RNA synthesis, killing both resting (limited activity) cells and CLL cells undergoing active DNA synthesis [144,145]. Cyclophosphamide like most DNA alkylating agents, kills CLL cells by forming DNA interstrand and intrastrand crosslinks by binding to the N-7 position on guanines[25]. Rituximab is a monoclonal antibody against the CD20 cell surface marker found on B-cells and CLL cells. In a randomized Phase III study of 817 young (median age 61 years), fit, treatment-naïve CLL patients, 409 patients received fludarabine-cyclophosphamide (FC) combination and 408 patients, FCR[140]. At 3 years post-randomization, FCR treatment led to a higher OR (90% versus 80%), CR (44% versus 22%), OS (87% versus 83%) and PFS (65% to 45%) than FC. Toxicities reported for FCR and FC treatments included neutropenia, leukocytopenia, infections and thrombocytopenia. Unfortunately, there was no survival benefit to FCR treatment in patients with *TP53* deletion[140]. The reasoning behind combining DNA-damaging agents like cyclophosphamide with nucleoside analogs like fludarabine is that the nucleoside analogs inhibit DNA repair that is induced by the alkylating agent[146].

A second chemoimmunotherapy combination used in CLL treatment is the bendamustine-rituximab (BR) combination; although, obinutuzumab is the most common monoclonal antibody used in the clinic. Bendamustine is an alkylating agent that demonstrated better activity as a single agent, compared to fludarabine[147]. However, in a study of fit CLL patients that compared FCR to BR, FCR treatment yielded longer PFS and higher CR, although BR resulted in a better toxicity profile[148]. Hence, FCR remains the treatment of choice in fit CLL patients without del(17p). In addition to FCR and BR there are other chemoimmunotherapy treatment regimens like chlorambucil-obinutuzumab and chlorambucil-ofatumumab.

Chlorambucil is another DNA alkylating agent while ofatumumab and obinutuzumab are both anti-CD20 monoclonal antibodies. A major limitation of chemotherapy and chemoimmunotherapy comes from the lack of significant improvements in the long-term prognoses of patients with high risk disease (del(11p), del(17p), etc.)[9]. Hence, in recent years, small molecule inhibitors have been investigated and approved for patients with high-risk disease at diagnosis and patients with chemoimmunotherapy-refractory disease.

Small molecule inhibitors

Small molecule inhibitors for CLL were developed based on knowledge of pathways contributing to CLL pathogenesis. These inhibitors have overall proven to be better alternatives for patients with historically dire prognoses with chemoimmunotherapy.

Ibrutinib

Ibrutinib is a first-in-class orally available irreversible inhibitor of BTK that functions by covalently binding to a cysteine residue (Cys-481) in the protein's ATP-binding/activation pocket, rendering the protein inactive[149,150]. Ibrutinib-mediated inhibition of BTK inhibits BTK autophosphorylation, a process critical to BTK's central role as a propagator of the BCR signal and this is evident in the inhibition of downstream proteins like ERK1/2 and the NF-kB pathway after ibrutinib treatment[83,150]. Ibrutinib is cytotoxic to CLL and other BCR-dependent lymphomas, although it is important to state that ibrutinib is known to also inhibit other kinases with sequence homology to BTK like EGFR (epidermal growth factor receptor), BLK (B-lymphocyte kinase) and ITK (IL-2-inducible T-cell kinase)[149,150]. Ibrutinib induces cell death in CLL cells via caspase-dependent apoptosis[83].

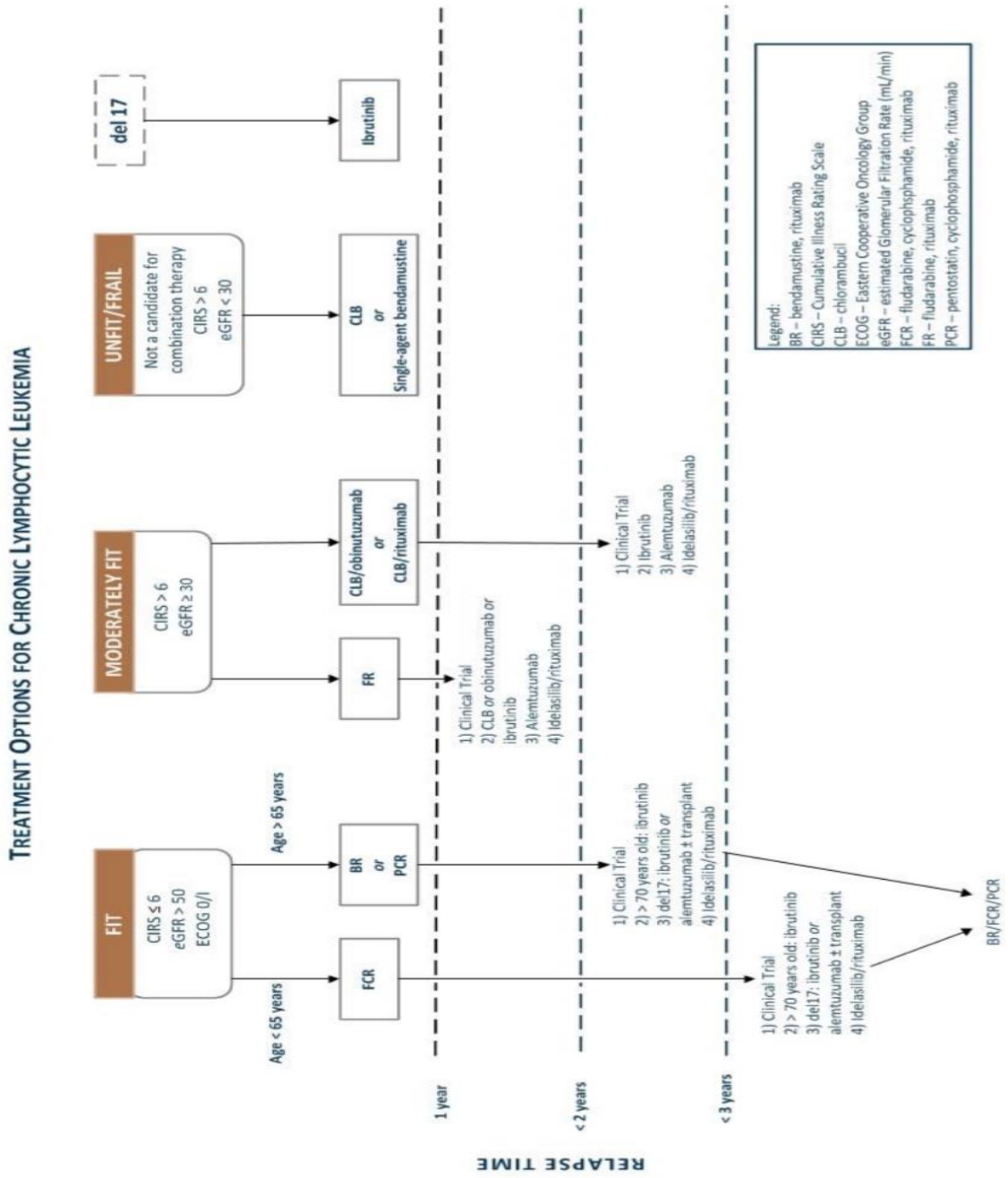


Figure iv. Chronic lymphocytic leukemia (CLL) treatment guidelines. An outline of the CLL treatment approach used in Manitoba, obtained from: CancerCare Manitoba disease management consensus recommendations for CLL (2015).

In CLL, ibrutinib was first evaluated in patients with refractory high-risk disease in a study of patients with a median of 4 previous therapies, unmutated *IGHV*, bulky nodes, del(11q)

and del(17p)[129]. In these patients, the OR was 71%, with reported reductions in nodal sizes with a concomitant lymphocytosis; nonetheless, lymphocyte counts eventually declined. Furthermore, the 2-year data showed a PFS and OS in 75% and 83% of patients, providing evidence for the durability of patient response to ibrutinib. This study demonstrated ibrutinib's potent activity in CLL, even in heavily pre-treated patients and this eventually led to ibrutinib being approved as a first-line of treatment for patients with high-risk disease[9].

Overall, the response of CLL patients on ibrutinib can be classified based on certain characteristics. Data from an 8-year follow-up study of single agent ibrutinib in first-line and relapsed/refractory CLL show that patient response is influenced by chromosomal abnormalities[151]. The OR rate was similar in first-line (89%) and relapsed/refractory (87%) CLL, with first-line treatment having a higher CR rate (35%) than relapsed/refractory disease (10%). Furthermore, estimated 7-year PFS was 83% in the first-line arm and 34% in the refractory setting[151]. Estimated 7-year OS was 84% (median follow-up of 87 months, median OS not reached) for first-line treatment and 55% (median follow-up of 82 months, median OS of 92 months) for relapsed/refractory disease. Despite wide and overlapping hazard ratios, the 7-year OS varied by the presence of chromosomal abnormalities. The order of the 7-year OS from highest to lowest were for patients with del(13q), patients without chromosomal abnormalities, del(11q), trisomy 12 and del(17p), respectively. The same trend was observed with PFS at 7-years, albeit with trisomy 12 patients having a higher PFS than del(11q) patients. Although responses were better than with chemoimmunotherapy, this study showed that patients with del(17p) have a poorer prognosis with ibrutinib treatment, relative to other factors.

Ibrutinib as monotherapy or in combination with other agents like rituximab has been shown to be superior in comparison to other therapies, both as first-line treatment and in

refractory cases[9,152]. Upon administration of ibrutinib, patients experience a rapid lymphocytosis concurrent with reductions in nodal size[129,153,154]. This is known to be due to ibrutinib-mediated disruptions of important CLL tumour microenvironment interactions like the chemokine CXCR4, forcing CLL cells out to the protected proliferation centres[154,155]. Side effects of ibrutinib include diarrhea, upper respiratory tract infections, arthralgia, fatigue and rashes[129]. Over time, patients may discontinue ibrutinib due to side effects, a transformation of their disease to the rapidly proliferating diffuse large B-cell lymphoma (Richter's transformation), or drug resistance.

Idelalisib

Idelalisib is an oral inhibitor of PI3Kδ, the class 1 PI3K upregulated and important to CLL cell proliferation and survival. Idelalisib induces caspase-dependent apoptosis in CLL cells, along with disruption of important survival signals from the tumour microenvironment such as CXCR4 and CXCR5-mediated signalling, and the important interactions between CLL cells, SCs and NLCs[90,98]. Due to idelalisib-mediated inhibition of CLL homing signals via the aforementioned receptors, like ibrutinib, idelalisib treatment results in rapid lymphocytosis and nodal reduction in CLL patients after treatment[156]. Moreover, idelalisib inhibits downstream BCR signalling through AKT and ERK[98]. In a phase I study of relapsed/refractory CLL, patients with a median of 5 previous treatments, bulky nodes, unmutated *IGHV* and *TP53* deletion/mutation, were treated with idelalisib[156]. For these high-risk patients, the OR was 72%, median PFS was approximately 16 months and OS at 3 years was 75%. Moreover, a nodal response was observed in 81% of the patients. Importantly, severe adverse effects after idelalisib treatment included pneumonia, neutropenic fever and diarrhea. Idelalisib has been combined with other agents like rituximab and ofatumumab and compared against monotherapy; both

combinations proved to be more efficacious than rituximab and ofatumumab monotherapy respectively[157,158]. Idelalisib is approved for both frontline and refractory treatment of CLL, but is rarely used because of toxicity.

Venetoclax

CLL cells express elevated levels of BCL-2, an anti-apoptotic protein, conferring a survival advantage to these cells. The elevated levels of BCL-2 in CLL cells is partly explained by their requirement of this protein to sequester the pro-apoptotic protein BIM[159]. Venetoclax is an oral inhibitor of the BCL-2 protein that induces apoptosis in CLL cells. In an initial study in refractory CLL, a single oral dose of venetoclax resulted in tumour lysis syndrome and a reduction of lymphadenopathy within 24 hours in all three patients enrolled in the study[160]. This finding led to the institution of a dose-escalation approach for oral venetoclax treatment. Stilgenbauer et al.[161] administered venetoclax to patients with treatment-refractory del(17p) CLL in a phase II study. At a median follow-up of 1 year, the OR was 79.4% with an OS of 86.7% and PFS of 72%. Significant (grade 3) adverse effects reported included anemia, neutropenia and thromobocytopenia, while grade 1 and 2 adverse events included diarrhea, nausea, fatigue and infections like nasopharyngitis. Venetoclax has been approved for refractory CLL and in patients with del(17p).

Other inhibitors

Other inhibitors being investigated or that have been recently approved for the treatment of CLL include acalabrutinib and duvelisib. Acalabrutinib is a second generation oral inhibitor of BTK, developed in attempt to mitigate the off-target-mediated adverse effects experienced by CLL patients taking ibrutinib. A preclinical study showed that acalabrutinib and ibrutinib exhibited similar characteristics *in vitro*, when administered to CLL cells[162]. Acalabrutinib and

ibrutinib were shown to: inhibit BTK and downstream BCR targets like PLCγ2 and ERK, inhibit chemokine production and migration of CLL cells, induce caspase-dependent apoptosis and inhibit total protein levels of the anti-apoptotic proteins BCL-2 and MCL-1[162]. However, when compared to ibrutinib, acalabrutinib did not exhibit significant activity against the SRC family kinases LCK (lymphocyte-specific protein tyrosine kinase) and SRC, or against the ITK and EGFR proteins[162,163]. Ibrutinib was found to inhibit all of the aforementioned proteins *in vitro*. These findings suggested that acalabrutinib may not induce off-target adverse events like bleeding and atrial fibrillation, induced by ibrutinib treatment.

Currently, clinical trials with acalabrutinib have reported very positive findings. An early study of acalabrutinib in relapsed, high-risk CLL reported an OR of 95% in all patients and an OR of 100% in del(17p) patients, with only one patient out of 61 progressing on the drug, after a median follow-up of 14 months[164]. An expansion of this study reported an OR of 94% that was not influenced by high-risk disease characteristics like del(17p) and *IGHV* mutation status[165]. Also, PFS was 36 months and 33 months for patients with del(17p) and a complex karyotype (greater than 3 chromosomal abnormalities) respectively. Most importantly, the occurrence of treatment-associated severe adverse events in these studies were low, compared to those reported with ibrutinib. These results in addition to other studies of acalabrutinib monotherapy and combination with agents like obinutuzumab, paint an promising picture of CLL treatment targeting BCR inhibition with acalabrutinib[166,167].

Duvelisib is an oral dual inhibitor of PI3Kδ and γ. PI3Kγ inhibition by duvelisib may be desired due to migration and stromal cell-adhesion functions of PI3Kγ[59]. In CLL, duvelisib has been shown to unsurprisingly induce similar adverse effects as idelalisib, but also importantly, duvelisib was effective in resistant/refractory CLL and in patients with high-risk disease features,

compared to agents like ofatumumab[168,169]. Duvelisib has been approved for resistant/refractory CLL after more than two prior therapies, based on its significant improvement of PFS, compared to ofatumumab monotherapy, albeit with a warning of possibly fatal toxicities[169].

Ibrutinib resistance in CLL

Despite the positive responses to ibrutinib treatment seen in CLL patients, as the inhibitor is increasingly used in the clinic and as more patients are observed over longer periods of time, resistance is being observed. An early study by Furman et al.[170] described ibrutinib resistance in a patient who initially responded to ibrutinib but developed resistance after 21 months. Sequencing data from samples collected before ibrutinib treatment, during response and at relapse, identified a mutation (C481S) in the ibrutinib-binding pocket of BTK. Furman et al. showed that C481S mutation resulted in a disruption of ibrutinib's covalent binding to BTK, resulting in a protein only reversibly bound by ibrutinib and this was demonstrated by the higher concentration (400-fold) required to inhibit BTK autophosphorylation in the mutant protein[170]. Importantly, this mutation was not present before ibrutinib treatment or during the period when the patient was responding to the inhibitor, showing that the C481S mutation was acquired during ibrutinib treatment.

Taking the initial study one step further, Woyach et al.[171] performed whole exome sequencing on six patients with samples collected at baseline and upon relapse, after ibrutinib treatment. This study reported the BTK C481S mutation in five of the six patients and three mutations in BTK's direct downstream target, PLCγ2 (R665W, L845F, S707Y). These mutations were not detected at baseline, but were present at relapse. As expected, functional analyses showed that the C481S mutation resulted in a protein bound reversibly by ibrutinib, but also that

ibrutinib demonstrated a lower affinity for the mutant BTK, leading to less effective inhibition of BTK autophosphorylation and downstream BCR pathway signalling (p-ERK and p-AKT)[171].

The PLCγ2 mutants R665W and L845F, displayed enhanced IgM-mediated calcium flux that was resistant to ibrutinib inhibition, suggesting that these mutants exhibit BTK-independent BCR signalling. Interestingly, in one patient at relapse, BTK was still inhibited by ibrutinib, but PLCγ2 phosphorylation was enhanced and in another patient with both BTK and PLCγ2 mutations, neither protein was inhibited by ibrutinib at relapse. Of importance, for all patients, no mutations were detected in other kinases (e.g. ITK, EGFR or BLK) with C481-homologous cysteines that are also irreversibly inhibited by ibrutinib[171]. In a follow-up study, PLCγ2 R665W-mediated ibrutinib resistance was shown to involve a BTK-bypass mechanism that depended SYK and LYN for PLCγ2 phosphorylation[172]. Taken together, these studies showed that ibrutinib resistance is mediated by mutations in BTK and/or PLCγ2 developed during ibrutinib therapy, that confer alternative BCR signalling.

Using patient samples and data from four different clinical trials of ibrutinib monotherapy or in combination with ofatumumab (combined n=308), Woyach et al.[173] showed that with longer follow-up (4 years), the estimated cumulative incidence of disease progression while on ibrutinib was 19%. BTK and/or PLCγ2 mutations were detected in 85% of patients progressing on ibrutinib, at a median of 9.3 months before clinical relapse. Negative independent risk factors for relapse while on ibrutinib included complex karyotype at baseline or del(17p). Interestingly, for patients 65 years or older without complex karyotype or del(17p), the risk of disease progression on ibrutinib was extremely low (1.9% at 4 years), while younger patients (< 65 years) with both complex karyotype and del(17p), had a higher risk of progression (44% at 4 years)[173]. Moreover, 53% of patients who discontinued ibrutinib therapy in these studies did so

because of disease progression while on the drug. This was a pivotal study because it examined the incidence of ibrutinib resistance, BTK and/or PLCγ2-mediated resistance and risk factors for ibrutinib resistance in a large enough cohort of patients with long follow-up. This study also reported in a large patient cohort, an important finding: BTK and/or PLCγ2 mutations are present *before* clinical relapse and are clonally selected for by ibrutinib therapy, a finding also reported in another study[173,174]. The presence and detectability of these mutations before clinical relapse in some patients provides a window of opportunity for alternative treatment plans, before disease progression.

Finally, although BTK and PLCγ2 mutations have been shown to be important in the majority of CLL progressions on ibrutinib, and are generally accepted as the main mechanisms driving ibrutinib resistance in CLL, other mutations and/or mechanisms are known and have been hypothesized to play a role. These include ibrutinib-mediated selection of CLL subclones with del(8p), which results in TRAIL-R haploinsufficiency (and subsequent TRAIL insensitivity) and aberrant FOXO3a nuclear/cytoplasmic subcellular localization in CLL/lymphoma cell lines[175,176].

PROJECT AIMS AND RATIONALE

Given the possibility of other mechanisms mediating ibrutinib resistance in CLL and the increasing incidence of patients progressing on the inhibitor, it is important to identify other mechanisms (if any) mediating ibrutinib resistance. Furthermore, it is important to state that the clinical course of CLL is known to be heterogeneous; therefore, more than one mechanism of resistance may be observed in a patient, e.g. the occurrence of both BTK and PLCγ2 mutations. For the above reasons, this project aimed to develop and characterize a cell line model of ibrutinib resistance, with the hope of identifying and integrating multiple mechanisms of resistance in a cell line.

Moreover, ibrutinib resistant cell line models developed and characterized were to be tested using current rescue therapies for ibrutinib-resistant CLL patients in order to evaluate clinical relevance. Also, the cell line models were to be tested with an array of CLL-relevant agents in hopes of identifying novel treatment strategies to overcome ibrutinib resistance. Finally, the mechanisms and treatment strategies identified using the cell line model of ibrutinib resistance were to be tested on freshly isolated CLL cells from patients.

Hypotheses

Upon continual/long-term treatment with ibrutinib in either a dose-escalation or constant dose regimen, cell lines will develop resistance to ibrutinib, which will be identified as cells growing normally in ibrutinib at concentration (s) toxic to parental cells. Ibrutinib-resistant cells will exhibit differences compared to their ibrutinib-sensitive counterparts, at the genomic, transcription, translation and/or signalling levels, that may or may not be directly linked to their mechanism of resistance to ibrutinib.

MATERIALS AND METHODS

Cell culture

Cell lines: Cell lines utilized and their diseases of origin are as follows: BJAB and RAJI cells (Burkitt's lymphoma), MEC-1 and I83 cells (CLL). All cells were cultured in RPMI 1640 media (R0883, Sigma Aldrich) supplemented with 10% fetal bovine serum, 1% volume/volume GlutaMax (L-glutamine substitute) and Penicillin-Streptomycin. Cells were split at a 1:5 or 1:7 ratio and cultured at 37ºC and 5% CO_2 until confluence. Cultured cells at confluence ($1.5x10^6$ – $2x10^6$ cells/mL) were counted (Bio-Rad cell counter) and resuspended at $1x10^6$ cells/mL in fresh media, for all experiments conducted.

Patient samples: Patient-derived chronic lymphocytic leukemia (CLL) B-cells isolated from whole blood and counted by the Manitoba CLL Tumour Bank as previously described[177], were received and resuspended at $1x10^7$ cells/mL in fresh serum-free hybridoma media (Life technologies™) and allowed to recover overnight. After recovery, cells were treated for 72 hours at $5x10^6$ and $1x10^7$ cells/mL for flow cytometry and western blot experiments, respectively.

B-cell receptor pathway inhibitors

Inhibitors of the B-cell receptor pathway were used in all studies conducted. The inhibitors used and their targets are as follows: **ibrutinib** (BTK), **idelalisib** (PI3Kδ), **copanlisib** (PI3K α,β,δ,γ) and **ravoxertinib** (ERK1/2). All inhibitors were purchased from Selleckchem, except copanlisib (APExBIO). Catalog numbers for all agents are outlined in Table 2, and a schematic of the inhibitors in the context of the BCR can seen in Figure vii.

Flow cytometry

Cell viability and total cell death were investigated via flow cytometry analysis of annexin V and 7-Aminoactinomycin D (7-AAD), markers of apoptosis and total cell death

respectively, in a previously established protocol [178]. Cells negative for both annexin V and 7-AAD were deemed live/viable cells, while total cell death was defined as cells positive for both annexin V and 7-AAD. The fraction of dead cells (FDC) was determined by subtracting the percentage of cells alive (annexin V and 7-AAD negative) from 100 and making the resulting value a fraction of 100 (dividing by 100).

Synergy-antagonism studies

Synergy-antagonism studies were conducted in order to determine the relationship between agents being combined in cell lines and patient samples. Inhibitors were serially diluted (six to seven total concentrations, including zero) and arranged in the horizontal or vertical axis of 96-well plates for combination studies, as outlined in the image below (Figure v-B). After treatment, cells were stained with annexin V and 7-AAD and run on the flow cytometer. Results were analyzed using the Combenefit software[179].

Combenefit: Combenefit is a free bioinformatics software developed by the Cancer Research UK Cambridge Institute that enables visual presentation and statistical analysis of the effect of drug combinations, using different established models like BLISS and LOEWE[179]. All drug combinations were analyzed using the Loewe model of synergy. Briefly, the Loewe model determines synergy and antagonism in a drug combination by comparing the effect observed with the drug combination to linear portions of individual agent dose-response (D-r) curves to determine any shifts (D-r shift) or differences, relative to a theoretical additive effect expected. If a drug combination effect is greater than additive, it is deemed synergistic and if a drug combination exerts an effect less than additive, it is deemed antagonistic[180]. Combenefit exports images depicting synergy and/or antagonism and increases the intensity of the designated colour

in relation to the magnitude of the observed effect. Sample combenefit-generated images using the Loewe model are outlined below (Figure v).

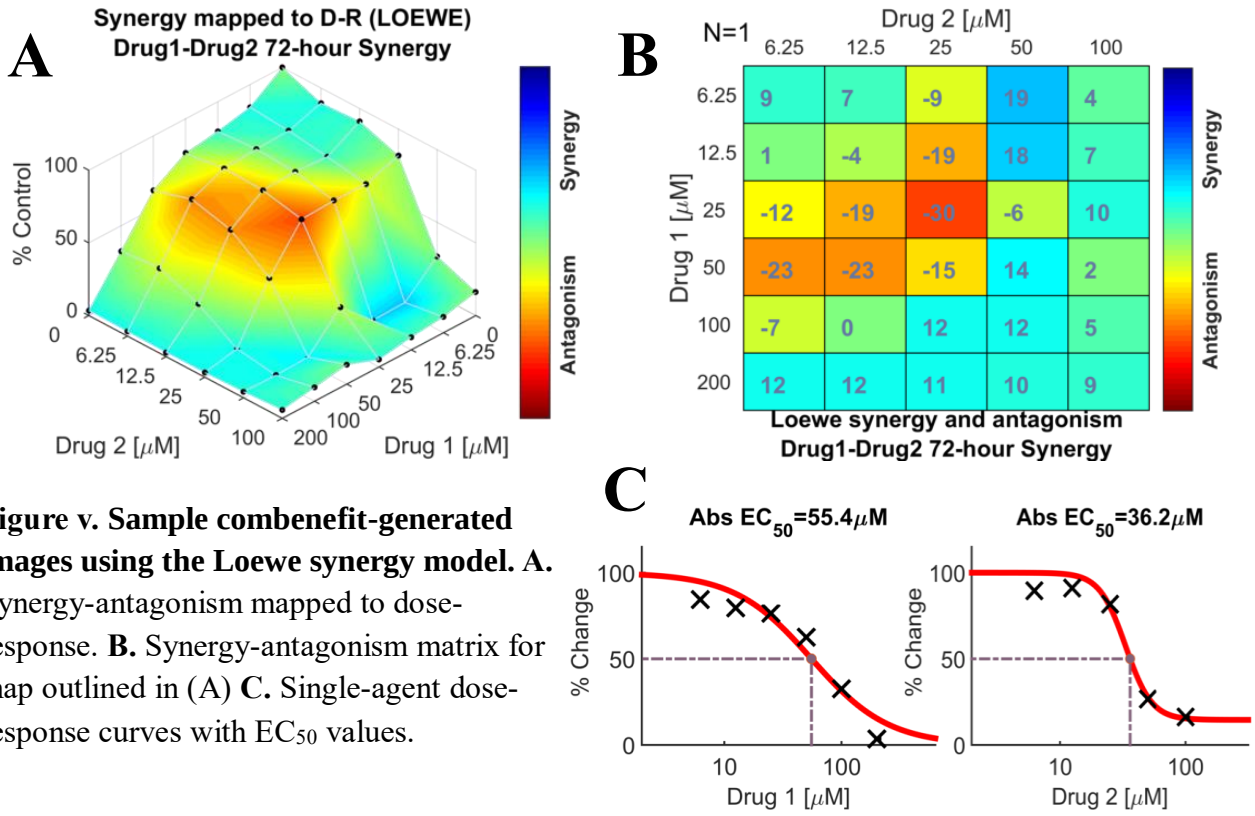


Figure v. Sample combenefit-generated images using the Loewe synergy model. A. Synergy-antagonism mapped to dose-response. **B.** Synergy-antagonism matrix for map outlined in (A) **C.** Single-agent dose-response curves with EC_{50} values.

Development of an ibrutinib-resistant BJAB cell line (IBR10^2 cells)

An ibrutinib-resistant BJAB cell line was developed via a dose-escalation approach. A target concentration of 20μM ibrutinib was chosen based on data from multiple ibrutinib-treated patient-derived CLL cells, which show a median EC_{50} (effective concentration to kill 50% of cells) of 10μM at 72 hours (BJAB 72-hour EC_{50} = 1.6μM; data not shown). Hence, cells growing at a concentration two-fold greater than CLL cell EC_{50} and 12-fold greater than BJAB EC_{50}, were considered ibrutinib-resistant.

BJAB cells were cultured as described above until confluence then counted and resuspended at $5x10^5$ or $1x10^6$ cells/mL. After resuspension, ibrutinib was added to these cells at

different concentrations (5, 10 or 20µM), and the cells were then incubated. Upon confluence (if reached), the cells were washed and resuspended either at the same concentration (if starting at

Table 2: B-cell Receptor (BCR) pathway inhibitor general information and targets.

Inhibitor	Information
Ibrutinib (PCI-32765)	Bruton's Tyrosine Kinase (BTK) inhibitor. Selleckchem, Catalog #: S2680
Idelalisib (CAL-101, GS-1101)	Phosphatidylinositol-3-kinase δ (PI3Kδ) inhibitor. Selleckchem, Catalog #S2226
Copanlisib (BAY 80-6946)	Pan-Phosphatidylinositol-3-kinase (PI3K) inhibitor. APExBIO, Catalog #B2178
Ravoxertinib (GDC-0994)	Extracellular signal-Regulated Kinase 1 and 2 (ERK1/2) inhibitor. Selleckchem, Catalog #S7554

$1x10^6$ cells/mL), or split into the two different cell concentrations specified above, then treated again with ibrutinib at the same, or double the initial concentration. This multifactorial process of creating ibrutinib-resistant BJAB cells is outlined in the diagram below (Figure vi). Upon creation of seven different ibrutinib-resistant BJAB cell lines, the $IBR10^2$ clone was chosen for further analysis, based on a pilot study examining BTK, AKT and ERK signalling in three of the seven cell lines (see results below). $IBR10^2$ cells are BJAB cells treated at $1x10^6$ cells/mL with 10µM ibrutinib twice ($IBR10^2$) before being exposed to the target concentration of 20µM ibrutinib, until resistance (confluence after at least two rounds of 20µM ibrutinib) was achieved.

Protein expression studies

Protein expression studies were conducted via western blot. Briefly, after drug treatment, cells were mixed and transferred to appropriate tubes, centrifuged, washed with PBS and pelleted. These pellets were processed on the same day, or stored at -80°C for processing at a later time. Cell pellets were treated with a NP-40-containing protein lysis buffer, with trituration to promote lysis, followed by incubation at 4ºC. Post-incubation, the lysate-pellet solution was centrifuged at a high speed (13,000 RPM) at 4ºC to obtain a protein lysate. Protein lysates were

quantified using the Bradford's method and an equal mass of protein (40µg/well for cell lines and 15-20µg/well for patient-derived cells) mixed with Lithium Dodecyl Sulfate (LDS)-containing loading dye and heated at 97°C. This mixture was then loaded to pre-cast bis-tris plus gels and run at 150 Volts (V) for 75-120 minutes. Gels were transferred onto nitrocellulose membranes via wet transfer overnight at 20V or for 1.5 hours at 110V. Successful transfer was determined via Ponceau S staining. Nitrocellulose membranes were blocked with 5% milk before probing with primary antibodies (diluted in 5% milk) overnight at 4°C. Membranes were treated with appropriate secondary antibodies (also diluted in 5% milk) for 1 hour at room temperature, washed, treated with ECL substrate then exposed to reveal bands. Information on all antibodies used, along with full compositions of buffers utilized can be found in Table 3 below.

Analysis of western blot results

Upon completion of western blots, images of bands were analyzed using the free National Institutes of Health (NIH) software, imagej[181]. Imagej was used to analyze the intensity of desired protein bands (determined by appropriate ladder size) across different wells/treatments. The raw values obtained from imagej were analyzed as follows, for the sample protein BTK. For proteins with activated counterparts e.g. phosphorylated/activated BTK (p-BTK), the values

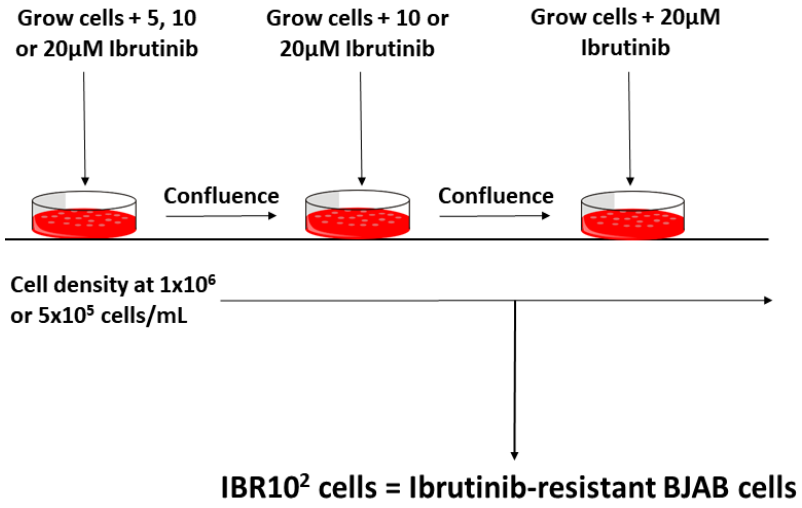


Figure vi. Schematic of the creation of an ibrutinib-resistant BJAB cell line. BJAB cells were treated with 5, 10 or 20µM ibrutinib in sequential order (for cells starting at 5 and 10µM), while cell density was manipulated at each junction (confluence), generating multiple clones.
Illustration from: http://www.clker.com/cliparts/V/8/M/H/l/F/cho-cell-petri-dish-hi.png

obtained from p-BTK are normalized relative to total BTK protein levels (i.e. p-BTK/BTK). In situations where BTK and p-BTK were obtained from different membranes, each protein was normalized to its loading control (Vinculin, VINC) first, before normalizing activated protein to total protein levels (i.e. [p-BTK/VINC1]/[BTK/VINC2]). After normalization for loading and total protein, each value was then normalized to untreated control for each experiment and comparisons made between treatment groups.

Table 3: General information on antibodies and buffers used for protein expression analysis studies.

Antibody/Buffer	Information
P-BTK (Rabbit)	Tyrosine-223 Phosphorylated/activated Bruton's Tyrosine Kinase (p-BTK), 78kDa, Cell Signalling Technologies, Catalog #87141
BTK (Rabbit)	Bruton's Tyrosine Kinase (BTK), 77kDa, Cell Signalling Technologies, Catalog #3533
P-AKT (Rabbit)	Serine-473 Phosphorylated/activated Protein Kinase B (p-AKT), 60kDa, Cell Signalling Technologies, Catalog #9271
AKT (Rabbit)	Protein Kinase B (AKT), 60kDa, Cell Signalling Technologies, Catalog #4691
P-ERK (Rabbit)	Phosphorylated/activated Extracellular signal-Regulated Kinase 1 and 2 (p-ERK1/2) 42/44kDa (Threonine 202/Tyrosine 204), Cell Signalling Technologies, Catalog #4370
ERK (Mouse)	Extracellular signal-Regulated Kinase 1 and 2 (ERK1/2) 42/44kDa, Cell Signalling Technologies, Catalog #9107
VINC (Mouse)	Vinculin (VINC), 120kDa, Abcam, Catalog #ab18058
Lysis buffer	50 mM Tris, 200 mM NaCl, 0.2% NP-40, 1% Tween-20, 1 mM NaF, 1 mM $Na_3VO_4.2H_2O$, 50 mM β-glycerophosphate, 2 mM PMSF, and protease inhibitors
Running buffer	50mM MOPS, 50mM Tris, 1.025mM EDTA, 0.1%SDS
Transfer buffer	25mM TRIS-HCL, 192mM Glycine, 0.03% SDS in 20% methanol
10X TBS-T	20mM Tris, 150mM NaCl, 0.1% Tween 20, pH 7.4

Microarray studies

BJAB and IBR10[2] cells were treated with 5μM ibrutinib, 80μM idelalisib and combination, then incubated for 24 hours for microarray analysis. RNA was extracted from these cells using the Qiagen RNeasy #74134 kit, according to the manufacturer's protocol. Extracted RNA was sent out for processing and Clariom S microarray by ThermoFisher Scientific in the

United States. ThermoFisher's Transcriptome Analysis Console (TAC) Software was used to analyze the expression data, comparing BJAB to IBR10^2 cells.

Data and Statistical analyses

Inhibitor single dose-response curves. Comparisons of inhibitor dose-response curves between BJAB and IBR10^2 cells was done via unpaired two-tailed T-tests at every concentration. P-values were corrected for multiple comparisons using the Holm-Sidak method.

Cell viability/death experiments. Cell viability/death was compared across groups using a two-way ANOVA with Sidak's multiple comparisons tests conducted across all treatment groups and time points for sensitive and resistant cells, with multiplicity-adjusted P-values reported.

Combination index analyses. Combination index (CI) calculations and accompanying analyses were conducted as previously described[182,183].

Protein expression analyses. For every protein analyzed, single agent treatments were compared to combination and untreated controls for sensitive and resistant cells, using a two-way ANOVA with Sidak's correction for multiple comparisons. Multiplicity-adjusted P-values were generated.

For all studies and analyses described above, P-values generated were interpreted at an alpha of 5% ($\alpha = 0.05$), using the GraphPad Prism® 6 software.

Microarray data analysis. The TAC software provides information on each gene/target available in the Clariom S with enough reads for expression analysis in the cells. Information provided include a fold change from BJAB relative to IBR10^2 cells, as well as, pathways in which these targets are players in. The pathway analysis also provides the most important pathways based on count (number of altered targets per pathway) and a Fisher's test-based significance value. TAC conducts a Fisher's Exact Test, using the number of overlapping and non-overlapping genes that

pass the filtering criteria in a pathway, then provides a significance value. The significance value is the negative log base 10 of the p-value ($-Log_{10}$(p-value)) obtained from the Fisher's Exact Test. For reference, a p-value of 0.05 gives a significance value of 1.301; therefore, using an $\alpha<0.05$ significance level, TAC significance values greater than 1.301 were deemed statistically significant. For this thesis, only the analysis of untreated BJABs compared to IBR10[2] cells was conducted. The top 20 BCR pathway/CLL/cancer-related hits based on count were recorded, then these hits were re-analyzed after including a filter for fold change of greater than 1.5 or less than -1.5. For the second analysis, the pathway significance value provided by TAC was also recorded. An unbiased top 20 pathways were also analyzed in like manner.

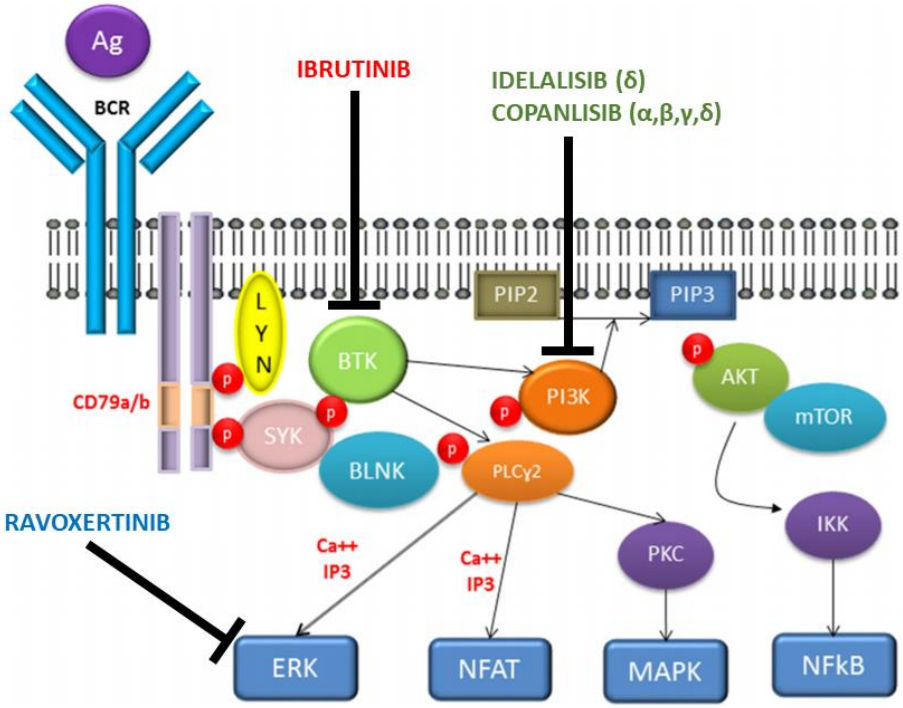


Figure vii. The B-cell receptor pathway highlighting inhibitors used. A simplified schematic of the B-cell receptor pathway highlighting the inhibitors used for the studies conducted. The inhibitors and their targets are as follows: Ibrutinib (BTK), Idelalisib (PI3Kδ), Ravoxertinib (ERK1/2), Copanlisib (PI3Kα, β, δ, γ). Illustration modified from Chavez, J.C., Sahakian, E., & Pinilla-Ibarz, J. (2013). Ibrutinib: an evidence-based review of its potential in the treatment of advanced chronic lymphocytic leukemia. *Core Evidence, 8,* 37 - 45.

RESULTS

IBR10^2 cells have the best resistance profile out of three ibrutinib-resistant BJAB cell lines

As described above, multiple ibrutinib-resistant cell lines were created, but only one could be chosen for further analysis and characterization. This decision was made based on the resistant cell lines readily available for a pilot study. These cell lines were IBR5$^{1/2}$, IBR5^1 and IBR10^2. IBR5$^{1/2}$ are BJAB cells treated with 5μM ibrutinib before exposure to 20μM ibrutinib (at 5x10^5 cells/mL, ½ of 1x^6 cells/mL), IBR5^1 are BJAB cells treated with 5μM ibrutinib once before exposure to 20μM ibrutinib (at 1x^6 cells/mL) and IBR10^2 are BJAB cells treated with 10μM ibrutinib twice before exposure to 20μM ibrutinib (at 1x10^6 cells/mL). The afore-mentioned cell lines were treated with ibrutinib (5 and 20μM) and idelalisib (80μM) for 24 hours, after which cell viability and western blot were performed and compared to sensitive BJAB cells. Strikingly, cell viability data showed IBR5^1 and IBR10^2 having a distinct, more resistant profile compared to IBR5$^{1/2}$, which had a viability profile closer to BJAB cells (Figure 1B). The percentage of cells alive after 20μM ibrutinib treatment were 56% (BJAB), 54% (IBR5$^{1/2}$), 87% (IBR5^1) and 93% (IBR10^2; Figure 1B). These responses clearly showcased IBR10^2 cells as the most resistant to ibrutinib; idelalisib treatment was included in this study to see how the cells responded to another BCR pathway inhibitor. IBR10^2 cells had the highest percentage of cells alive after 80μM idelalisib treatment (65%), although, the differences between all four cell lines was lower (≤18%) compared to their responses to ibrutinib (≤39%; Figure 1B).

Western blot analysis of BCR pathway proteins in the three ibrutinib-resistant cell lines above supported the cell viability data reported. As expected, only BJAB cells expressed p-BTK, which was completely inhibited by ibrutinib at both concentrations, with idelalisib having

virtually no effect on ibrutinib signalling (Figure 1A). Analysis of p-AKT signalling showed an increase in baseline AKT phosphorylation in IBR5[1] and IBR10[2] cells but reduced AKT activation at baseline in IBR5[1/2] cells.

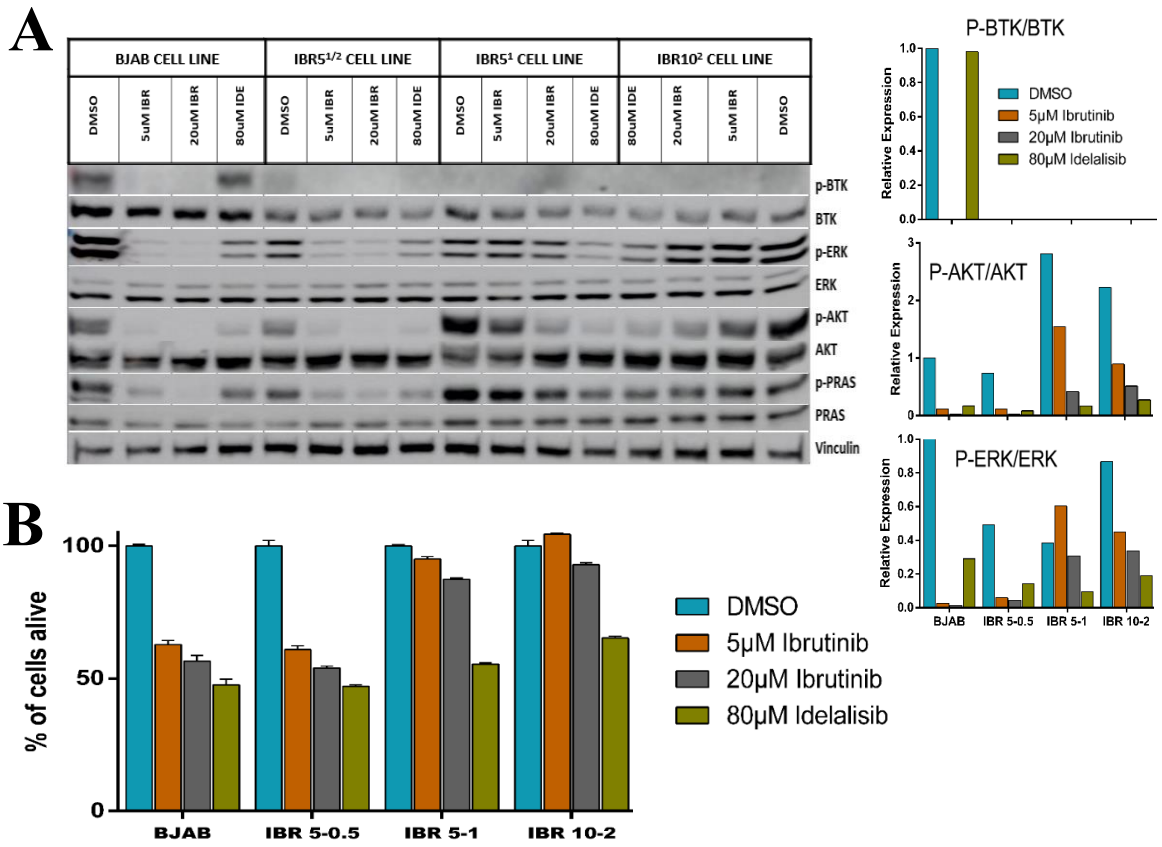


Figure 1. IBR10[2] cells are most resistant to ibrutinib and idelalisib treatment. A. Effect of BTK and PI3Kδ inhibition on sensitive (BJAB) and ibrutinib-resistant (IBR5[1/2], IBR5[1] and IBR10[2]) BJAB cells. Sensitive and resistant cells were treated with ibrutinib (5 and 20μM) and 80μM idelalisib for 24 hours, then run on a western blot. For densitometry, all values were normalized to BJAB DMSO; N=1. **B.** Cell viability data for the experiment described in (A). N=1, n=3, error bar = mean ± SEM. Cell line responses were normalized to their respective DMSO.

Furthermore, IBR10[2] cells were most resistant to AKT inhibition as they start lower than IBR5[1] cells (highest baseline AKT activation), but are inhibited to a lower extent after idelalisib use (Figure 1A). At the level of p-ERK, all three resistant cell lines had lower levels of ERK

activation at baseline, compared to sensitive cells (Figure 1A). However, IBR5$^{1/2}$ cells had the lowest levels of ERK phosphorylation at baseline, and IBR10^{2} cells had the most. Importantly, after inhibitor use, IBR10^{2} cells maintained higher levels of ERK signalling compared to IBR5$^{1/2}$ and IBR5^{1} cells. Together, the cell viability and western blot data suggested that IBR10^{2} cells had the best resistance profile because they were most resistant to cell death and BCR pathway inhibition at the p-AKT and p-ERK levels.

IBR10^{2} cells are resistant to B-cell receptor pathway inhibition

BJAB and IBR10^{2} cells were treated with inhibitors of the B-cell receptor (BCR) pathway for 72 hours and compared to respective untreated cells. The inhibitors used and their targets are as follows: ibrutinib (BTK), idelalisib (PI3Kδ), copanlisib (PI3K α,β,δ,γ) and ravoxertinib (ERK1/2). For ibrutinib treatment, IBR10^{2} cells were completely resistant to cell death relative to BJAB cells, for every concentration evaluated (Figure 2A). The EC_{50} for ibrutinib at 72 hours was 1.6μM for BJABs and 20.6μM for IBR10^{2} cells ($p<0.001$; Figure 2A). Ravoxertinib treatment resulted in a similar trend as IBR10^{2} cells had a higher EC_{50} (23.8μM) than BJAB cells (7.98μM; Figure 2C). Specifically, the difference in cell death response was larger at higher concentrations ($p<0.0001$) than at lower concentrations ($p<0.01$) investigated (Figure 2C). Although IBR10^{2} cells displayed higher EC_{50} values overall, the difference in EC_{50} (ΔEC_{50}) was lower ($0.49\mu M \leq \Delta EC_{50} \geq 0.04\mu M$) with PI3K inhibitor treatment relative to ibrutinib and ravoxertinib ($19\mu M \leq \Delta EC_{50} \geq 15.8\mu M$; Figure 2A, B). For idelalisib, the EC_{50} for IBR10^{2} and BJAB cells were 7.12μM and 6.63μM respectively, with statistical significance achieved only at 2.5μM ($p = 0.002$; Figure 2B). Copanlisib treatment led to statistically significant differences in cell death at 0.025μM and 0.05μM ($p\leq0.0004$), with EC_{50} for BJAB and IBR10^{2} cells of 0.03μM and 0.07μM respectively (Figure 2D). Taken together, the above

results confirm IBR10^2 resistance to BTK signalling (ibrutinib and ravoxertinib resistance), while suggesting a sensitivity of IBR10^2 cells to PI3Kδ inhibition, given the similarity in the dose response curves for idelalisib between sensitive and resistant cells.

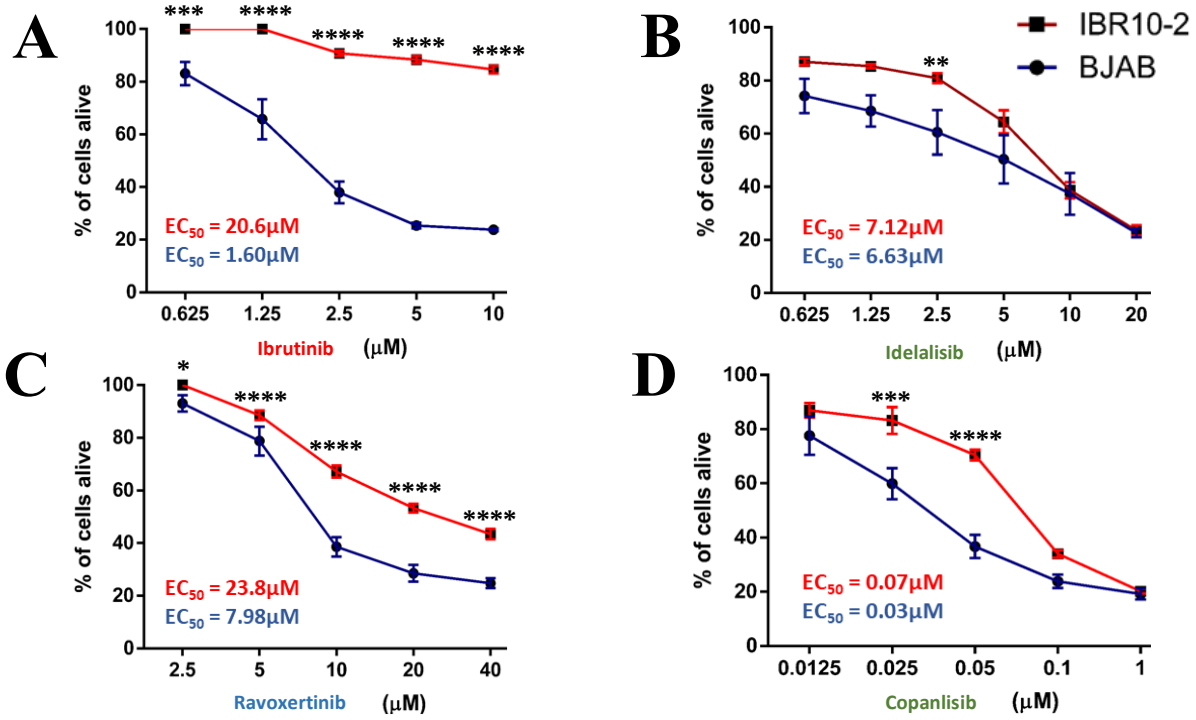


Figure 2. IBR10^2 cells show resistance to B-cell receptor (BCR) pathway inhibitors. Dose-response curves show IBR10^2 resistance to the following BCR pathway inhibitors after 72-hour treatment: **A.** Ibrutinib (BTK), **B.** Idelalisib (PI3Kδ), **C.** Ravoxertinib (ERK1/2), **D.** Copanlisib (PI3Kα, β, δ, γ). 13≤ N ≥3, error bars = mean ± SEM. * = p<0.05, ** = p<0.01, *** = p<0.001, **** = p<0.0001.

The PI3K-AKT pathway is crucial to IBR10^2 and BJAB cell survival

A washout experiment was conducted to investigate the mechanism of resistance and expression levels of BCR pathway proteins in IBR10^2 cells. Woyach et al., 2014 showed in a patient with both the BTK C481S and a PLCγ2 mutation, that ibrutinib treatment did not result in

a reduction of BTK, ERK or PLCγ2 activation; rather, these cells had consistent BCR signalling[171]. IBR10^2 cells cultured at 20μM ibrutinib until confluent were put on ibrutinib-free media and allowed to grow normally for 5 days, with pellets sampled for protein analysis every 24 hours; BJAB cells were also taken at confluence and treated in the same manner then samples from both cell lines were compared to each other. At confluence on 20μM ibrutinib, IBR10^2 cells displayed no p-BTK and identical p-AKT (none) and p-ERK levels as BJAB cells (Figure 3). In contrast, BJAB cells expressed low levels of p-BTK at confluence. In IBR10^2 cells, this baseline changed, with a 100-fold increase in p-AKT at 24 hours, with levels reaching a peak around 200-fold at 48 hours, followed by a decline at 72 hours then a plateau at about the same level as at 24 hours on days 4 and 5 (Figure 3).

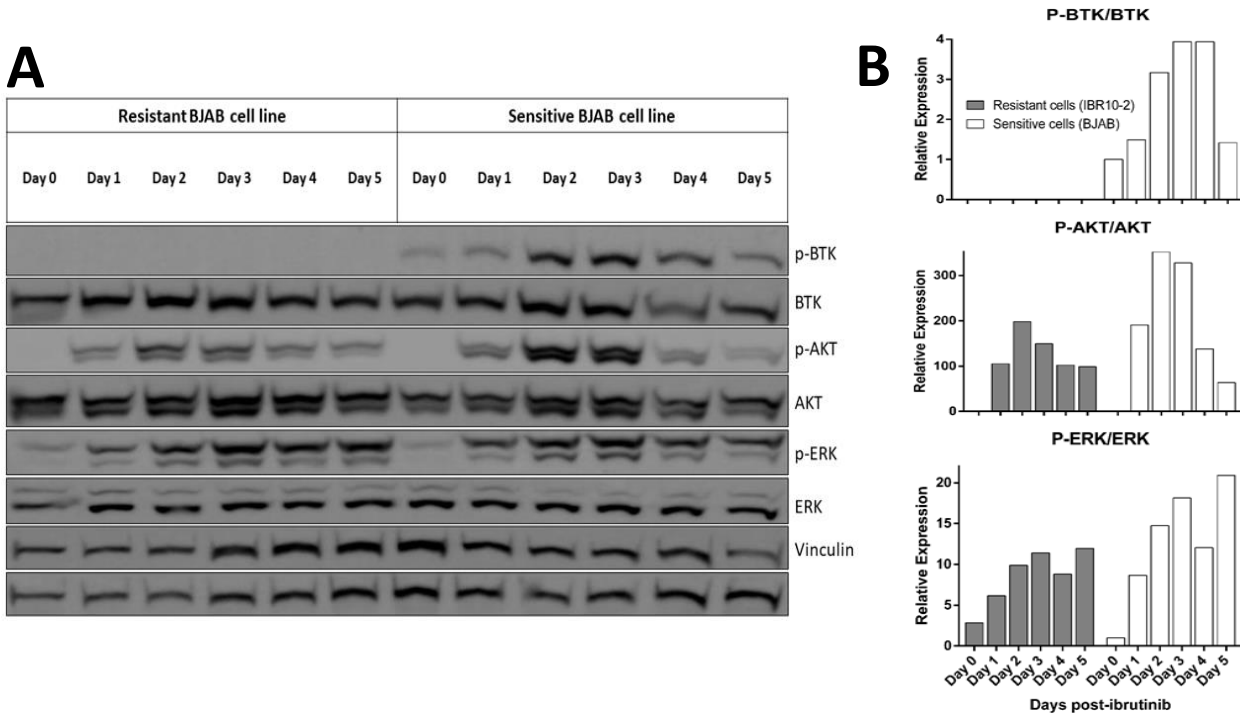


Figure 3. B-cell receptor signalling is downregulated in IBR10^2 cells. A. Baseline BJAB (sensitive) and IBR10^2 (resistant) cell signalling. IBR10^2 cells were cultured at 20μM ibrutinib till confluence then resuspended in ibrutinib-free media for 5 days for a western blot. BJAB cells were cultured till confluence then resuspended at the same cell concentration as IBR10^2 cells in fresh media. **B.** Densitometry data for the western blot described in (A). All values were normalized to sensitive BJAB DMSO at day 0, N=1.

BJAB p-AKT followed the same pattern as IBR10^2 cells, albeit with higher levels, but also, p-AKT levels never plateaued in BJABs but decreased continually till the last day, which had expression levels 63.5-fold greater than day 0 (Figure 3). With BJAB day 0 expression as a starting point, p-ERK activation in IBR10^2 cells increased steadily to 11.4 times day 0 levels at 72 hours; after this, p-ERK levels decreased on day 4, then increased again on day 5 to 12-fold day 0 levels (Figure 3). It is important to state that IBR10^2 cells at confluence (day 0) on 20μM ibrutinib expressed 2.85-fold more p-ERK than BJAB cells at confluence. For BJAB cells, p-ERK followed exactly the same pattern as IBR10^2 cells, but at higher expression levels with the day 3 levels being 14.75-fold and day 5 peak of 20.9-fold day 1's (Figure 3). This study provided some support to the dose-response studies suggesting an importance of the PI3K-AKT pathway in IBR10^2 resistance mechanism, given the fact that p-AKT levels plateaued instead of continually decreasing. Also, the p-ERK data adds an important bit of information because it showed that IBR10^2 cells overall, express lower levels of important BCR pathway proteins. However, the findings made above should be interpreted with the knowledge that this is only one repetition.

Taking the above study further, BJAB and IBR10^2 cells were treated with ibrutinib, idelalisib, copanlisib and combinations (ibrutinib-idelalisib, copanlisib-idelalisib) for 24, 48 and 72 hours. Viability and total cell death were measured in these cells relative to untreated BJAB cells at 24 hours. At 24 hours, there were no significant changes in the number of live cells in both BJAB and IBR10^2 cells across all treatments, save for idelalisib single treatment in IBR10^2 cells (29% decrease in viability, $p = 0.03$; Figure 4B). Other results are reported below.

BJAB cells. Single and combination treatments as described above resulted in a minimum 55% increase (90% in copanlisib-idelalisib) in total cell death relative to untreated controls at 24 hours

($p<0.001$ in all cases; Figure 4C). In the untreated control, the number of viable BJAB cells increased sequentially from 24 to 72 hours ($p<0.0001$), while total cell death was stable from 24 to 48 hours, and decreased by 27% at 72 hours (non-significant, n.s.; Figure 4A, C). Ibrutinib treatment blunted the increase in cell viability from 24 to 48 hours four-fold ($p<0.0001$), while resulting in a daily increase in total cell death from 24 to 72 hours ($p<0.0001$ for all comparisons; Figure 4A, C). There was no change in viability from 48 to 72 hours in ibrutinib-treated BJAB cells. With idelalisib treatment, there was no increase in the number of live BJAB cells at 24 and 48 hours; the number of live cells increased slightly at 72 hours, albeit to 51% below untreated cells at 72 hours ($p<0.0001$; Figure 4A). Idelalisib treatment resulted in a 38% increase in total cell death from 24 to 48 hours ($p = 0.021$); however, total cell death decreased 55% from 48 to 72 hours on idelalisib ($p<0.0001$), consistent with the increase in live cells (Figure 4C).

Similar to idelalisib treatment, there was a 30% reduction in the number of live BJAB cells from 24 to 48 hours ($p = 0.0012$) and a 50% increase in live cells from 48 to 72 hours ($p<0.0001$) with copanlisib treatment (Figure 4A). Furthermore, BJAB cells treated with copanlisib experienced an 83% increase in total cell death from 24 to 48 hours ($p<0.0001$) and total cell death remained unchanged from 48 to 72 hours (Figure 4C). The ibrutinib-idelalisib combination resulted in a 43% reduction in the number of live BJAB cells from 24 to 48 hours ($p<0.0001$) and an 8% further reduction from 48 to 72 hours (n.s.; Figure 4A). At 72 hours, the ibrutinib-idelalisib combination reduced BJAB cell viability by 8% (n.s.) and 120% ($p<0.0001$) relative to ibrutinib and idelalisib single treatments, respectively (Figure 4B). Also, ibrutinib-idelalisib combination increased total BJAB cell death by 113% from 24 to 48 hours and 115% from 48 to 72 hours ($p<0.0001$). At 72 hours, ibrutinib-idelalisib combination resulted in 100%

and 250% more total cell death compared to ibrutinib and idelalisib alone respectively, in BJAB cells ($p<0.0001$; Figure 4B).

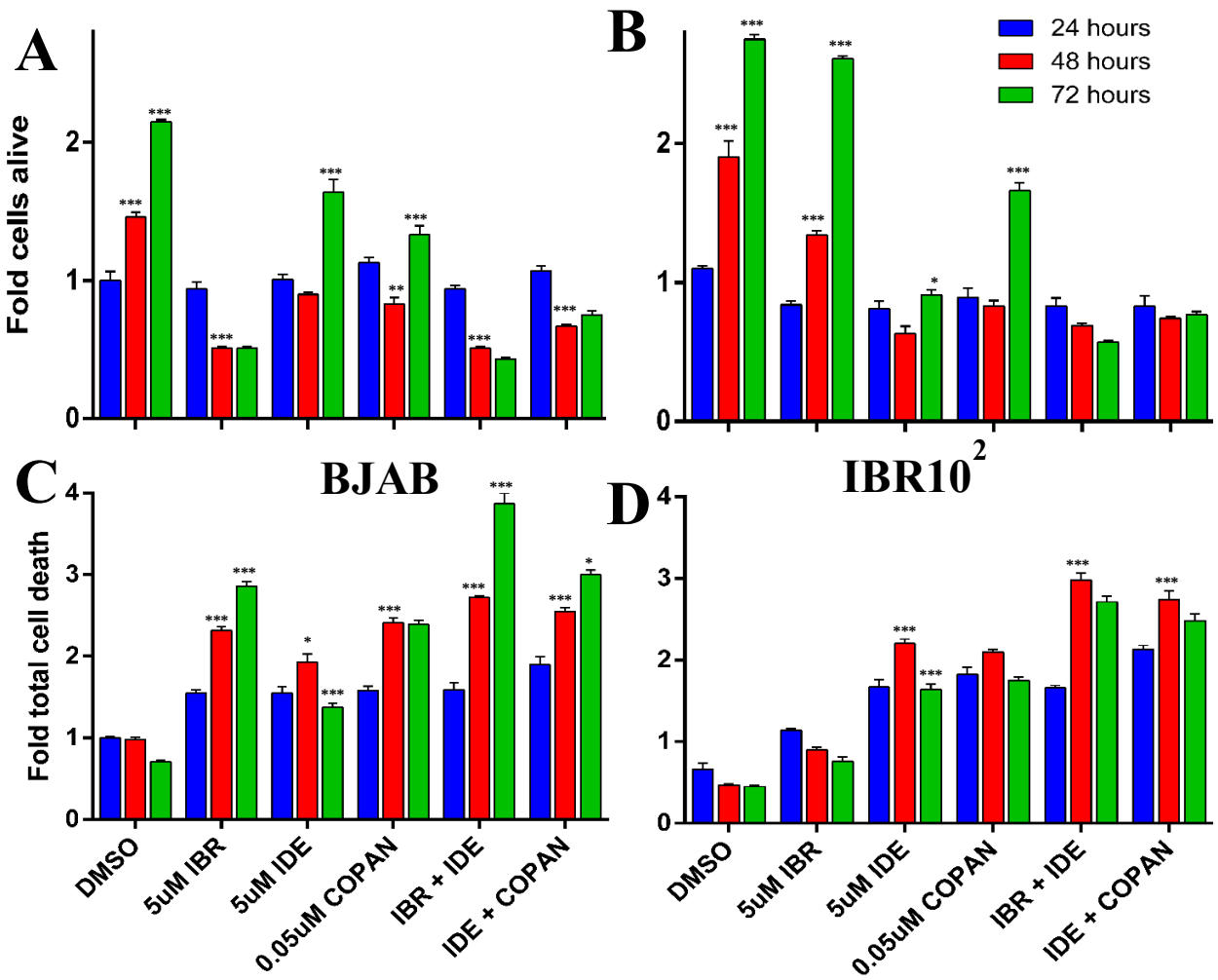


Figure 4. IBR10^2 cells rely on the PI3K-AKT pathway for survival. BJAB and IBR10^2 cells were treated with ibrutinib (IBR), idelalisib (IDE) and copanlisib (COPAN) alone and in combination for 24, 48 and 72 hours. Cell viability in BJAB **(A)** and IBR10^2 cells **(B)** and total cell death after treatment in BJAB **(C)** and IBR10^2 cells **(D)** are reported. All treatments were normalized to untreated BJAB cells at 24 hours. Error bars = mean ± SEM. * = $p<0.05$, ** = $p<0.01$, *** = $p<0.001$, **** = $p<0.0001$, for every bar compared to the time point before it.

The cellular responses to the single agents in each combination was compared to the combination effect at every time point, in order to show the benefit (if any) of combination treatment relative to single agents. Ibrutinib-idelalisib combination induced 7% (n.s.), 39% and

121% ($p<0.0001$) more reduction in the number of live BJAB cells at 24, 48 and 72 hours respectively, relative to idelalisib treatment alone (Figure 4A). In contrast, ibrutinib-idelalisib combination did not exert any additional benefit compared to ibrutinib treatment at any time point. Total cell death was increased by 4% (n.s.), 40% ($p = 0.011$) and 101% ($p<0.0001$) relative to ibrutinib single treatment at 24, 48 and 72 hours, respectively (Figure 4C). Relative to idelalisib, ibrutinib-idelalisib combination increased total cell death by 4% (n.s.), 79% and 249% ($p<0.0001$) at 24, 48 and 72 hours, respectively (Figure 4C). Copanlisib-idelalisib combination decreased BJAB cell viability by 6% (n.s.), 16% (n.s.) and 58% ($p<0.0001$) relative to copanlisib alone at 24, 48 and 72 hours respectively (Figure 4A). Compared to idelalisib alone, copanlisib-idelalisib reduced BJAB cell viability by 6% (n.s.), 23% ($p = 0.045$) and 89% ($p<0.0001$) at 24, 48 and 72 hours respectively (Figure 4A).

Total cell death was further increased by copanlisib-idelalisib combination relative to copanlisib alone by 32% (n.s.), 14% (n.s.) and 61% ($p<0.0001$) at 24, 48 and 72 hours respectively (Figure 4C). Increases of 35% ($p=0.054$), 62% and 162% ($p<0.0001$) were observed in total cell death with copanlisib-idelalisib combination compared to idelalisib treatment alone at 24, 48 and 72 hours respectively (Figure 4C).

In summary, the above results show that ibrutinib induces cell death in BJAB cells in a time-dependent manner. Also, BTK-PI3K inhibition resulted in significant cell death compared to either agent alone at 48 and 72 hours, highlighting a combination effect that may be synergistic or additive in nature.

IBR10^2 cells. In the study described above for BJAB cells, the number of live untreated IBR10^2 cells increased approximately 80% every day from 24 to 72 hours ($p<0.0001$) and total cell death remained constant during this time period (Figure 4B). At 24 hours, single and combination

treatments induced a minimum of 48% increase in total cell death (range 48% to 147%; $p<0.001$) relative to untreated controls, with copanlisib-idelalisib treatment inducing the most increase in cell death (Figure 4D). Importantly, the number of live IBR10^2 cells increased by a minimum of 50% every day from 24 to 72 hours ($p<0.0001$), while total cell death did not change significantly during the same period with ibrutinib treatment (Figure 4B). With idelalisib treatment, IBR10^2 cell viability reduced non-significantly from 24 to 48 hours, and rebounded to approximately baseline at 72 hours ($p=0.046$; Figure 4B). Idelalisib increased IBR10^2 total cell death by 53% from 24 to 48 hours ($p=0.0002$) and cells recover 56% from 48 to 72 hours ($p<0.0001$; Figure 4D).

The number of live IBR10^2 cells after copanlisib treatment did not change from 24 to 48 hours, then increased 83% from 48 to 72 hours ($p<0.0001$; Figure 4B). Copanlisib treatment did not result in any significant changes in the number of dead IBR10^2 cells over time, although, total IBR10^2 cell death relative to untreated control at 24 hours was 116%, 140% and 109% greater with copanlisib at 24, 48 and 72 hours respectively ($p<0.0001$; Figure 4D). In order to best outline the effects of combination treatments, total cell death relative to single agents alone will be reported. Relative to single treatment, ibrutinib-idelalisib combination resulted in 52%, 208% and 195% more cell death than ibrutinib ($p \leq 0.0002$) and 1% (n.s.), 78% and 107% ($p<0.0001$) more cell death than idelalisib alone at 24, 48 and 72 hours respectively (Figure 4D). Likewise, relative to single agent treatment at 24, 48 and 72 hours, copanlisib-idelalisib combination induced 31% (n.s.), 64% and 73% ($p<0.0001$) more cell death than copanlisib and 46%, 54% and 84% ($p \leq 0.0017$) more cell death than idelalisib alone respectively (Figure 4D). Finally, apart from 24 hours where copanlisib-idelalisib treatment resulted in 47% more total cell

death ($p = 0.0012$), ibrutinib-idelalisib and copanlisib-idelalisib combination treatments resulted in approximately the same amount of total cell death (Figure 4D).

Taken together, the above results confirm $IBR10^2$ resistance by showing an increase in viable cells over time on ibrutinib, but also outline $IBR10^2$ sensitivity to PI3K inhibition. In addition, $IBR10^2$ cells were shown to be extremely sensitive to ibrutinib-idelalisib and copanlisib-idelalisib combinations, suggesting that an additive or synergistic effect is occurring.

PI3K inhibitors sensitize $IBR10^2$ cells to ibrutinib treatment

Synergy-antagonism analyses

Given the cell death and viability results from the time course experiments above, the specific relationship observed in ibrutinib-idelalisib, ibrutinib-copanlisib and copanlisib-idelalisib combination treatments were investigated further using synergy-antagonism studies. For these studies, BJAB and $IBR10^2$ cells were treated with varying concentrations of ibrutinib, idelalisib and copanlisib in dose-response grids for 72 hours and synergism, antagonism or additivity was determined relative to single agent dose-response curves, using the Loewe synergy model. Firstly, although the ibrutinib dose-response scales were four-fold different, the same range of concentrations was used for idelalisib in both BJAB and $IBR10^2$ cells (Figure 5A). When combined, ibrutinib and idelalisib were slightly synergistic in BJAB cells, but in $IBR10^2$ cells, idelalisib at low concentrations (1.25µM) completely sensitized the cells to ibrutinib treatment, resulting in more than 50% cell death ($p<0.05$) at 5µM ibrutinib (normal EC_{50} = 20.6µM, Figure 5A, B).

Similarly, ibrutinib-copanlisib combination was mildly synergistic in BJAB cells but significantly synergistic in $IBR10^2$ cells, with 5µM ibrutinib killing more than 50% of cells when combined with 25nM copanlisib ($p<0.05$; Figure 5A, B).

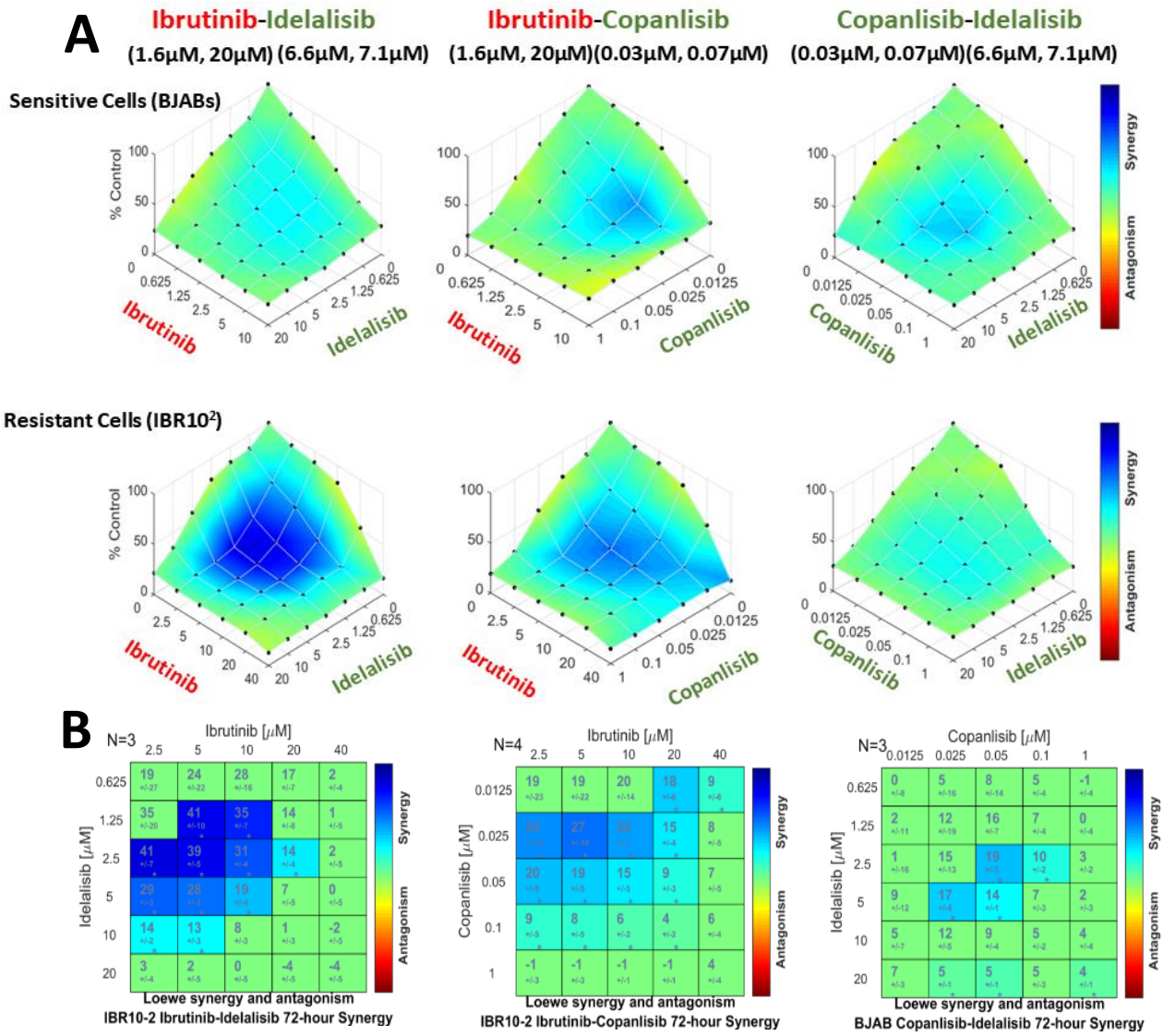


Figure 5. IBR10^2 cells are sensitive to PI3K inhibitor treatment. A. Synergy-antagonism analyses of the effect of BTK-PI3Kδ and pan-PI3K-PI3Kδ inhibition on BJAB and IBR10^2 cells. BJAB and IBR10^2 cells were treated with the specified ranges of the different B-cell receptor pathway inhibitors (ibrutinib, idelalisib and copanlisib) for 72 hours. Brackets indicate drug EC_{50} for (sensitive, resistant) cells. **B.** Combenefit-generated Loewe synergy-antagonism matrices of significant concentration combinations of inhibitors investigated in (A). 4≤ N ≥3 for all combinations. * = p<0.05, ** = p<0.01.

Finally, copanlisib-idelalisib combination was investigated in both BJAB and IBR10^2 cells. Copanlisib-idelalisib combination was more synergistic in cell killing in BJAB than in

IBR10^2 cells, although, the most significant synergistic relationship was observed with ibrutinib-idelalisib combination in IBR10^2 cells (Figure 5A). It is important to state that for every combination reported above, antagonism was expected, not additivity nor synergy, given previous data in our laboratory, using patient-derived CLL cells.

Protein expression analyses of BCR signalling

To explain the above findings, protein analyses via western blot were performed to assess the BCR signalling events resulting in the observed synergy in BJAB and IBR10^2 cells. BJAB and IBR10^2 cells were treated with ibrutinib, idelalisib, copanlisib and combinations (ibrutinib-idelalisib, ibrutinib-copanlisib and copanlisib-idelalisib) for 48 hours. The 48-hour time point was chosen because synergistic cell death was observed at 72 hours; therefore, relevant signalling events should be observed 24 hours prior, before the cells die. BTK, AKT and ERK activation levels were the focus on these analyses, given the inhibitors in use. Protein analyses showed that all inhibitors led to reductions in their target proteins p-BTK (ibrutinib) and p-AKT (idelalisib, copanlisib) in BJAB cells (Figure 6A). For p-AKT, idelalisib and copanlisib treatment resulted in 40-50% lower levels relative to control in IBR10^2 cells (n.s.), but only 20-40% in BJAB cells (n.s.), separating these cell lines with respect to PI3K inhibition sensitivity (Figure 6B). Furthermore, ibrutinib-idelalisib combination resulted in 85% and 65% ($p = 0.0002$, 0.0075) greater reduction in p-AKT than ibrutinib and idelalisib alone respectively, in BJAB cells (Figure 6A, B). For IBR10^2 cells, ibrutinib-idelalisib combination resulted in 63% greater reduction in p-AKT than ibrutinib alone ($p=0.011$), but no additional benefit relative to idelalisib single treatment (Figure 6B).

The ibrutinib-copanlisib combination yielded similar results as ibrutinib-idelalisib in BJAB cells, leading to 71% and 29% ($p = 0.0027$, n.s.) greater reduction in p-AKT than ibrutinib

and copanlisib alone, respectively (Figure 6A, B). In IBR10^2 cells, ibrutinib-copanlisib combination induced 64% and 5.6% (p = 0.0089, n.s.) more reduction in p-AKT than ibrutinib and copanlisib single treatments, respectively (Figure 6A, B). Finally, there was additional benefit in reducing AKT activation with the combination of idelalisib and copanlisib for both BJAB and IBR10^2 cells, but the results did not reach statistical significance.

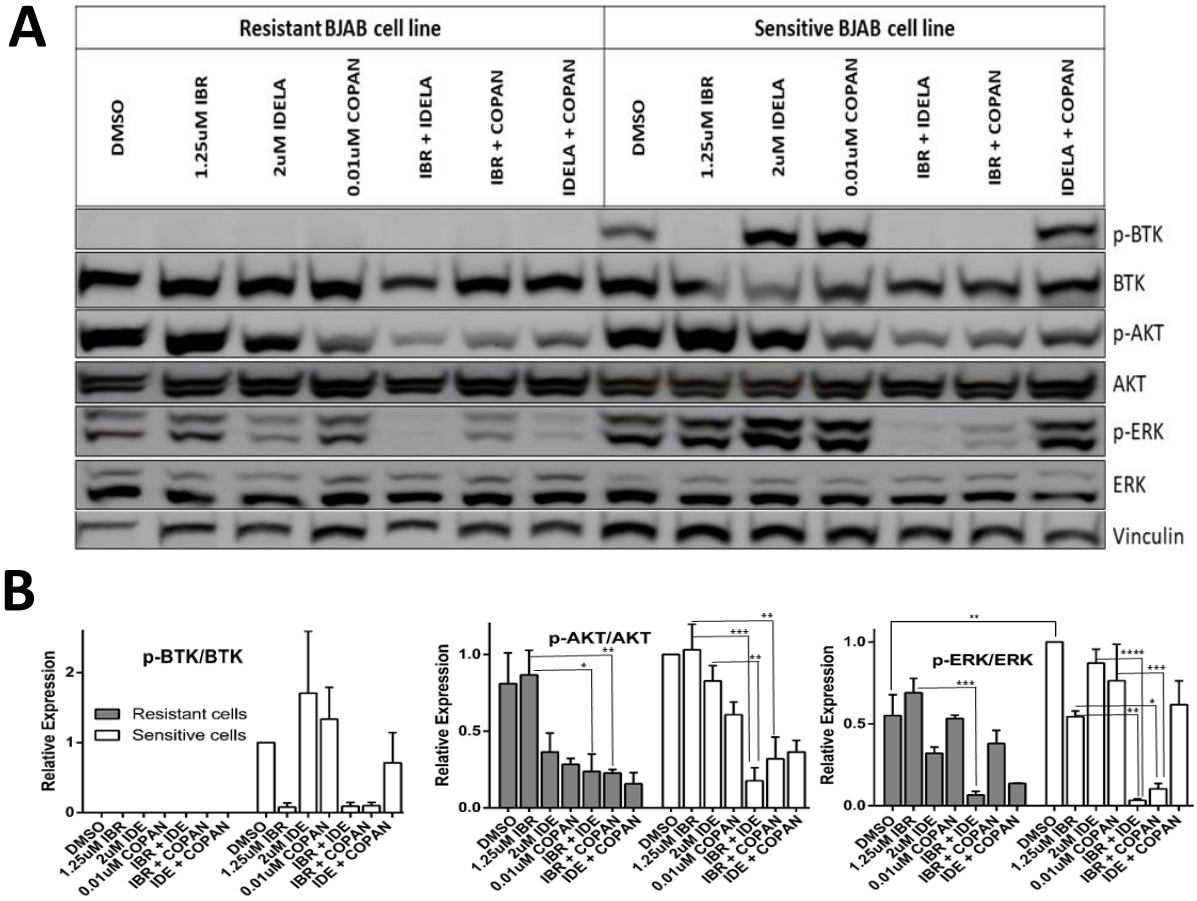


Figure 6. Ibrutinib-idelalisib combination inhibits ERK activation in BJAB and IBR10^2 cells. A. Effect of BTK-PI3Kδ and pan-PI3K-PI3Kδ inhibition on BJAB and IBR10^2 cells. BJAB (sensitive) and IBR10^2 (resistant) cells were treated with 1.25μM ibrutinib (IBR), 2μM idelalisib (IDELA), 0.01μM copanlisib (COPAN) and combination for 48 hours for a western blot. **B.** Densitometry data for the western blot described in (A). All values were normalized to sensitive BJAB DMSO, N=3, error bars = mean ± SEM. * = p<0.05, ** = p<0.01, *** = p<0.001, **** = p<0.0001.

Since ERK activation is important to both BTK and PI3K signalling, p-ERK levels were also assessed. Notably, IBR10^2 cells displayed 45% less baseline activation of ERK ($p = 0.001$) compared to BJAB cells, consistent with an absence of BTK signalling (Figure 6B). Ibrutinib treatment resulted in a 46% reduction in p-ERK in BJAB cells ($p = 0.025$), but had no effect on IBR10^2 cells (Figure 6B). Importantly, idelalisib and copanlisib single treatment did not induce any significant reductions in p-ERK for both BJAB and IBR10^2 cells. However, ibrutinib-idelalisib combination led to 51% and 84% ($p = 0.0084$, $p<0.0001$) greater reduction in p-ERK relative to ibrutinib and idelalisib single treatments respectively, in BJAB cells (Figure 6A, B). In IBR10^2 cells, ibrutinib-idelalisib combination induced 62% and 25% ($p = 0.0007$, n.s.) more reduction of p-ERK compared to ibrutinib and idelalisib alone, respectively (Figure 6A, B).

The ibrutinib-copanlisib combination induced a 44% and 66% ($p = 0.036$, 0.0003) greater reduction in p-ERK relative to ibrutinib and copanlisib alone respectively, in BJAB cells (Figure 6). Surprisingly, ibrutinib-copanlisib did not confer any statistically significant additional benefit in p-ERK reduction compared to single agents in IBR10^2 cells. Lastly, idelalisib-copanlisib combination did not result in any significant reductions in p-ERK in comparison to the single agents alone in either cell line (Figure 6). Collectively, the above data offer some insight into the observations previously made in cell death and synergy studies, showing a combined effect especially with ibrutinib-idelalisib combination, in both BJAB and IBR10^2 cells in BCR pathway protein activation. Additionally, these results highlight an important cellular event at the centre of the observed differences between BJAB and IBR10^2 response to PI3K inhibition: ERK activation.

BTK and PI3K-AKT signalling terminate with ERK activation in BJAB cells

ERK activation was shown to be important to BJAB and IBR10^2 cell survival; hence, ibrutinib, idelalisib and copanlisib were combined with the ERK inhibitor ravoxertinib for 72 hours. Antagonism was expected in all combinations for both cell lines.

Synergy-antagonism analyses

As hypothesized based on the findings in figure 6, in BJAB cells, a combination of ravoxertinib and idelalisib was strongly antagonistic. In contrast, IBR10^2 cells only displayed minor antagonism and surprisingly, synergy at certain concentration combinations, which allowed more than 50% of cells to be killed at 10µM ravoxertinib (normal EC_{50} = 23.8µM) in combination with only 0.625µM idelalisib ($p<0.05$; Figure 7B). Combining ravoxertinib with copanlisib resulted in strong antagonism in BJAB cells as well, and like with idelalisib, this antagonism was greatly reduced in IBR10^2 cells, which also displayed synergy. Ravoxertinib-copanlisib combination was antagonistic at lower concentrations of ravoxertinib (5µM, $p<0.05$) but synergistic at other concentrations ($p<0.05$, Figure 7B). Lastly, ravoxertinib combined with ibrutinib was strongly antagonistic in BJAB cells, but also the most antagonistic combination in IBR10^2 cells (Figure 7A). Once again, low concentrations of ravoxertinib (5µM, $0.05<p<0.01$) were antagonistic with ibrutinib, while 80µM ravoxertinib was synergistic with all concentrations of ibrutinib ($0.05<p<0.01$); however, given the high concentration, the observed synergy might be ERK-independent (Figure 7B). Taken together, the above results confirm ERK as a common effector protein in the BTK and AKT pathways in BJAB cells, but show a biphasic effect when ERK is inhibited along with upstream BCR proteins BTK and AKT in IBR10^2 cells, warranting further investigation into relevant signalling events.

Protein expression analyses

Ravoxertinib combined with ibrutinib, idelalisib and copanlisib was shown above to be biphasic in synergy-antagonism studies; therefore, protein analysis via western blot was performed to assess signalling changes responsible for this effect. Unfortunately, a sufficient number of experiments could not be completed to confidently investigate this question.

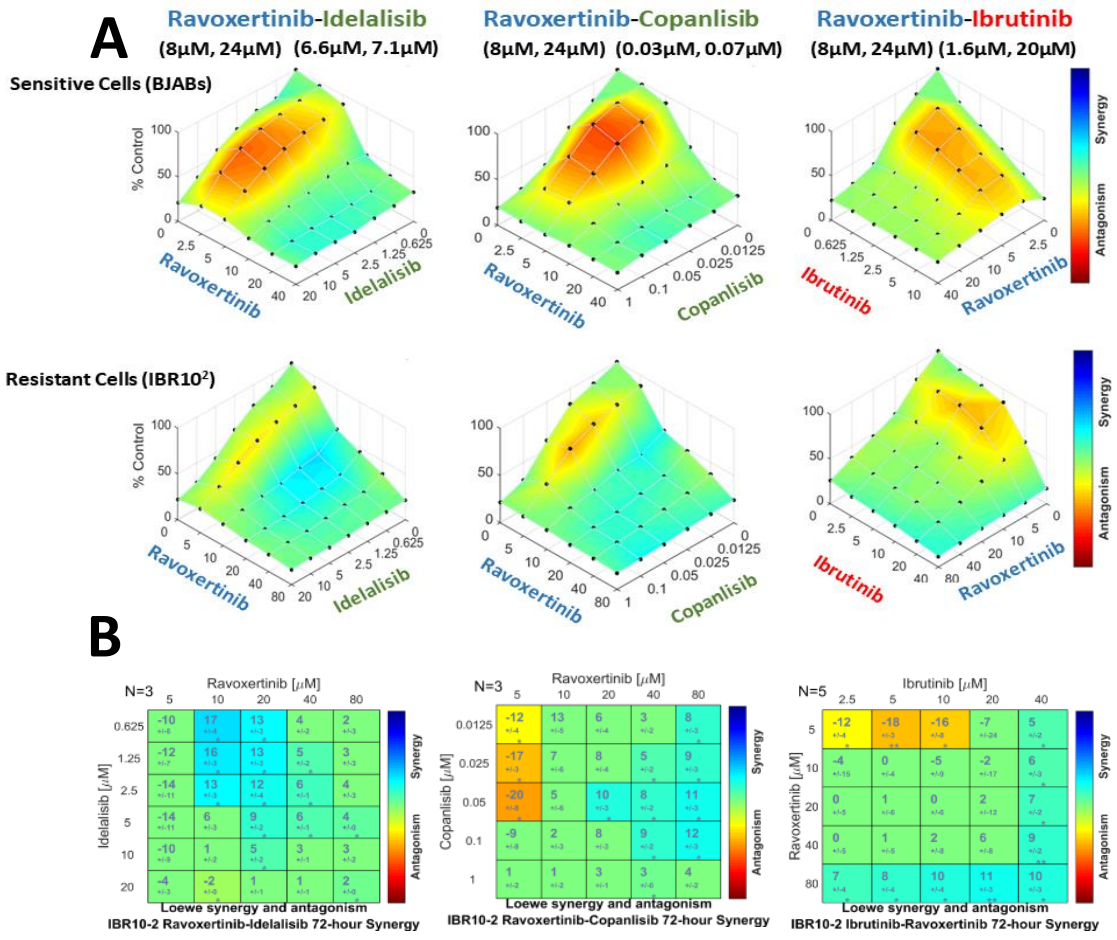


Figure 7. Inhibition of ERK activation is biphasic in IBR10^2 cells. A. Synergy-antagonism analyses of the effect of ERK-PI3Kδ, ERK-pan-PI3K, and BTK-ERK inhibition on BJAB and IBR10^2 cells. BJAB and IBR10^2 cells were treated with the specified ranges of the different B-cell receptor pathway inhibitors (ravoxertinib, ibrutinib, idelalisib and copanlisib) for 72 hours. Brackets indicate drug EC_{50} for (sensitive, resistant) cells. **B.** Combenefit-generated Loewe synergy-antagonism matrices of significant concentration combinations of inhibitors investigated in (A). 5≤ N ≥3 for all combinations. * = p<0.05, ** = p<0.01.

Idelalisib-ibrutinib/copanlisib combination leads to cooperative cell death in CLL cells

Results obtained above were cell line-based, so freshly isolated CLL patient cells were needed to investigate the relevance of the current model of ibrutinib resistance. Initial studies with all patient cells examined showed an expected pattern: upon stimulation with CD40L/IL-4, CLL cells become completely resistant to the PI3K-AKT pathway inhibitors idelalisib and copanlisib (data not shown). However, in order to mimic the CLL microenvironment *in vivo*, all results reported below were obtained from stimulated cells. The combination of all patient cells used showed an inability of idelalisib and copanlisib to kill 100% of cells, even at high concentrations (Figure 8A). On the other hand, ibrutinib treatment resulted in sufficient cell death at the concentrations used, irrespective of stimulation. To investigate the findings made with the IBR10^2 cell line, CLL cells were treated with idelalisib in combination with ibrutinib or copanlisib. Since it was determined in Figure 6 that PI3Kδ was important to IBR10^2 survival as seen with ibrutinib-idelalisib combination, and given the limited availability of patient samples, the ibrutinib-copanlisib combination was not investigated in CLL cells.

Preliminary studies combining the above three agents showed a greater combined effect with idelalisib-ibrutinib/copanlisib combinations. Moreover, the combined effect was greater at concentrations where idelalisib single treatment resulted in more cell death (Figure 8B). Specifically, when combined with 10μM ibrutinib, 100μM and 200μM idelalisib resulted in 58% ($p<0.0001$) and 34% ($p = 0.0198$) more cell death respectively (Figure 8B). Also, 5μM ibrutinib combined with 200μM idelalisib resulted in 56% more cell death than ibrutinib alone ($p<0.0001$). Idelalisib-copanlisib combination also yielded promising results in CLL cells. 20μM copanlisib combined with 100 and 200μM idelalisib induced 25% ($p = 0.0045$) and 55% ($p<0.0001$) more cell death respectively, than copanlisib alone (Figure 8B). Furthermore,

addition of 20µM copanlisib to 100 and 200µM idelalisib yielded 27% (p = 0.0005) and 24% (p=0.0037) more cell death respectively, than idelalisib single treatment.

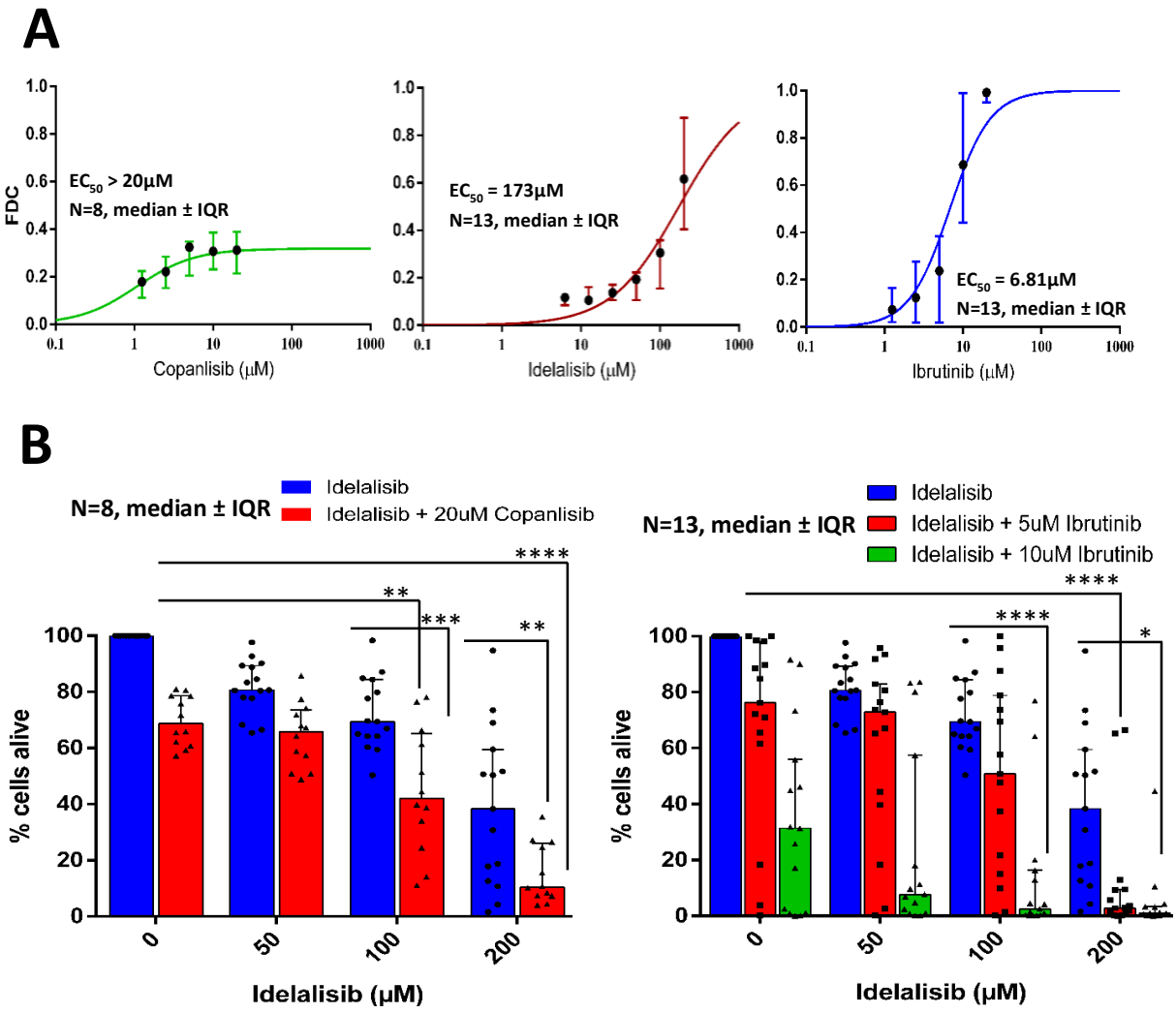


Figure 8. Idelalisib-ibrutinib/copanlisib combination results in greater cell death in CLL cells. A. Combined dose-response curves for copanlisib, idelalisib and ibrutinib. CLL cells were treated with the aforementioned agents for 72 hours. N numbers and error bars specified above. **B.** Effects of idelalisib-copanlisib/ibrutinib combinations in CLL cells. CLL cells were treated with the specified concentrations of idelalisib in combination with copanlisib (20µM) or ibrutinib (5 and 10µM), for 72 hours. N and error bars specified above. FDC: Fraction of dead cells* = p<0.05, ** = p<0.01, *** = p<0.001, **** = p<0.0001.

The preliminary results reported above with idelalisib-ibrutinib/copanlisib combinations on CLL cells show that the findings made with IBR10^2 cell line may be clinically relevant, given the greater cytotoxicity achieved with the combinations. However, the exact nature of the combination effect (synergy or antagonism) cannot be determined from these studies.

Ibrutinib-idelalisib combination leads to synergistic cell death in CLL cells

Further analysis of the results obtained from Figure 8 above, revealed that ibrutinib-idelalisib combination resulted in synergistic cell death in CLL cells. Using the patient cells above, the combination index of two concentrations of ibrutinib over a range of idelalisib was examined. At 50, 100 and 200µM idelalisib, 10µM ibrutinib resulted in a median combination index (CI) of 0.80, 0.70 and 0.52 respectively, suggesting an increasing synergistic effect (Figure 9). Also, 5µM ibrutinib resulted in a median CI of 0.68 and 0.50 at 100 and 200µM idelalisib,

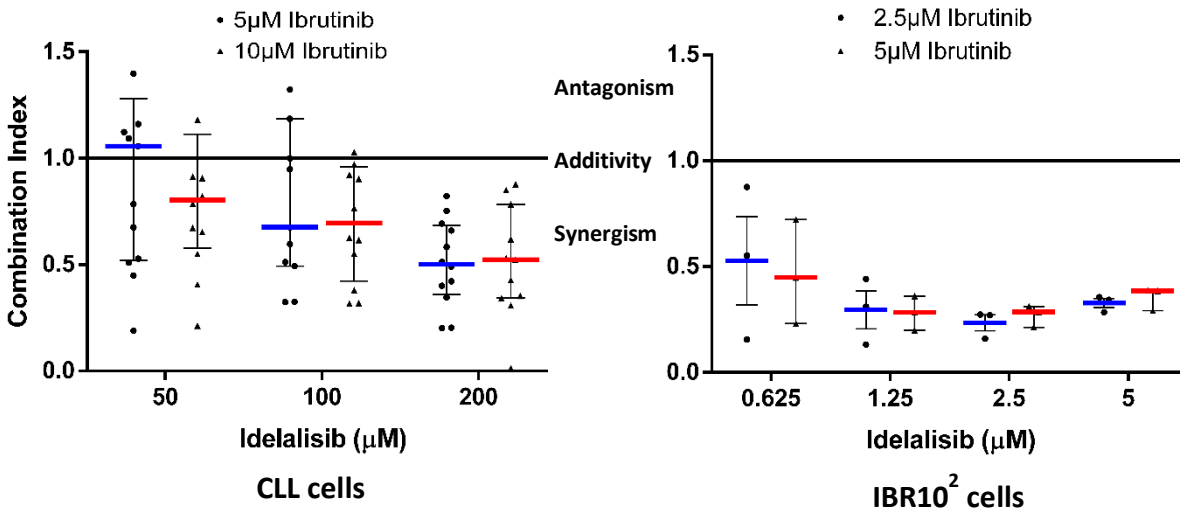


Figure 9. Ibrutinib-idelalisib combination is synergistic in CLL. Graph of median combination index (CI) for ibrutinib-idelalisib combinations in stimulated (CD40L/IL-4) CLL cells, treated for 72 hours at the specified concentrations. 9≥N≤10, blue and red lines = median CI values for 5 and 10µM ibrutinib respectively. Error bars = IQR, CI = 1= additive, CI < 1=synergy, CI>1=antagonism. For comparison, the ibrutinib-idelalisib 72-hour synergy previously reported using the Loewe synergy method, is represented using the CI method (N=3). 8 data points cut off from CLL cell graph (CI>1.5).

respectively. Like with the viability study, the CI decreased with increasing idelalisib concentrations; this is important because the proposed synergy was only evident in CLL cells at concentrations of idelalisib that induced enough cell death as single treatments. Unfortunately, a similar analysis could not be conduced for idelalisib-copanlisib combinations because copanlisib never induced enough cell death for a linear portion of the dose-response curve to be reached. However, the data also suggests synergy, given the magnitude of the effect seen with the combination. For the purposes of having a direct comparison, the most synergistic concentrations of the ibrutinib-idelalisib combination in IBR10[2] cells were also analyzed using the CI method. As expected, the synergistic combinations resulted in CI values well below 1, reaching as low as 0.23 when 2.5µM ibrutinib was combined with 2.5µM idelalisib. Information on the patients whose cells were utilized in the above studies can be found on table 4 below.

Finally, the effect of ibrutinib-idelalisib combination was evaluated in ibrutinib resistant CLL cells in the same manner as described above. There were cells from a total of five ibrutinib-resistant patients; unfortunately, for two of these patients, the individual agents did not meet the isobologram requirement for CI analyses to be conducted by the algorithm used. Therefore, these patient cells were not utilized in the final dose-response curves or CI graphs below (Figure 10 A and C). After removing data for the ibrutinib-treated patients, in all CD40L/IL-4 stimulated patients, there was a shift in the dose-response curves from the previous data; ibrutinib-resistant patients had a higher EC_{50} of 10.69µM compared to 7.12µM for ibrutinib, and for idelalisib, resistant patients' EC_{50} was 224.4µM compared to 136.8µM (NS; Figure 10A).

Ibrutinib-idelalisib combination was also found to elicit a statistically significant increase in cell death in ibrutinib-resistant CLL cells. At 200µM idelalisib, the addition of either 5µM or 10µM ibrutinib resulted in a statistically significant reduction in cell viability by 40% (p=0.007)

and 56% (p=0.0001) respectively (Figure 10B). Also, the addition of 10µM ibrutinib resulted in a significant reduction in cell viability at 50µM and 100µM idelalisib by 64% (p=0.0002) and 65% (p<0.0001) respectively (Figure 10B). On the flip side, the addition of idelalisib only led to statistically significant reductions in cell viability by 72% (p<0.0001) and 53% (p=0.006) at 5µM and 10µM ibrutinib respectively, when combined with 200µM idelalisib (Figure 10B). The above reductions in cell viability with ibrutinib-idelalisib combination translated to synergy with CI analysis in ibrutinib resistant CLL.

Table 4: CLL Patient responses to ibrutinib, idelalisib and copanlisib, with patient information.

Sample	Ibrutinib EC_{50}	Idelalisib EC_{50}	Copanlisib EC_{50}	Age	Gender	RAI stage	WBC	LDT	IGVH	Zap70	FISH	Treatments (before sampling)
1	>20	>300	>20	80	F	RAI 2	106	>12	M	0	del 13q 14.2 (77.6%)	CLB
2	16.672	107.152	>20	68	F	Rai 0	77.5	>12	M	0	no fish	none
3	16.558	108.393	>20	59	M	RAI 4	133	<6	U	6	normal	IB
4	5.61	115.345	>20	72	M	RAI 2	63.4	<12	U	15	del 11 (18.4%), trisomy 12 (43.6%)	FLU, FCR
5	5.365	236.592	>20	69	M	RAI 1	52.1	>12	not done	12	no fish	none
6	2.65	116.681	>20	70	M	RAI 1	35.3	>12	not done	1.35	no fish	none
7	3.286	149.279	>20	63	F	RAI 1	30.8	>12	M	not done	no fish	none
3	0.39	99.312	>20	59	M	RAI 4	123	<6	U	6	normal	IB
8	8.255	121.899	>20	83	M	RAI 4	60.3	>12	M	not done	normal	none
9	9.258	>300	>20	63	M	RAI 2	16.7	<12	U	1	del 11 (24%), del 13q14.3 (49.5%)	FCR, BR + IDE, IB
10	9.953	129.122	>20	62	F	RAI 3	17.5	<12	U	13	normal	RCD, IB
11	7.308	>300	>20	78	M	RAI 3	12.1	<12	U	6	trisomy 12 (47.1%)	FR, FCR, IB
4	6.945	251.768	>20	72	M	RAI 2	109	<12	U	15	del 11 (18.4%), trisomy 12 (43.6%)	FLU, FCR
12	9.561	>300	>20	82	F	SLL	45.6	<6	U	45	del 11 (48%), del 13q14.3 (34%), del 13q 14.3.2 (29%)	IB
13	7.921	294.491	>20	66	M	RAI 1	27	>12	U	not done	no fish	none
Median	7.615µM	121.90µM	>20	69								

FISH: Fluorescence-in-situ hybridization, M: Mutated, U: unmutated, CLB: Chlorambucil, FCR: Fludarabine-cyclophosphamide-rituximab, IB: ibrutinib, IDE: idelalisib, FR: fludarabine-rituximab, BR: bendamustine-rituximab, flu: fludarabine, RCD: rituximab-cyclophosphamide-dexamethasone, WBC: white blood cell count, LDT: lymphocyte doubling time, no fish: FISH not done. Patients are numbered according to sampling date; patient numbers in yellow are patient sampled more than once. NOTE: two ibrutinib-resistant patients are missing from the above list, due to late sampling.

Although the CI analysis from stimulated ibrutinib resistant CLL cells followed a similar trend as ibrutinib-naïve cells, the interquartile range could not be calculated, given the small sample size of three, resulting in larger error bars (Figure 10C).

The PI3K-AKT and MAPK-ERK pathways are altered at the RNA level in IBR10^2 cells

Microarray analysis conducted as detailed in the methods section provided crucial information on changes at the RNA expression level in IBR10^2 cells relative to BJABs. TAC pathway analysis showed that the PI3K-AKT pathway and larger signalling cascades it is connected to, are altered in IBR10^2 cells. Specifically, the RNA expression of targets in these pathways are significantly reduced in these cells. Some of these pathways (in order of decreasing significance) include the JAK-STAT pathway (4.69), Toll-like receptor pathway regulation (3.45), AXL signalling pathway (3.39), IL-4 signalling (2.44), the MAPK-ERK signalling pathway (2.36) and PTEN (phosphatase and tensin homolog) regulation (2.27; Table 5). This data, although only N=1, provides more support for the results presented above on the importance of the PI3K and MAPK-ERK pathways to IBR10^2 cell survival. Specifically, it shows that even though ERK1/2 are not directly inhibited at the RNA level (less than 1.5-fold change), the expression of other targets in that pathway (e.g. MAP3K8 and NF-kB1/2) is reduced. Furthermore, the microarray data provide other pathways that might complete the picture on mechanism (s) driving ibrutinib resistance in IBR10^2 cells. Additionally, although its significance level is lower than all other pathways highlighted above and below, the BCR pathway was identified in the expression analysis as being significantly reduced in IBR10^2 cells relative to BJABs (Table 5). This is of extreme importance because the targets identified not only support the data above but also provide evidence that boosts the probability of the currently proposed mechanism of IBR10^2 cell resistance.

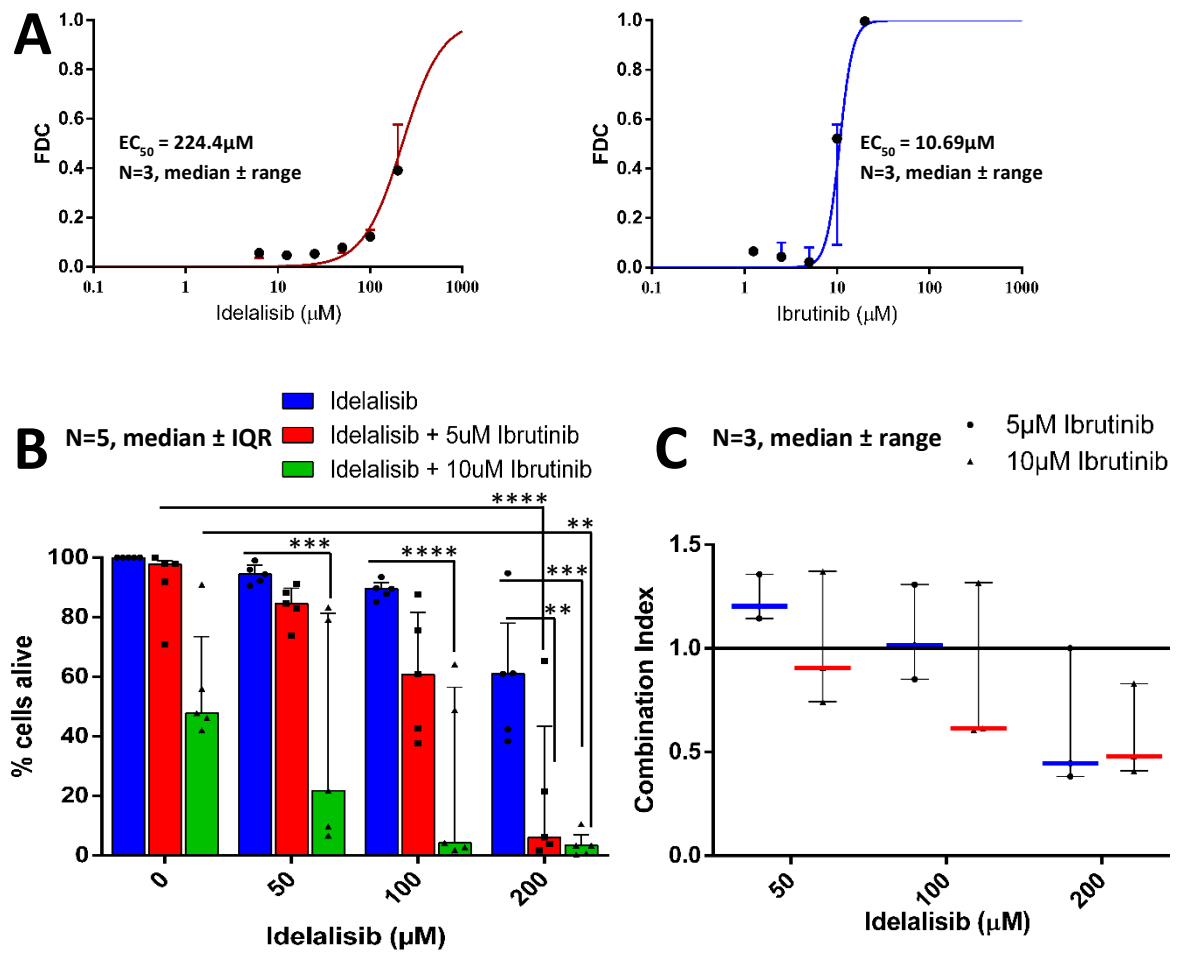


Figure 10. Ibrutinib-idelalisib combination is synergistic in ibrutinib resistant CLL. A. Combined dose-response curves for idelalisib and ibrutinib. CLL cells were treated with the aforementioned agents for 72 hours. N numbers and error bars specified above. **B.** Effects of ibrutinib-idelalisib combination in ibrutinib resistant CLL cells. CLL cells were treated with the specified concentrations of idelalisib in combination with ibrutinib (5 and 10µM) for 72 hours. N number and error bars specified above. **C.** Graph of median combination index (CI) for ibrutinib-idelalisib combinations in stimulated (CD40L/IL-4) ibrutinib resistant CLL cells, treated for 72 hours at the specified concentrations. N=3, blue and red lines = median CI values for 5 and 10µM ibrutinib respectively. Error bars = range, CI = 1= additive, CI < 1=synergy, CI>1=antagonism. FDC: Fraction of dead cells* = $p<0.05$, ** = $p<0.01$, *** = $p<0.001$, **** = $p<0.0001$.

Table 5: Transcriptome analysis console (TAC)-generated pathways of interest obtained from microarray analysis of baseline gene expression in IBR10^2 cells relative to BJABs.

Pathway	Number of targets altered		Targets >1.5 (reduced in IBR10-2)		Targets < -1.5 (increased in IBR10-2)	
	Downregulated	Upregulated	Downregulated	Significance	Upregulated	Significance
JAK/STAT	57	54	16	**4.69**	1	**0.42**
Cell cycle checkpoints	9	8	2	**4.17**	1	**2.9**
Regulation of Toll-like receptor signalling pathway	76	58	17	**3.45**	3	**0.1**
AXL signalling pathway	67	59	15	**3.39**	1	**0.27**
Interactions between immune cells and micro-RNAs in tumour microenvironment	21	9	8	**2.87**	N/A	**N/A**
Autophagy	16	14	6	**2.74**	1	**0.24**
Toll-like receptor signalling related to Myd88	19	11	6	**2.66**	1	**0.23**
TNF-related Weak Inducer of Apoptosis (TWEAK) signalling pathway	22	18	7	**2.57**	N/A	**N/A**
Focal adhesion-PI3K-AKT-mTOR signalling pathway	142	159	25	**2.54**	11	**0.42**
PI3K-AKT signalling pathway	168	171	27	**2.47**	12	**0.39**
IL-4 signalling pathway	31	13	8	**2.44**	N/A	**N/A**
MAPK Signalling pathway	127	118	21	**2.36**	10	**0.61**
PTEN regulation	7	5	1	**2.27**	1	**1.17**
PIP3 activates AKT signalling	7	6	1	**2.26**	N/A	**N/A**
Toll-like receptor signalling pathway	55	47	11	**2.21**	4	**0.27**
Chemokine signalling pathway	80	84	14	**1.68**	5	**0.09**
RANKL/RANK (Receptor Activator of NF-kB) signalling pathway	31	24	6	**1.46**	3	**0.68**
B-cell receptor signalling pathway	55	41	9	**1.35**	2	**0**
NRF2 pathway	80	62	11	**1.18**	2	**0.35**
Integrin-mediated cell adhesion	46	53	8	**1.04**	6	**1.16**
TGF-beta signalling pathway	62	71	10	**1.02**	3	**0**
Cell cycle	46	68	2	**0.74**	1	**0.57**
miR-targeted genes in leukocytes	47	67	10	**0.47**	1	**1.02**
miR-targeted genes in lymphocytes	159	203	24	**0.13**	4	**2.76**
PKC-gamma calcium signalling pathway in ataxia	8	13	1	**0**	4	**2.49**

The top five BCR pathway players identified by the TAC software to be expressed at lower levels in IBR10^2 cells in decreasing order were: CD19 (2.29), FOXO1 (2.22), TEC (2.11), LCK (1.87) and SYK (1.81; Table 6). Of the 9 total targets listed in Table 6, five of them function upstream (CD19) or downstream (FOXO1, MALT1, NFKB1, RPS6KA1) of PI3K-AKT pathway, cementing this pathway as being at the center of IBR10^2 cells' ibrutinib resistance. Of note, the other differentially expressed BCR pathway genes are connected to the regulation of signal initiation. SYK is a major player in initiating the BCR signalling cascade and its expression levels are reduced in IBR10^2 cells. Moreover, LCK and SHP-1 (PTPN6) are involved with SYK regulation and their expression is also reduced in IBR10^2 cells. LCK and SYK inhibition would theoretically reduce overall BCR signalling, but more so BTK-ERK signalling. The reduced expression of SHP-1 is likely related to modifying the BCR signal initiating to match the already reduced expression of SYK, allowing for lower levels of signalling. Altogether, the BCR pathway genes with reduced expression in IBR10^2 cells, highlight changes to BCR pathway initiation, but also to PI3K-AKT signalling. As expected, all the genes related to the PI3K-AKT pathway that appear on this list, are also on the specific list of genes altered within the PI3K-AKT pathway (Table 7).

Other pathways with significantly reduced expression of targets included: cell cycle checkpoints (4.17), autophagy (2.74) and TNF-related weak inducer of apoptosis (TWEAK) signalling pathways (2.57; Table 5). These pathways suggest that downstream PI3K-ERK signalling might not be the only way IBR10^2 cells evade ibrutinib-induced apoptosis. This is because all three pathways listed above are related to cell death and might explain other ways IBR10^2 cells survive at high ibrutinib concentrations.

Just as important, pathways containing targets with increased expression in IBR10^2 cells were observed. Only three pathways achieved statistical significance and they were: cell cycle checkpoints, miR-targeted genes in lymphocytes and the PKC-gamma calcium signalling in ataxia (Table 5). The significant alteration of cell cycle checkpoint highlights it for further study because certain targets were upregulated and others downregulated. Also, it is important to state that PKC activity is crucial to BTK-PLCγ2-ERK1/2 signalling and could add to the current evidence for altered ERK signalling. The above analysis notwithstanding, when analysing all genes with increased IBR10^2 expression, other statistically significant pathways were identified and outlined in Supplementary table 7. Interestingly, with a few exceptions like cell cycle checkpoints and miR-targeted genes, most of these pathways were not as obviously connected to CLL, ibrutinib treatment or the BCR pathway as the reduced pathways were. For this reason, the top 100 genes upregulated in IBR10^2 cells are outlined in Supplementary Table 9 and all 60 genes from pathways identified in Supplementary Table 7 were sorted in Supplementary Table 8 by fold change. Overall, these pathways were essential cellular pathways not unique to CLL or B-cells, such as metabolism, cell cycle regulation and cell-to-cell/cell-to-extracellular matrix communication (Supplementary Table 7). Taken together, the results obtained from the microarray analysis provide support for the cell death/viability and protein expression studies that show a crucial role for the PI3K-AKT and MAPK-ERK pathways in IBR10^2 resistance mechanism. However, the expression data also provide alternative pathways that could individually or in tandem with the PI3K-AKT-ERK pathways, influence IBR10^2 cells response to various BCR pathway inhibitors, including ibrutinib and idelalisib.

Table 6: Genes within the B-cell receptor pathway with reduced expression in IBR10[2] cells relative to BJABs.

Pathway	Overall Significance	Targets	Fold change	Brief description of function/roles in B-cells or otherwise
B-cell receptor (BCR) pathway	**1.35**	CD19	**2.29**	PI3K-AKT signalling; B-cell proliferation, survival[37,184]
		FOXO1	**2.22**	FOXO1 is a transcription factor that plays a role in apoptosis (involved with FasL, TRAIL, transactivates pro-apoptotic protein bim). Involved in cell cycle regulation, inhibited by AKT and ERK[185].
		TEC	**2.11**	Tec-deficient B-cells display enhanced survival, proliferation and p-AKT expression (BTK-dependent), when stimulated with anti-CD40 and rIL-4, compared to wild-type B-cells[186]. TEC and BTK expression levels are also positively correlated in CLL cells[186].
		LCK	**1.87**	LCK mediates SYK phosphorylation and proximal BCR signalling in CLL cells; LCK inhibition or reduction reduces BCR-mediated increases in p-AKT, p-ERK and IKK (IκB kinase) [187]. LCK levels correlate with BCR signal strength in CLL cells[187].
		SYK	**1.81**	BCR signal activation (CD79a/b phosphorylation), amplification and activation of important downstream targets like BTK[37].
		MALT1	**1.69**	MALT1 is a proto-oncogene and the human paracaspase. MALT1 mediates the BCR pathway, downstream of the PI3K-AKT pathway[188]. MALT1 induces NF-kB activation[188].
		NFKB1	**1.68**	NFKB1 translation produces a DNA-binding subunit of the NF-kB complex (p105). The NF-kB pathway is an effector involved in BCR-mediated apoptosis in B-cells[189,190].
		RPS6KA1	**1.64**	RPS6KA1 encodes a ribosomal S6 kinase (RSK) family member (p90RSK). This kinase is phosphorylated and activated by ERK1/2 and can turn activate IκB, to mediate cellular functions including apoptosis and survival[191,192].
		PTPN6	**1.51**	PTPN6 is also known as SHP-1, a phosphatase important to BCR pathway negative regulation[37]. In the absence of SHP-1 phosphatase activity, SYK was hyper-phosphorylated and hyperactive; therefore, SHP-1 is a negative regulator of SYK and therefore, BCR activation[193]. SHP-1 has also been shown to de-phosphorylate LCK[194].

Abbreviations: PI3K (Phosphatidylinositol-3-kinase), AKT (Protein kinase B), FOXO1 (Forkhead box protein O1), FasL (Fas ligand), TRAIL (TNF-related apoptosis-inducing ligand), ERK (extracellular signal-regulated kinase), TEC (tyrosine-protein kinase), BTK (Bruton's tyrosine kinase), CD40 (cluster of differentiation 40), IL-4 (interleukin-4), LCK (lymphocyte-specific protein tyrosine kinase), SYK (spleen tyrosine kinase), MALT1 (mucosa-associated lymphoid tissue lymphoma translocation protein 1), RPS6KA1 (ribosomal protein s6 kinase alpha-1), PTPN6

Table 7: Genes within the PI3K-AKT pathway with reduced expression in IBR10[2] cells relative to BJABs.

Pathway	Overall Significance	Targets	Fold change	Brief description of function/roles
PI3K-AKT pathway	**2.47**	IRS1	**4.14**	IRS1 is an adapter protein and a substrate for the insulin receptor (INSR). IRS1 overexpression has been shown to enhance the anti-apoptotic function of bcl-2 and it also associates with bcl-XL[195]. IRS1 stimulation also activates the PI3K-AKT pathway[195].
		SGK1	**4.13**	SGK1 is a kinase downstream of the PI3K-AKT pathway that has been shown to regulate FOXO1[196]. SGK1 has also been shown to promote cell survival by phosphorylating the downstream PI3K-AKT substrate FOXO3a[197].
		CREB5	**3.52**	CREB5 is a transcription factor in the cAMP-Responsive Element binding protein (CREB) family. CREBs have been implicated in the proliferation and survival of B and T-cells by modulating the expression of genes like Mcl-1 and NF-kB activation[198]. CREB is activated by PKC in a BTK/PLCγ2-dependent manner, PI3K-AKT signalling (via the BCR pathway) and possibly the MAPK protein p38[199–202].
		JAK3	**2.83**	JAK3 belongs to the JAK family of kinases. JAK3 has been shown to enhance IL-4 signalling in B-cells[203].
		CDKN1A	**2.79**	CDKN1A is also known as p21. P21 is an inhibitor of cyclin-dependent kinases and PCNA, and is transcriptionally regulated by p53 to induce growth (G1) cell cycle arrest in response to exogenous or endogenous DNA damage[204,205].
		IL4R	**2.44**	IL-4R encodes the IL-4 receptor, which when ligated in CLL cells, signals through the PI3K-AKT pathway[206]. IL-4 (along with CD40) stimulation has been shown to increase expression levels of the receptors of the pro-survival TNF superfamily members BAFF and APRIL in CLL cells[206]. This increase correlated with an increase in CLL cell viability.
		CD19	**2.29**	PI3K-AKT signalling; B-cell proliferation, survival[37,184]
		JAK2	**2.29**	JAK2 plays an important role in the JAK/STAT pathway, which is important to CLL cell survival. BCR ligation activates JAK3 and its downstream target STAT3; STAT3 is constitutively phosphorylated in CLL cells[207,208]. JAK inhibition has been shown to activate SHP-1 and boost ibrutinib's apoptotic activity in CLL-BMSC co-culture[208]. Finally, JAK2 has been shown to activate BTK and contribute to integrin activation in CLL cells, after CXCL12 treatment[209].
		IL2RG	**2.25**	IL2RG encodes the γ chain of the IL-2 receptor, which associates with IL-4R, upon IL-4 binding[210]. IL-2 signalling has been shown to promote B-cell proliferation and to signal through the PI3K-AKT, MAPK-ERK and JAK-STAT pathways[211,212].
		LPAR1	**2.19**	
		PRKAA2	**1.9**	
		COL4A6	**1.85**	

	SYK	**1.81**	BCR signal activation (CD79a/b phosphorylation), amplification and activation of important downstream targets like BTK[37].
	PRKAA1	**1.79**	
	ITGA7	**1.69**	
	NFKB1	**1.68**	NFKB1 translation produces a DNA-binding subunit of the NF-kB complex (p105). The NF-kB pathway is an effector involved in BCR-mediated apoptosis in B-cells[189,190].
	TLC1A	**1.67**	
	NTRK2	**1.66**	
	CSF1R	**1.62**	
	PIK3CD	**1.62**	PIK3CD encodes the δ isoform of p110 PI3K. CLL cells signal through p110δ-AKT pathway upon BCR activation or IL-4/CD40L stimulation to promote survival[213,214].
	NOS3	**1.6**	
	PDGFD	**1.58**	
	LPAR5	**1.58**	
	IFNA2	**1.56**	
	HSP90B1	**1.55**	
	TLR4	**1.53**	
	THEM4	**1.52**	

Abbreviations: PI3K (Phosphatidylinositol-3-kinase), AKT (Protein kinase B), FOXO1 (Forkhead box protein O1), ERK (extracellular signal-regulated kinase), BTK (Bruton's tyrosine kinase), CD40 (cluster of differentiation 40), IL-4 (interleukin-4), SYK (spleen tyrosine kinase), RPS6KA1 (ribosomal protein s6 kinase alpha-1), SHP-1 (src homology region 2 domain-containing phosphatase-1), IRS1 (insulin receptor substrate-1), bcl-1 (b-cell lymphoma 2), bcl-XL (b-cell lymphoma-extra large), serine/threonine-protein kinase-1), cAMP (cyclic adenosine monophosphate), Mcl-1 (induced myeloid leukemia cell differentiation protein), PKC (protein kinase C), PLCγ2 (phospholipase Cγ2), MAPK (mitogen-activated protein kinase), JAK (Janus kinase), PCNA (proliferating cell nuclear antigen), TNF (tumour necrosis factor), BAFF (B-cell activating factor) APRIL (a proliferation-inducing ligand), STAT (signal transducer

DISCUSSION

A hyperactive BCR pathway is known to be pivotal for CLL cell growth and survival in the microenvironment; for this reason, small molecule inhibitors targeting key BCR proteins have been highly effective in CLL treatment. The approval of ibrutinib for refractory disease treatment changed the prognostic landscape of CLL. This is because patients previously thought to have no other options, such as those with high-risk disease (e.g. del (17p)) and refractory for multiple treatments, responded to the drug[129]. However, years into ibrutinib approval, resistance is now a concern because ibrutinib-resistant patients have very limited options that they may or may not respond to. The currently accepted mechanism of ibrutinib resistance, present in about 85% of resistant patients, involves mutations in BTK and/or PLCγ2[173]. Nevertheless, a human cell line model of ibrutinib resistance that encapsulates this resistance mechanism, or one that may account for the remaining 15% of patients does not exist. The current study using BJAB cells provides one such possible model to allow for better understanding of the signalling events underlying ibrutinib resistance, the BCR pathway in CLL and how CLL cells may alter it in response to long-term treatment.

Identification of a novel cell line model of ibrutinib resistance

The ibrutinib-resistant cell line developed here, IBR10^2 cells, appear to overcome ibrutinib treatment by limiting BCR pathway signalling at the protein and RNA levels and rely primarily on PI3Kδ-AKT signalling for their survival (Figure 5, table 6). Additionally, IBR10^2 cells limit the expression of a myriad of other cell death-related pathways and increase the expression of essential cellular pathways in order to survive ibrutinib treatment (Table 5, supplemental tables 1-9). Specifically, we show that IBR10^2 cells cultured on ibrutinib for extended periods of time exhibit no BTK activation and consequently only activate ERK1/2 at

about 50% of levels exhibited by parental sensitive cells (Figure 6). We also provide evidence that BTK signalling through the BCR pathway accounts for approximately 50% of ERK1/2 activation in BJAB cells. At the RNA expression level, microarray analysis at baseline showed that IBR10^2 cells inhibit overall BCR pathway signalling but also express lower levels of key PI3Kδ-AKT and MAPK-ERK pathway players, while altering essential cellular processes like cell cycle and metabolism (Tables 6 and 7, supplementary tables 6 and 7). Finally, from the standpoint of treatment, we provide evidence for combining ibrutinib and idelalisib, as this combination led to synergistic cell death in IBR10^2 cells and synergistically inhibited p-ERK in sensitive cells (Figures 5 and 6). Also, ibrutinib-idelalisib combination was shown to be synergistic in ibrutinib-naïve and ibrutinib-resistant CLL cells (Figures 9 and 10). The key findings guiding the mechanism (s) of resistance proposed above are discussed below.

Initial protein expression analyses showed a complete ablation of BTK activation, suggesting a resistance mechanism involving BTK-independent BCR signalling in IBR10^2 cells (Figure 3). IBR10^2 cells' baseline response to BCR pathway inhibitors showed a sensitivity to PI3K-AKT inhibition as they did not significantly differ from the sensitive cell line. Further investigation into this response demonstrated a statistically significant increase in cell death with ibrutinib-idelalisib combination, in both ibrutinib-sensitive and resistant cells, in a time-dependent manner (Figure 4). More importantly, at 48-hours post-treatment in IBR10^2 cells, this combined effect on cell death was 208% and 78% ($p<0.01$) greater than ibrutinib and idelalisib single treatments respectively (Figure 4D). At 72 hours, the effect remained and was still significant. Firstly, this finding was counter-intuitive because current research and BCR pathway knowledge suggests cross-resistance to idelalisib in ibrutinib-resistant patients. Therefore, finding a combined effect this great was unexpected and the signalling events had to be

elucidated. In order to discern the true nature of the above combined effect, synergy-antagonism studies were conducted and at best, we expected ibrutinib-idelalisib combination to be additive. This is because our work using unstimulated CLL patient cells shows antagonism when these agents are combined. However, these studies demonstrated in IBR10^2 cells, profound statistically significant synergy with ibrutinib-idelalisib combinations at very low concentrations of both agents (Figure 5). Just as important, synergy was also observed in BJAB cells, but the synergistic effect was less than that observed in IBR10^2 cells. This difference in response further suggested an alteration in PI3K signalling in IBR10^2 cells. Using targeted low concentrations derived from the synergy-antagonism studies, western blots were performed to investigate signalling events in IBR10^2 cells compared to sensitive BJABs.

At a signalling level, we found that ERK1/2, an effector downstream of both BTK and PI3K-AKT, was likely responsible for the differences in response observed. This is because IBR10^2 cells expressed about 45% less p-ERK at baseline ($p=0.001$) compared to BJAB cells (Figure 6). Interestingly, after treatment with ibrutinib at a concentration that completely ablates BTK expression, we found that sensitive BJAB cells expressed 46% less p-ERK ($p=0.025$; Figure 6). Based on these findings, we concluded that in BJAB cells, BTK signalling was responsible for about 45% of baseline ERK phosphorylation. Moreover, we hypothesized that IBR10^2 cells at least partly developed resistance to ibrutinib by permanently inhibiting BTK-mediated ERK signalling, which explains their baseline p-ERK levels. This study also shed light on the signalling events mediating the ibrutinib-idelalisib combination effect in both sensitive and resistant cells. In sensitive BJAB cells, 2µM idelalisib inhibited AKT activation by approximately 17% (n.s.) but inhibited AKT activation by 45% (n.s.) in IBR10^2 cells, demonstrating IBR10^2 cells' heightened sensitivity to PI3K-AKT inhibition (Figure 6). Also, this

concentration of idelalisib reduced p-ERK by 13% and 23% (n.s.) in BJAB and IBR10^2 cells respectively, despite IBR10^2 cells expressing 45% less p-ERK at baseline (Figure 6). In combination, ibrutinib-idelalisib resulted in 97% ($p<0.0001$) and 44% ($p=0.015$) reduction in ERK activation in BJAB and IBR10^2 cells respectively, compared to their corresponding untreated controls (Figure 6). This ablation of ERK in BJAB cells confirmed at a signalling level that ibrutinib-idelalisib combination is synergistic. It is important to state that the combination effect on p-ERK inhibition was greater in BJAB cells because of their intact baseline p-ERK levels. Nevertheless, a combined effect was also observed in IBR10^2 cells and was significantly greater than ibrutinib but not idelalisib single treatment (Figure 6).

The above protein expression study also shed light on IBR10^2 cell signalling response to various inhibitors and combinations. On this note, there was a combined effect on ERK signalling with ibrutinib-idelalisib combination, but not ibrutinib-copanlisib combination (Figure 6). This showed that inhibition of PI3Kδ specifically, in combination with ibrutinib use was responsible for the synergistic effect observed in these cells. Additionally, in IBR10^2 cells, idelalisib-copanlisib combination had a combined inhibitory effect on ERK signalling (Figure 6). Of importance, in BJAB cells, ibrutinib-copanlisib and ibrutinib-idelalisib combinations inhibited p-ERK almost identically; however, idelalisib-copanlisib combination had no effect on ERK signalling (Figure 6). These findings highlighted that in addition to the baseline differences in BTK-ERK signalling, there may exist relevant PI3K isoform-specific differences in signalling between BJAB and IBR10^2 cells. Furthermore, these PI3K isoform differences could play roles in other aspects of IBR10^2 cell signalling not explored in our studies. Finally, this protein expression study showed a statistically significant combined inhibition of AKT activation in BJAB but not IBR10^2 cells, with ibrutinib-idelalisib combination treatment (Figure 6). This

finding solidified ERK signalling as the likely culprit responsible for the observed synergy in IBR10^2 cells.

Another synergy-antagonism study performed confirmed ERK as a downstream target of both BTK and PI3K-AKT signalling. In these studies, the combination of ibrutinib or idelalisib with the ERK inhibitor ravoxertinib was antagonistic in BJAB cells and to a lesser extent in IBR10^2 cells (Figure 7). In order to assess the relevance of the findings discussed above, we examined the efficacy of ibrutinib-idelalisib combination on CD40L/IL-4-stimulated CLL cells from treatment-naïve, ibrutinib-treated and ibrutinib-resistant patients. When all patient-derived cells were analyzed together, synergy was observed with ibrutinib-idelalisib combination (Figure 9). Also, synergy could not be assessed in copanlisib-idelalisib combination because copanlisib elicited less than 50% cell death at the maximum concentration used. In a separate analysis, cells derived from three ibrutinib-resistant CLL patients were treated as described above for the other CLL cells. Cell viability analyses confirmed a statistically significant reduction in cell viability with ibrutinib-idelalisib combination at different concentrations (Figure 10B). Although our current data shows a trend towards synergy, the trend was not statistically determined in cells obtained from CLL patients presenting with clinical ibrutinib resistance, because only three patients were sampled. Nevertheless, our results show a combined effect with ibrutinib-idelalisib combination in both ibrutinib-naïve and ibrutinib-resistant CD40L/IL-4 stimulated CLL cells.

In addition to inhibiting survival signals from the BCR pathway, ibrutinib treatment also disrupts the survival-promoting microenvironment in CLL PCs in the lymph nodes. The microarray data mentioned above revealed an important finding regarding IBR10^2 cells: they have reduced expression of important CLL tumour microenvironment-related pathways and respective targets. In particular, IBR10^2 cells expressed CCL5, IL4R, JAK2 and 3 among others,

at levels lower than in BJAB cells (Supplementary tables 1 and 5). This finding was interesting because it suggested that ibrutinib action in the CLL tumour microenvironment may be captured at the gene expression level in this model. The BCR pathway induces the expression of CCL3 and 4 and is involved in crosstalk with multiple microenvironment cytokines and other stimuli[215]. Ibrutinib and idelalisib treatment disrupt the BCR pathway; for this reason and via other actions in the tumour microenvironment, ibrutinib and idelalisib administration result in rapid lymphocytosis in CLL patients. Essentially, these agents force CLL cells out of their protective environments in the PCs, leading to CLL cell death. Unfortunately, this aspect of ibrutinib (and idelalisib) function cannot be captured with the current single cell culture model. Even so, reduced TNF and TRAF1 expression levels, in addition to the other genes and pathways outlined in the appendix, signify that long-term ibrutinib treatment may alter the expression of important CLL tumour microenvironment survival signals in cell line models, even in the absence of co-culturing (Supplementary table 5).

Other pathways identified by the TAC software analysis of the microarray data that could contribute to the model of ibrutinib resistance described above, include the IL-4, JAK-STAT, AXL, TNF Weak Inducer of Apoptosis (TWEAK) and Autophagy signalling pathways (Supplementary tables 1-5). This finding is supported by Landau et al., 2017[216], as they found most of the pathways and the expression of some of the targets (CCL5, DUSP2, LCK and IL4R) identified in our resistant cell line to be reduced when comparing CLL patient cells during ibrutinib treatment to cells sampled at baseline. Landau et al. also describe the phenotype of CLL cells on ibrutinib as having overall reduced BCR signalling, activation and proliferation. This phenotype in addition to alterations in cell cycle identified in both their study and ours, show that the phenotype and mechanism of resistance we report is observed in some patients during

ibrutinib therapy and at resistance. Providing further support for our expression study, Palma et al., 2018[217] found two genes from our dataset (TNF and DUSP2) to be upregulated in CLL cells sampled from the lymph nodes of patients, compared to cells from the peripheral blood. Notably, ibrutinib treatment led to a reduction of transcription levels of these genes as we have reported. To close this section, it is imperative to state that while the two studies referenced above only found the expression of a few of our gene targets to be altered, both studies identified the same pathways we identified and sometimes a different subunit of the same protein.

The microarray analysis also identified some genes and pathways that are upregulated in IBR10^2 cells relative to BJABs. These pathways were not obviously connected to ibrutinib treatment, the BCR pathway or CLL. Nonetheless, these findings were important because from a pathway point-of-view, they showed that IBR10^2 cells also display alterations of basic cellular processes including cell cycle regulation and metabolism (Supplementary table 7). Looking closer at the upregulated genes individually made it clearer that some of these targets may actually influence drug resistance and be of relevance to CLL. Examples of targets that stood out include: MAP2K6 (MAPK kinase – MAPKK6/MKK6/MEK6), MAP2K5 (MEK5), MAPK7 (ERK5), TAB1 (MAPKK kinase-7-interacting protein-1), CASP9 (caspase 9), CYP3A4 (cytochrome P450 3A4), CYP2E1, IKBKG (IκK-γ) and DEPTOR (DEP domain containing mTOR-interacting protein), amongst many others (Supplementary tables 8 and 9). MKK6 is a known activator of the p38 MAPK pathway, which is constitutively active in CLL and contributes to their survival in stromal cell co-culture[218–220]. In relation, TAB1 is a known activator of p38; since both MKK6 and TAB1 expression are increased, this suggests a role for the p38 MAPK pathway in IBR10^2 resistance[221]. On the other hand, MEK5 is the direct activator of the ERK5 pathway and both genes are upregulated in IBR10^2 cells; the ERK5 pathway has

been implicated in various cellular responses like proliferation, differentiation and apoptosis[222,223].

CYP3A4 is the known metabolizer of ibrutinib in the body and ibrutinib has been shown to be an inhibitor of CYP3A4; there is no known connection between CYP2E1 and ibrutinib metabolism[224,225]. Even so, it was difficult to determine from the literature the extent (if any) of B-cells (malignant or otherwise) expressing the CYP3A4 protein. Nonetheless, CYP3A4 and CYP2E1 gene expression levels were increased in IBR10^2 cells, possibly once again showing clinical implications in a preclinical model, but also that CYP3A4 and maybe CYP2E1 upregulation contribute to IBR10^2 cells' increasingly multifaceted mechanism of evading ibrutinib-mediated cell death. Interestingly, IBR10^2 cells express higher levels of caspase 9, the apoptotic protein; the purpose and possible contribution of this effect cannot be determined at this time, because caspase-9 is needed to initiate the apoptotic pathway. Finally, IKK-γ is a part of the IKK complex and is important for NF-kB activation; DEPTOR is an inhibitor of mTOR that also activates AKT, and its expression is deregulated in malignancies[226–228]. Taken together, the above targets and their distinct but connected pathways highlight other mechanisms that may underlie or aid IBR10^2 cells in their acquired resistance to long-term ibrutinib treatment.

Limitations and applicability of findings

Given the importance of the BCR pathway to CLL and the use of a Burkitt's lymphoma cell line (BJAB) for our investigations, it is necessary to discuss some important points. Firstly, BJAB cells were derived from a patient with EBV-negative Burkitt's lymphoma and the cell line harbours a *TP53* mutation[229,230]. Although, it is unclear if the cells have a functional p53 protein because they still have two alleles present. These factors are important to know because they potentially influence how the cells respond to various treatments and determine their similarity to

both clinical Burkitt's lymphoma and CLL, given the importance of p53 mutation/deletion status in CLL treatment response in patients. Secondly, the B-cells in Burkitt's lymphoma (BL) are driven by a mechanism different from what is seen in CLL. BL cells from most patients are known to harbour a translocation (t(8;14) (q24;q32)) that allows expression of the oncogenic transcription factor Myc, to be mediated by enhancer elements associated with immunoglobulin genes, which are highly active in B-cells[231]. This deregulation of Myc expression drives the lymphoma; thus, if the mechanism driving the malignancy is different at baseline, how the cells respond to chronic ibrutinib treatment may be different, which may hamper the applicability of our findings to CLL. In contrast, the driving mechanisms for other lymphomas involve translocations but also altered BCR signalling, DNA damage and apoptosis pathways[93,94].

Thirdly, it is important to state that studying a cell line for drug resistance is different from studying a primary tumour. Importantly, a CLL-derived cell line was not used for our investigations because the EC_{50} for ibrutinib in CLL cell lines available to us (MEC-1 and I83), were much higher than our desired concentration for resistance (20µM). This observation put the potential resistant cell lines farther from the clinically-relevant concentration of ibrutinib (0.3µM) and at higher risks for off-target effect-mediated ibrutinib resistance[232]. Moreover, preliminary studies we conducted showed that I83 cells did not express BTK and had very low levels of p-ERK. Finally, after establishing the $IBR10^2$ cell line, we attempted to develop similar cell lines using MEC-1 and I83, but all efforts proved unsuccessful. As a result of the origin of the cell line used, our studies must be interpreted with caution, as baseline signalling differences between Burkitt's lymphoma and CLL, may render our findings more relevant to other B-cell lymphomas than CLL.

Another category of factors affecting the applicability of our findings in the clinic involves the limitations of studying drug resistance *in vitro*. Firstly, IBR10^2 cells must be described in contrast to CLL cells derived from ibrutinib-resistant patients. On this note, one similarity between our findings on IBR10^2 cells and western blots done on ibrutinib-resistant CLL patient cells, is that ibrutinib no longer has an effect on p-ERK levels on both cell types. However, CLL patients with BTK and/or PLCγ2 mutations do not express reduced baseline ERK activation as was reported here[171,172]. Furthermore, these patient cells still have BTK activation, whereas IBR10^2 cells have ablated their BTK signalling. The above differences notwithstanding, it is important to highlight that studies investigating the effect of BTK and/or PLCG2 mutations in CLL, typically use cell lines like HEK293 and DT40 to investigate downstream signalling effects[171,172]. Therefore, there may be aspects of our findings that are applicable to clinical CLL ibrutinib resistance. It is also necessary to state that none of the studies assessed investigated p-AKT expression on CLL cells from ibrutinib-resistant patients, but their cell line models appear to match our findings with respect to ibrutinib treatment having no effect on p-AKT levels[171].

Secondly, for a complicated disease like CLL where the microenvironment heavily influences disease, it is difficult to approximate clinical disease *in vitro*. To combat this, we used CD40L/IL-4 stimulation on the CLL cells sampled from patients in our studies. For *in vitro* studies, CLL cells are typically stimulated using CD40L/IL-4 or IgM. IgM stimulates the BCR pathway by ligating the BCR, which leads to SYK, LYN and BTK activation; CD40L/IL-4 stimulation primarily stimulates the PI3K-AKT pathway, promoting CLL cells' resistance to cell death via BCR pathway inhibitors, especially PI3K inhibitors. CD40L/IL-4 stimulation was chosen for our investigations because of convenience, as our laboratory primarily uses this method but more importantly, because IBR10^2 cells display altered PI3K-AKT signalling. As a

result, CD40L/IL-4 was used in order to test the synergism between ibrutinib and idelalisib, using stimulation that leads to significant upregulation of PI3K-AKT signalling. As a result of this choice in reagents, it is unclear if the synergism we observed will occur with IgM stimulation, although the current literature suggests that it may not.

In relation to the above, another limitation of the studies reported here is the use of clinically-relevant concentrations. The concentrations of idelalisib used in our studies of CLL cells that showed synergy, were significantly higher (up to 200μM) than the reported clinically-relevant maximum plasma concentration of idelalisib (5.18μM)[232]. The reason for this difference in idelalisib concentration used, was the stimulation of the CLL cells with CD40L/IL-4 before treatment. It was observed early on in our studies that upon stimulation with CD40L/IL-4, CLL cells were completely resistant to PI3K-AKT inhibition, requiring very high concentrations (>100μM) for cell death to be induced. This was expected because CD40L/IL-4 is known to stimulate the PI3K-AKT pathway, the same pathway inhibited by idelalisib. For this reason, CD40L/IL-4 stimulation increased the EC_{50} of idelalisib in CLL cells (EC_{50} = 173μM in this study). This observation meant that in order to investigate the effects of ibrutinib-idelalisib combination in CLL cells, the use of clinically relevant concentrations was no longer an option. Nevertheless, the synergy we report between ibrutinib and idelalisib may still be a true effect. In support of our model, we observed synergy with ibrutinib at concentrations of idelalisib that were half the clinically relevant maximum concentration in $IBR10^2$ cells, and all signalling studies were conducted at 2μM idelalisib, a concentration also lower than the clinically-relevant maximum concentration (5.18μM).

Secondly, although the set concentration to establish ibrutinib resistance (20μM) was based on *in vitro* findings, it is still much higher than the maximum clinically-relevant

concentration of ibrutinib in the blood (0.3μM)[232]. This difference, coupled with the promiscuous receptor-binding nature of ibrutinib may have resulted in a cell line model of resistance that is very different from what is observed in the clinic. This factor notwithstanding, preclinical models and clinical findings are rarely in sync with respect to concentrations used, because *in vitro* studies sometimes require higher concentrations of inhibitors to achieve a comparable level of cell death as is observed *in vivo*. Therefore, a deeper characterization of this cell line model will determine its clinical applicability. Thirdly, the response of CLL cells *in vitro* for our ibrutinib studies must be addressed. This is because cells from patients who display clinical resistance to ibrutinib responded to ibrutinib *in vitro* (at a higher concentration) and it has not escaped our attention that this may be due to an off-target effect. Additionally, cells from patients currently responding on ibrutinib, when given additional ibrutinib *in vitro*, responded. This also may be due to an off-target effect, given ibrutinib's receptor-binding nature. Finally, off-target effects may also account for the synergy observed in CLL cells in our studies, due to the high (>100μM) concentrations of idelalisib used.

Unfortunately, we were unable to determine the mutation status of BTK and PLCγ2 in IBR10^2 cells, for the purpose of this thesis. Nonetheless, we infer based on current literature that these cells likely do not harbour a BTK or PLCγ2 mutation. This is because patient cells with BTK mutations still exhibit BTK activation (express p-BTK) and those with PLCγ2 mutations have been shown to have increased ERK activation (high p-ERK)[171,172]. Neither of these findings were made in our cell line model. Nevertheless, the results presented above show that it is possible for malignant B-cells to alter sub-pathways within the BCR pathway, in response to long-term drug-induced selection. This phenomenon may apply to either CLL or other B-cell malignancies. In conjunction with the above limitation, some major conclusions about IBR10^2

resistance mechanism were drawn from data with insufficient replications (N=1 data). These conclusions were drawn from the microarray data and the washout protein expression experiment, both showing reduced BCR pathway signalling in IBR10^2 cells. In order to increase confidence in the proposed model, these studies must be repeated and appropriate statistical analyses conducted.

In summary, our cell line model provides evidence of a novel pathway of ibrutinib resistance involving PI3Kδ-AKT and altered ERK signalling, that is susceptible to ibrutinib-idelalisib combination treatment. We also report similar findings in patient-derived CLL cells. However, the applicability of our findings is limited by our use of a Burkitt's lymphoma cell line to investigate CLL ibrutinib resistance, the use of high concentrations of ibrutinib and idelalisib in our studies, and the dissimilarity between our model and clinical CLL ibrutinib resistance. Nevertheless, Kapoor et al.[176] provide some evidence for the applicability of our findings, as they conducted a study very similar to ours and described a mechanism of ibrutinib resistance involving deregulated PI3K signalling in both CLL and ABC DLBCL cells. Also, another study by de Rooij et al.[233], showed that ibrutinib and idelalisib synergistically inhibited BCR-mediated adhesion interactions in MCL and CLL patient-derived cells. These studies provide support for different aspects of our findings in the IBR10^2 cell line and show its potential applicability beyond CLL. Of note, other studies investigating BTK and PI3K dual inhibition in CLL and other lymphomas also exist[234–236].

SUMMARY OF FINDINGS

With an array of cell death, synergy-antagonism, protein expression and transcriptomic studies, we have done preliminary characterization of a novel ibrutinib-resistant BJAB-derived cell line, IBR10^2. IBR10^2 cells display an ibrutinib resistance mechanism characterized by overall reduced signalling through the BCR pathway. IBR10^2 cells have been shown to be completely resistant to ibrutinib via cell death and protein expression analyses and have also been shown to have a unique sensitivity to PI3K inhibition. We show here the importance of ERK activation to traditional BTK and PI3K-AKT signalling within the BCR pathway, in the context of ibrutinib resistance in these cells. Overall, our results show that IBR10^2 cells have ablated BTK activation, express 50% less ERK activity at baseline compared to sensitive BJAB cells, are highly sensitive to PI3K inhibition and that ibrutinib-idelalisib combination is synergistically cytotoxic to these cells in an ERK-dependent manner. In support of our proposed mechanism of resistance, transcriptomic analyses showed reduced expression of BCR, PI3K-AKT and MAPK pathway targets; although, we acknowledge that other basic cellular pathways likely play a role in IBR10^2 cells resistance mechanism. We also show that ibrutinib-idelalisib is synergistically cytotoxic to CD40L/IL-4-stimulated CLL cells. In summary, we introduce a new model of CLL ibrutinib resistance, identify a combination treatment to overcome this resistance and provide data on ibrutinib-idelalisib cross-reactivity that could prove vital in the future. Nonetheless, studies determining the BTK and PLCγ2 mutation status, and investigations into IBR10^2 cell response to current treatments used by ibrutinib-refractory CLL patients are warranted.

SIGNIFICANCE

The development and current characterization of IBR10^2 cells revealed a novel mechanism of ibrutinib-resistance, developed in response to long-term treatment with ibrutinib. This model joins other studies that report a role for the PI3K-AKT pathway in the development of resistance to ibrutinib. However, the specific mechanism described here involves downstream ERK signalling and an apparent rewiring of the traditional BCR signalling pathway, in response to ibrutinib, in addition to ibrutinib-mediated reduction in the expression of BCR pathway proteins at the mRNA level. Unfortunately, it is unlikely that these mechanisms of resistance co-exist with the currently accepted mechanism of resistance driving up to about 90% of all ibrutinib-resistant CLL patients (BTK and/or PLCγ2 mutations)[173]. Nevertheless, this mechanism may account for some of the remaining patients who do not present with mutations in either BTK or PLCγ2. Despite the above statements, it is yet to be determined whether BJAB or IBR10^2 cells possess a mutation in PLCγ2 or BTK. In summary, the model of ibrutinib-resistance presented here contributes to the growing field of studies on ibrutinib resistance in CLL and other B-cell malignancies, and holds promise as a model that can be interrogated in future preclinical studies to hopefully validate and identify new rescue therapies for patients presenting with ibrutinib resistance.

FUTURE DIRECTIONS

As has been alluded to in the results and discussion segments, characterization of the IBR10^2 cell line is far from complete, and there are still many questions left to be answered with respect to how these cells respond to ibrutinib, PI3K and ERK inhibition. Specifically, protein expression studies in BJAB and IBR10^2 cells treated with ravoxertinib-ibrutinib/ idelalisib/ copanlisib combinations need to be conducted to determine how signalling changes in response to ERK-BTK/PI3K inhibition. Furthermore, the mutation status of BTK and PLCγ2 need to be determined and if possible, transcriptomic and genomic analyses of BJAB and IBR10^2 cells at baseline and in response to ibrutinib, idelalisib, copanlisib and combination need to be done to see what changes (if any) exist at the gene and transcription levels with statistically evaluable repetitions.

Specifically, given the results discussed above, the contributions of the p38, ERK5, cell cycle (checkpoints and the G2/M phases), JAK-STAT and AXL pathways and the effects of miR-mediated gene expression should be investigated in the context of the BCR and PI3K-AKT pathways, in order to determine if there is a connection between the alterations in gene expression observed. Taking things forward, the individuality of the upregulated gene expression profile of IBR10^2 cells should be exploited as it makes the assessment of the use of inhibitors possible. This is because identifying an upregulated gene central to IBR10^2 resistance mechanism and inhibiting it may provide another avenue for combination therapies akin to ibrutinib-idelalisib that sensitize the cells to ibrutinib treatment. Another opportunity that the above approach provides, is the identification of novel applications of drugs already approved. This is because identification of say a transporter central to IBR10^2 cells' resistance might allow

for the use of an already approved blocker in addition to ibrutinib; this could be an inexpensive solution that is needed, given the high cost of using small molecule inhibitors in the clinic.

With respect to the clinical applicability of the IBR10^2 cell line model, upon establishment of the above parameters and a better understanding of the model, the cells need to be treated with current rescue therapies used for ibrutinib-resistant patients, including Venetoclax and duvelisib, to see how they respond. Also, novel combination therapies using current and proposed agents for the treatment of CLL should be utilized to isolate the inhibitors/group of inhibitors the cells are sensitive to, so that data-driven alternative treatments for ibrutinib-refractory CLL patients may be devised. Finally, given that the IBR10^2 cell line was developed from a Burkitt's lymphoma patient and Burkitt's lymphoma has a different driving mechanism than CLL, our findings should be investigated for their relevance to Burkitt's and other lymphomas.

REFERENCES

1. Chronic Lymphocytic Leukemia - Cancer Stat Facts [Internet]. SEER. [cited 2020 Apr 28]. Available from: https://seer.cancer.gov/statfacts/html/clyl.html

2. Seftel MD, Demers AA, Banerji V, Gibson SB, Morales C, Musto G, et al. High incidence of chronic lymphocytic leukemia (CLL) diagnosed by immunophenotyping: A population-based Canadian cohort. Leuk Res. 2009 Nov 1;33(11):1463–8.

3. Melo JV, Catovsky D, Galton DAG. The relationship between chronic lymphocytic leukaemia and prolymphocytic leukaemia. Br J Haematol. 1986;63(2):377–87.

4. Hallek M, Cheson BD, Catovsky D, Caligaris-Cappio F, Dighiero G, Döhner H, et al. iwCLL guidelines for diagnosis, indications for treatment, response assessment, and supportive management of CLL. Blood. 2018 Jun 21;131(25):2745–60.

5. Moreau EJ, Matutes E, A'Hern RP, Morilla AM, Morilla RM, Owusu-Ankomah KA, et al. Improvement of the Chronic Lymphocytic Leukemia Scoring System With the Monoclonal Antibody SN8(CD79b). Am J Clin Pathol. 1997 Oct 1;108(4):378–82.

6. Ginaldi L, De Martinis M, Matutes E, Farahat N, Morilla R, Catovsky D. Levels of expression of CD19 and CD20 in chronic B cell leukaemias. J Clin Pathol. 1998 May;51(5):364–9.

7. Deans JP, Polyak MJ. FMC7 is an epitope of CD20. Blood. 2008 Feb 15;111(4):2492–2492.

8. Alapat. D, Coviello-Malle JM, Owens R, Qu P, Barlogie B, Shaughnessy JD, et al. Diagnostic Usefulness and Prognostic Impact of CD200 Expression in Lymphoid Malignancies and Plasma Cell Myeloma. Am J Clin Pathol. 2012 Jan;137(1):93–100.

9. Hallek M. Chronic lymphocytic leukemia: 2020 update on diagnosis, risk stratification and treatment. Am J Hematol. 2019;94(11):1266–87.

10. Marti GE, Rawstron AC, Ghia P, Hillmen P, Houlston RS, Kay N, et al. Diagnostic criteria for monoclonal B-cell lymphocytosis. Br J Haematol. 2005;130(3):325–32.

11. Johnston JB, Parikh SA, Gibson SB, Kenderian SJ, Kay NE. Chronic Lymphocytic Leukemia. In: Wintrobe's Clinical Hematology. 14th ed. Lippincott Williams & Wilkins; 2018. p. 1948–85.

12. Rai KR, Sawitsky A, Cronkite EP, Chanana AD, Levy RN, Pasternack BS. Clinical staging of chronic lymphocytic leukemia. Blood. 1975 Aug;46(2):219–34.

13. Binet JL, Auquier A, Dighiero G, Chastang C, Piguet H, Goasguen J, et al. A new prognostic classification of chronic lymphocytic leukemia derived from a multivariate survival analysis. Cancer. 1981;48(1):198–206.

14. Kikushige Y, Ishikawa F, Miyamoto T, Shima T, Urata S, Yoshimoto G, et al. Self-Renewing Hematopoietic Stem Cell Is the Primary Target in Pathogenesis of Human Chronic Lymphocytic Leukemia. Cancer Cell. 2011 Aug 16;20(2):246–59.

15. Gaidano G, Foà R, Dalla-Favera R. Molecular pathogenesis of chronic lymphocytic leukemia. J Clin Invest. 2012 Oct 1;122(10):3432–8.

16. Zhang S, Kipps TJ. The Pathogenesis of Chronic Lymphocytic Leukemia. Annu Rev Pathol. 2014;9:103–18.

17. Fabbri G, Dalla-Favera R. The molecular pathogenesis of chronic lymphocytic leukaemia. Nat Rev Cancer. 2016 Mar;16(3):145–62.

18. Packham G, Krysov S, Allen A, Savelyeva N, Steele AJ, Forconi F, et al. The outcome of B-cell receptor signaling in chronic lymphocytic leukemia: proliferation or anergy. Haematologica. 2014 Jul;99(7):1138–48.

19. Messmer BT, Messmer D, Allen SL, Kolitz JE, Kudalkar P, Cesar D, et al. In vivo measurements document the dynamic cellular kinetics of chronic lymphocytic leukemia B cells. J Clin Invest. 2005 Mar 1;115(3):755–64.

20. Burger JA. Nurture versus Nature: The Microenvironment in Chronic Lymphocytic Leukemia. Hematology. 2011 Dec 10;2011(1):96–103.

21. Edelmann J, Klein-Hitpass L, Carpinteiro A, Führer A, Sellmann L, Stilgenbauer S, et al. Bone marrow fibroblasts induce expression of PI3K/NF-κB pathway genes and a pro-angiogenic phenotype in CLL cells. Leuk Res. 2008 Oct 1;32(10):1565–72.

22. Herishanu Y, Pérez-Galán P, Liu D, Biancotto A, Pittaluga S, Vire B, et al. The lymph node microenvironment promotes B-cell receptor signaling, NF-κB activation, and tumor proliferation in chronic lymphocytic leukemia. Blood. 2011 Jan 13;117(2):563–74.

23. International CLL-IPI working group. An international prognostic index for patients with chronic lymphocytic leukaemia (CLL-IPI): a meta-analysis of individual patient data. Lancet Oncol. 2016 Jun;17(6):779–90.

24. Döhner H, Stilgenbauer S, Benner A, Leupolt E, Kröber A, Bullinger L, et al. Genomic aberrations and survival in chronic lymphocytic leukemia. N Engl J Med. 2000 Dec 28;343(26):1910–6.

25. Sampath D, Plunkett W. The role of DNA repair in chronic lymphocytic leukemia pathogenesis and chemotherapy resistance. Curr Oncol Rep. 2007 Sep 1;9(5):361–7.

26. Seiffert M, Dietrich S, Jethwa A, Glimm H, Lichter P, Zenz T. Exploiting biological diversity and genomic aberrations in chronic lymphocytic leukemia. Leuk Lymphoma. 2012 Jun 1;53(6):1023–31.

27. Döhner H, Stilgenbauer S, James MR, Benner A, Weilguni T, Bentz M, et al. 11q Deletions Identify a New Subset of B-Cell Chronic Lymphocytic Leukemia Characterized by Extensive Nodal Involvement and Inferior Prognosis. Blood. 1997 Apr 1;89(7):2516–22.

28. Morrison C, Sonoda E, Takao N, Shinohara A, Yamamoto K, Takeda S. The controlling role of ATM in homologous recombinational repair of DNA damage. EMBO J. 2000 Feb 1;19(3):463–71.

29. Zenz T, Mertens D, Küppers R, Döhner H, Stilgenbauer S. From pathogenesis to treatment of chronic lymphocytic leukaemia. Nat Rev Cancer. 2010 Jan;10(1):37–50.

30. Austen B, Skowronska A, Baker C, Powell JE, Gardiner A, Oscier D, et al. Mutation Status of the Residual ATM Allele Is an Important Determinant of the Cellular Response to Chemotherapy and Survival in Patients With Chronic Lymphocytic Leukemia Containing an 11q Deletion. J Clin Oncol. 2007 Dec 1;25(34):5448–57.

31. Jain P, Keating M, Thompson PA, Trinh L, Wang X, Wierda W, et al. High fluorescence in situ hybridization percentage of deletion 11q in patients with chronic lymphocytic leukemia is an independent predictor of adverse outcome. Am J Hematol. 2015 Jun;90(6):471–7.

32. Calin GA, Dumitru CD, Shimizu M, Bichi R, Zupo S, Noch E, et al. Frequent deletions and down-regulation of micro- RNA genes miR15 and miR16 at 13q14 in chronic lymphocytic leukemia. Proc Natl Acad Sci. 2002 Nov 26;99(24):15524–9.

33. Veronese A, Pepe F, Chiacchia J, Pagotto S, Lanuti P, Veschi S, et al. Allele-specific loss and transcription of the miR-15a/16-1 cluster in chronic lymphocytic leukemia. Leukemia. 2015 Jan;29(1):86–95.

34. Cimmino A, Calin GA, Fabbri M, Iorio MV, Ferracin M, Shimizu M, et al. miR-15 and miR-16 induce apoptosis by targeting BCL2. Proc Natl Acad Sci. 2005 Sep 27;102(39):13944–9.

35. Rassenti LZ, Jain S, Keating MJ, Wierda WG, Grever MR, Byrd JC, et al. Relative value of ZAP-70, CD38, and immunoglobulin mutation status in predicting aggressive disease in chronic lymphocytic leukemia. Blood. 2008 Sep 1;112(5):1923–30.

36. Schroeder HW, Cavacini L. Structure and Function of Immunoglobulins. J Allergy Clin Immunol. 2010 Feb;125(2 0 2):S41–52.

37. Woyach JA, Johnson AJ, Byrd JC. The B-cell receptor signaling pathway as a therapeutic target in CLL. Blood. 2012 Aug 9;120(6):1175–84.

38. Rolli V, Gallwitz M, Wossning T, Flemming A, Schamel WWA, Zürn C, et al. Amplification of B Cell Antigen Receptor Signaling by a Syk/ITAM Positive Feedback Loop. Mol Cell. 2002 Nov 1;10(5):1057–69.

39. Yamamoto T, Yamanashi Y, Toyoshima K. Association of Src-Family Kinase Lyn with B-Cell Antigen Receptor. Immunol Rev. 1993;132(1):187–206.

40. Fearon DT, Carroll MC. Regulation of B lymphocyte responses to foreign and self-antigens by the CD19/CD21 complex. Annu Rev Immunol. 2000;18:393–422.

41. Carter RH, Fearon DT. CD19: lowering the threshold for antigen receptor stimulation of B lymphocytes. Science. 1992 Apr 3;256(5053):105–7.

42. Liu C, Miller H, Hui KL, Grooman B, Bolland S, Upadhyaya A, et al. A Balance of Bruton's Tyrosine Kinase and SHIP Activation Regulates B Cell Receptor Cluster Formation by Controlling Actin Remodeling. J Immunol. 2011 Jul 1;187(1):230–9.

43. Cheng PC, Dykstra ML, Mitchell RN, Pierce SK. A Role for Lipid Rafts in B Cell Antigen Receptor Signaling and Antigen Targeting. J Exp Med. 1999 Dec 6;190(11):1549–60.

44. Pike LJ. Lipid rafts bringing order to chaos. J Lipid Res. 2003 Apr 1;44(4):655–67.

45. Kabak S, Skaggs BJ, Gold MR, Affolter M, West KL, Foster MS, et al. The Direct Recruitment of BLNK to Immunoglobulin α Couples the B-Cell Antigen Receptor to Distal Signaling Pathways. Mol Cell Biol. 2002 Apr 15;22(8):2524–35.

46. Engels N, Wollscheid B, Wienands J. Association of SLP-65 / BLNK with the B cell antigen receptor through a non-ITAM tyrosine of Ig-α. Eur J Immunol. 2001;31(7):2126–34.

47. Hashimoto S, Iwamatsu A, Ishiai M, Okawa K, Yamadori T, Matsushita M, et al. Identification of the SH2 domain binding protein of Bruton's tyrosine kinase as BLNK--functional significance of Btk-SH2 domain in B-cell antigen receptor-coupled calcium signaling. Blood. 1999 Oct 1;94(7):2357–64.

48. Fu C, Turck CW, Kurosaki T, Chan AC. BLNK: a Central Linker Protein in B Cell Activation. Immunity. 1998 Jul 1;9(1):93–103.

49. Dal Porto JM, Gauld SB, Merrell KT, Mills D, Pugh-Bernard AE, Cambier J. B cell antigen receptor signaling 101. Mol Immunol. 2004 Jul 1;41(6):599–613.

50. Park H, Wahl MI, Afar DEH, Turck CW, Rawlings DJ, Tam C, et al. Regulation of Btk Function by a Major Autophosphorylation Site Within the SH3 Domain. Immunity. 1996 May 1;4(5):515–25.

51. Saito K, Tolias KF, Saci A, Koon HB, Humphries LA, Scharenberg A, et al. BTK Regulates PtdIns-4,5-P2 Synthesis: Importance for Calcium Signaling and PI3K Activity. Immunity. 2003 Nov 1;19(5):669–77.

52. Petro JB, Rahman SMJ, Ballard DW, Khan WN. Bruton's Tyrosine Kinase Is Required for Activation of Iκb Kinase and Nuclear Factor κb in Response to B Cell Receptor Engagement. J Exp Med. 2000 May 15;191(10):1745–54.

53. Khan WN, Alt FW, Gerstein RM, Malynn BA, Larsson I, Rathbun G, et al. Defective B cell development and function in Btk-deficient mice. Immunity. 1995 Sep 1;3(3):283–99.

54. Jean S, Kiger AA. Classes of phosphoinositide 3-kinases at a glance. J Cell Sci. 2014 Mar 1;127(5):923–8.

55. Chantry D, Vojtek A, Kashishian A, Holtzman DA, Wood C, Gray PW, et al. p110δ, a Novel Phosphatidylinositol 3-Kinase Catalytic Subunit That Associates with p85 and Is Expressed Predominantly in Leukocytes. J Biol Chem. 1997 Aug 1;272(31):19236–41.

56. Targets of B-cell antigen receptor signaling: the phosphatidylinositol 3-kinase/Akt/glycogen synthase kinase-3 signaling pathway and the Rap1 GTPase. Immunol Rev. 2000;176(1):47–68.

57. Pleiman CM, Hertz WM, Cambier JC. Activation of phosphatidylinositol-3' kinase by Src-family kinase SH3 binding to the p85 subunit. Science. 1994 Mar 18;263(5153):1609–12.

58. Ramadani F, Bolland DJ, Garcon F, Emery JL, Vanhaesebroeck B, Corcoran AE, et al. The PI3K Isoforms p110α and p110δ are Essential for Pre-B Cell Receptor Signaling and B Cell Development. Sci Signal. 2010 Aug 10;3(134):ra60.

59. Ali AY, Wu X, Eissa N, Hou S, Ghia J-E, Murooka TT, et al. Distinct roles for phosphoinositide 3-kinases γ and δ in malignant B cell migration. Leukemia. 2018;32(9):1958–69.

60. Miao B, Skidan I, Yang J, Lugovskoy A, Reibarkh M, Long K, et al. Small molecule inhibition of phosphatidylinositol-3,4,5-triphosphate (PIP3) binding to pleckstrin homology domains. Proc Natl Acad Sci U S A. 2010 Nov 16;107(46):20126–31.

61. Bellacosa A, Chan TO, Ahmed NN, Datta K, Malstrom S, Stokoe D, et al. Akt activation by growth factors is a multiple-step process: the role of the PH domain. Oncogene. 1998 Jul;17(3):313–25.

62. Gold MR, Scheid MP, Santos L, Dang-Lawson M, Roth RA, Matsuuchi L, et al. The B Cell Antigen Receptor Activates the Akt (Protein Kinase B)/Glycogen Synthase Kinase-3 Signaling Pathway Via Phosphatidylinositol 3-Kinase. J Immunol. 1999 Aug 15;163(4):1894–905.

63. Zhuang J, Hawkins SF, Glenn MA, Lin K, Johnson GG, Carter A, et al. Akt is activated in chronic lymphocytic leukemia cells and delivers a pro-survival signal: the therapeutic potential of Akt inhibition. Haematologica. 2010 Jan;95(1):110–8.

64. Ghosh S, May MJ, Kopp EB. NF-kappa B and Rel proteins: evolutionarily conserved mediators of immune responses. Annu Rev Immunol. 1998;16:225–60.

65. Vigorito E, Gambardella L, Colucci F, McAdam S, Turner M. Vav proteins regulate peripheral B-cell survival. Blood. 2005 Oct 1;106(7):2391–8.

66. Ruland J, Mak TW. Transducing signals from antigen receptors to nuclear factor κB. Immunol Rev. 2003;193(1):93–100.

67. Stadanlick JE, Kaileh M, Karnell FG, Scholz JL, Miller JP, Quinn Iii WJ, et al. Tonic B cell antigen receptor signals supply an NF-κB substrate for prosurvival BLyS signaling. Nat Immunol. 2008 Dec;9(12):1379–87.

68. Hashimoto A, Okada H, Jiang A, Kurosaki M, Greenberg S, Clark EA, et al. Involvement of Guanosine Triphosphatases and Phospholipase C-γ2 in Extracellular Signal–regulated Kinase, c-Jun NH2-terminal Kinase, and p38 Mitogen-activated Protein Kinase Activation by the B Cell Antigen Receptor. J Exp Med. 1998 Oct 5;188(7):1287–95.

69. Johnson GL, Lapadat R. Mitogen-activated protein kinase pathways mediated by ERK, JNK, and p38 protein kinases. Science. 2002 Dec 6;298(5600):1911–2.

70. Dolmetsch RE, Lewis RS, Goodnow CC, Healy JI. Differential activation of transcription factors induced by Ca 2+ response amplitude and duration. Nature. 1997 Apr;386(6627):855–8.

71. Ono M, Bolland S, Tempst P, Ravetch JV. Role of the inositol phosphatase SHIP in negative regulation of the immune system by the receptor Fc(gamma)RIIB. Nature. 1996 Sep 19;383(6597):263–6.

72. Scharenberg AM, El-Hillal O, Fruman DA, Beitz LO, Li Z, Lin S, et al. Phosphatidylinositol-3,4,5-trisphosphate (PtdIns-3,4,5-P3)/Tec kinase-dependent calcium signaling pathway: a target for SHIP-mediated inhibitory signals. EMBO J. 1998 Apr 1;17(7):1961–72.

73. Carver DJ, Aman MJ, Ravichandran KS. SHIP inhibits Akt activation in B cells through regulation of Akt membrane localization. Blood. 2000 Aug 15;96(4):1449–56.

74. Bolland S, Pearse RN, Kurosaki T, Ravetch JV. SHIP Modulates Immune Receptor Responses by Regulating Membrane Association of Btk. Immunity. 1998 Apr 1;8(4):509–16.

75. Pani G, Kozlowski M, Cambier JC, Mills GB, Siminovitch KA. Identification of the tyrosine phosphatase PTP1C as a B cell antigen receptor-associated protein involved in the regulation of B cell signaling. J Exp Med. 1995 Jun 1;181(6):2077–84.

76. Nishizumi H, Horikawa K, Mlinaric-Rascan I, Yamamoto T. A Double-Edged Kinase Lyn: A Positive and Negative Regulator for Antigen Receptor–mediated Signals. J Exp Med. 1998 Apr 20;187(8):1343–8.

77. Hibbs ML, Harder KW, Armes J, Kountouri N, Quilici C, Casagranda F, et al. Sustained Activation of Lyn Tyrosine Kinase In Vivo Leads to Autoimmunity. J Exp Med. 2002 Dec 16;196(12):1593–604.

78. Kim M, Carman CV, Springer TA. Bidirectional Transmembrane Signaling by Cytoplasmic Domain Separation in Integrins. Science. 2003 Sep 19;301(5640):1720–5.

79. de Gorter DJJ, Beuling EA, Kersseboom R, Middendorp S, van Gils JM, Hendriks RW, et al. Bruton's Tyrosine Kinase and Phospholipase Cγ2 Mediate Chemokine-Controlled B Cell Migration and Homing. Immunity. 2007 Jan 1;26(1):93–104.

80. Spaargaren M, Beuling EA, Rurup ML, Meijer HP, Klok MD, Middendorp S, et al. The B Cell Antigen Receptor Controls Integrin Activity through Btk and PLCγ2. J Exp Med. 2003 Nov 17;198(10):1539–50.

81. Contri A, Brunati AM, Trentin L, Cabrelle A, Miorin M, Cesaro L, et al. Chronic lymphocytic leukemia B cells contain anomalous Lyn tyrosine kinase, a putative contribution to defective apoptosis. J Clin Invest. 2005 Feb 1;115(2):369–78.

82. Buchner M, Fuchs S, Prinz G, Pfeifer D, Bartholomé K, Burger M, et al. Spleen Tyrosine Kinase Is Overexpressed and Represents a Potential Therapeutic Target in Chronic Lymphocytic Leukemia. Cancer Res. 2009 Jul 1;69(13):5424–32.

83. Herman SEM, Gordon AL, Hertlein E, Ramanunni A, Zhang X, Jaglowski S, et al. Bruton tyrosine kinase represents a promising therapeutic target for treatment of chronic lymphocytic leukemia and is effectively targeted by PCI-32765. Blood. 2011 Jun 9;117(23):6287–96.

84. Ponader S, Chen S-S, Buggy JJ, Balakrishnan K, Gandhi V, Wierda WG, et al. The Bruton tyrosine kinase inhibitor PCI-32765 thwarts chronic lymphocytic leukemia cell survival and tissue homing in vitro and in vivo. Blood. 2012 Feb 2;119(5):1182–9.

85. Furman RR, Asgary Z, Mascarenhas JO, Liou H-C, Schattner EJ. Modulation of NF-κB Activity and Apoptosis in Chronic Lymphocytic Leukemia B Cells. J Immunol. 2000 Feb 15;164(4):2200–6.

86. Muzio M, Apollonio B, Scielzo C, Frenquelli M, Vandoni I, Boussiotis V, et al. Constitutive activation of distinct BCR-signaling pathways in a subset of CLL patients: a molecular signature of anergy. Blood. 2008 Jul 1;112(1):188–95.

87. Krysov S, Dias S, Paterson A, Mockridge CI, Potter KN, Smith K-A, et al. Surface IgM stimulation induces MEK1/2-dependent MYC expression in chronic lymphocytic leukemia cells. Blood. 2012 Jan 5;119(1):170–9.

88. Ringshausen I, Schneller F, Bogner C, Hipp S, Duyster J, Peschel C, et al. Constitutively activated phosphatidylinositol-3 kinase (PI-3K) is involved in the defect of apoptosis in B-CLL: association with protein kinase Cδ. Blood. 2002 Nov 15;100(10):3741–8.

89. Niedermeier M, Hennessy BT, Knight ZA, Henneberg M, Hu J, Kurtova AV, et al. Isoform-selective phosphoinositide 3′-kinase inhibitors inhibit CXCR4 signaling and overcome stromal cell–mediated drug resistance in chronic lymphocytic leukemia: a novel therapeutic approach. Blood. 2009 May 28;113(22):5549–57.

90. Herman SEM, Gordon AL, Wagner AJ, Heerema NA, Zhao W, Flynn JM, et al. Phosphatidylinositol 3-kinase-δ inhibitor CAL-101 shows promising preclinical activity in

chronic lymphocytic leukemia by antagonizing intrinsic and extrinsic cellular survival signals. Blood. 2010 Sep 23;116(12):2078–88.

91. Chen L, Huynh L, Apgar J, Tang L, Rassenti L, Weiss A, et al. ZAP-70 enhances IgM signaling independent of its kinase activity in chronic lymphocytic leukemia. Blood. 2008 Mar 1;111(5):2685–92.

92. Richardson SJ, Matthews C, Catherwood MA, Alexander HD, Carey BS, Farrugia J, et al. ZAP-70 expression is associated with enhanced ability to respond to migratory and survival signals in B-cell chronic lymphocytic leukemia (B-CLL). Blood. 2006 May 1;107(9):3584–92.

93. Seifert M, Scholtysik R, Küppers R. Origin and Pathogenesis of B Cell Lymphomas. In: Küppers R, editor. Lymphoma: Methods and Protocols [Internet]. New York, NY: Springer; 2019 [cited 2020 Dec 30]. p. 1–33. (Methods in Molecular Biology). Available from: https://doi.org/10.1007/978-1-4939-9151-8_1

94. Blombery PA, Wall M, Seymour JF. The molecular pathogenesis of B-cell non-Hodgkin lymphoma. Eur J Haematol. 2015;95(4):280–93.

95. Young RM, Phelan JD, Wilson WH, Staudt LM. Pathogenic B-cell receptor signaling in lymphoid malignancies: New insights to improve treatment. Immunol Rev. 2019;291(1):190–213.

96. Pedersen IM, Reed J. Microenvironmental Interactions and Survival of CLL B-cells. Leuk Lymphoma. 2004 Jan 1;45(12):2365–72.

97. Buchner M, Baer C, Prinz G, Dierks C, Burger M, Zenz T, et al. Spleen tyrosine kinase inhibition prevents chemokine- and integrin-mediated stromal protective effects in chronic lymphocytic leukemia. Blood. 2010 Jun 3;115(22):4497–506.

98. Hoellenriegel J, Meadows SA, Sivina M, Wierda WG, Kantarjian H, Keating MJ, et al. The phosphoinositide 3′-kinase delta inhibitor, CAL-101, inhibits B-cell receptor signaling and chemokine networks in chronic lymphocytic leukemia. Blood. 2011 Sep 29;118(13):3603–12.

99. Brugnoni D, Rossi G, Tucci A, Cattaneo R, Airo P. Study of CD40 ligand expression in B-cell chronic lymphocytic leukemia. Haematologica. 1995 Jan 1;80(5):440–2.

100. Younes A, Snell V, Consoli U, Clodi K, Zhao S, Palmer JL, et al. Elevated levels of biologically active soluble CD40 ligand in the serum of patients with chronic lymphocytic leukaemia. Br J Haematol. 1998;100(1):135–41.

101. von Bergwelt-Baildon M, Maecker B, Schultze J, Gribben JG. CD40 activation: potential for specific immunotherapy in B-CLL. Ann Oncol. 2004 Jun 1;15(6):853–7.

102. Kitada S, Zapata JM, Andreeff M, Reed JC. Bryostatin and CD40-ligand enhance apoptosis resistance and induce expression of cell survival genes in B-cell chronic lymphocytic leukaemia. Br J Haematol. 1999;106(4):995–1004.

103. Buhmann R, Nolte A, Westhaus D, Emmerich B, Hallek M. CD40-activated B-cell chronic lymphocytic leukemia cells for tumor immunotherapy: stimulation of allogeneic versus autologous T cells generates different types of effector cells. Blood. 1999 Mar 15;93(6):1992–2002.

104. Haiat S, Billard C, Quiney C, Ajchenbaum-Cymbalista F, Kolb J-P. Role of BAFF and APRIL in human B-cell chronic lymphocytic leukaemia. Immunology. 2006;118(3):281–92.

105. Long BW, Witte PL, Abraham GN, Gregory SA, Plate JM. Apoptosis and interleukin 7 gene expression in chronic B-lymphocytic leukemia cells. Proc Natl Acad Sci. 1995 Feb 28;92(5):1416–20.

106. Cordingley FT, Hoffbrand AV, Heslop HE, Turner M, Bianchi A, Reittie JE, et al. TUMOUR NECROSIS FACTOR AS AN AUTOCRINE TUMOUR GROWTH FACTOR FOR CHRONIC B-CELL MALIGNANCIES. The Lancet. 1988 Apr 30;331(8592):969–71.

107. Farahani M, Treweeke AT, Toh CH, Till KJ, Harris RJ, Cawley JC, et al. Autocrine VEGF mediates the antiapoptotic effect of CD154 on CLL cells. Leukemia. 2005 Apr;19(4):524–30.

108. Chen H, Treweeke AT, West DC, Till KJ, Cawley JC, Zuzel M, et al. In vitro and in vivo production of vascular endothelial growth factor by chronic lymphocytic leukemia cells. Blood. 2000 Nov 1;96(9):3181–7.

109. Ferrajoli A, Keating MJ, Manshouri T, Giles FJ, Dey A, Estrov Z, et al. The clinical significance of tumor necrosis factor-alpha plasma level in patients having chronic lymphocytic leukemia. Blood. 2002 Aug 15;100(4):1215–9.

110. Lee YK, Shanafelt TD, Bone ND, Strege AK, Jelinek DF, Kay NE. VEGF receptors on chronic lymphocytic leukemia (CLL) B cells interact with STAT 1 and 3: implication for apoptosis resistance. Leukemia. 2005 Apr;19(4):513–23.

111. Ferrajoli A, Manshouri T, Estrov Z, Keating MJ, O'Brien S, Lerner S, et al. High Levels of Vascular Endothelial Growth Factor Receptor-2 Correlate with Shortened Survival in Chronic Lymphocytic Leukemia. Clin Cancer Res. 2001 Apr 1;7(4):795–9.

112. Douglas RS, Capocasale RJ, Lamb RJ, Nowell PC, Moore JS. Chronic Lymphocytic Leukemia B Cells Are Resistant to the Apoptotic Effects of Transforming Growth Factor-β. Blood. 1997 Feb 1;89(3):941–7.

113. Aguilar-Hernandez MM, Blunt MD, Dobson R, Yeomans A, Thirdborough S, Larrayoz M, et al. IL-4 enhances expression and function of surface IgM in CLL cells. Blood. 2016 Jun 16;127(24):3015–25.

114. Guo B, Zhang L, Chiorazzi N, Rothstein TL. IL-4 rescues surface IgM expression in chronic lymphocytic leukemia. Blood. 2016 Jul 28;128(4):553–62.

115. Wagner SD. IL-4, IgM, and resistance to BTKi and PI3Kδi in CLL. Blood. 2016 Jun 16;127(24):2944–6.

116. Rothstein TL, Guo B. Receptor crosstalk: reprogramming B cell receptor signalling to an alternate pathway results in expression and secretion of the autoimmunity-associated cytokine, osteopontin. J Intern Med. 2009 Jun;265(6):632–43.

117. Burger JA, Tsukada N, Burger M, Zvaifler NJ, Dell'Aquila M, Kipps TJ. Blood-derived nurse-like cells protect chronic lymphocytic leukemia B cells from spontaneous apoptosis through stromal cell-derived factor-1. Blood. 2000 Oct 15;96(8):2655–63.

118. Pedersen IM, Reed J. Microenvironmental Interactions and Survival of CLL B-cells. Leuk Lymphoma. 2004 Jan 1;45(12):2365–72.

119. Eble JA, Haier J. Integrins in cancer treatment. Curr Cancer Drug Targets. 2006 Mar;6(2):89–105.

120. Sivina M, Hartmann E, Kipps TJ, Rassenti L, Krupnik D, Lerner S, et al. CCL3 (MIP-1α) plasma levels and the risk for disease progression in chronic lymphocytic leukemia. Blood. 2011 Feb 3;117(5):1662–9.

121. Greer JP, Arber DA, Glader BE, List AF, Means RM, Rodgers GM. Wintrobe's Clinical Hematology. 14th ed. Lippincott Williams & Wilkins; 2018. 8288 p.

122. Yoon J-Y, Lafarge S, Dawe D, Lakhi S, Kumar R, Morales C, et al. Association of interleukin-6 and interleukin-8 with poor prognosis in elderly patients with chronic lymphocytic leukemia. Leuk Lymphoma. 2012 Sep 1;53(9):1735–42.

123. Ghosh AK, Secreto C, Boysen J, Sassoon T, Shanafelt TD, Mukhopadhyay D, et al. The novel receptor tyrosine kinase Axl is constitutively active in B-cell chronic lymphocytic leukemia and acts as a docking site of nonreceptor kinases: implications for therapy. Blood. 2011 Feb 10;117(6):1928–37.

124. Kurtova AV, Balakrishnan K, Chen R, Ding W, Schnabl S, Quiroga MP, et al. Diverse marrow stromal cells protect CLL cells from spontaneous and drug-induced apoptosis: development of a reliable and reproducible system to assess stromal cell adhesion-mediated drug resistance. Blood. 2009 Nov 12;114(20):4441–50.

125. Cols M, Barra CM, He B, Puga I, Xu W, Chiu A, et al. Stromal Endothelial Cells Establish a Bidirectional Crosstalk with Chronic Lymphocytic Leukemia Cells through the TNF-Related Factors BAFF, APRIL, and CD40L. J Immunol. 2012 Jun 15;188(12):6071–83.

126. Seke Etet PF, Vecchio L, Nwabo Kamdje AH. Interactions between bone marrow stromal microenvironment and B-chronic lymphocytic leukemia cells: Any role for Notch, Wnt and Hh signaling pathways? Cell Signal. 2012 Jul 1;24(7):1433–43.

127. Forconi F, Moss P. Perturbation of the normal immune system in patients with CLL. Blood. 2015 Jul 30;126(5):573–81.

128. Rossmann ED, Lewin N, Jeddi-Tehrani M, Österborg A, Mellstedt H. Intracellular T cell cytokines in patients with B cell chronic lymphocytic leukaemia (B-CLL). Eur J Haematol. 2002;68(5):299–306.

129. Byrd JC, Furman RR, Coutre SE, Flinn IW, Burger JA, Blum KA, et al. Targeting BTK with Ibrutinib in Relapsed Chronic Lymphocytic Leukemia. N Engl J Med. 2013 Jul 4;369(1):32–42.

130. Green DR, Llambi F. Cell Death Signaling. Cold Spring Harb Perspect Biol [Internet]. 2015 Dec [cited 2020 Apr 21];7(12). Available from: https://www.ncbi.nlm.nih.gov/pmc/articles/PMC4665079/

131. Lavrik I, Golks A, Krammer PH. Death receptor signaling. J Cell Sci. 2005 Jan 15;118(2):265–7.

132. Pepper C, Hoy T, Bentley P. Elevated Bcl-2/Bax Are a Consistent Feature of Apoptosis Resistance in B-cell Chronic Lymphocytic Leukaemia and Are Correlated with In Vivo Chemoresistance. Leuk Lymphoma. 1998 Jan 1;28(3–4):355–61.

133. Pepper C, Lin TT, Pratt G, Hewamana S, Brennan P, Hiller L, et al. Mcl-1 expression has in vitro and in vivo significance in chronic lymphocytic leukemia and is associated with other poor prognostic markers. Blood. 2008 Nov 1;112(9):3807–17.

134. Petlickovski A, Laurenti L, Li X, Marietti S, Chiusolo P, Sica S, et al. Sustained signaling through the B-cell receptor induces Mcl-1 and promotes survival of chronic lymphocytic leukemia B cells. Blood. 2005 Jun 15;105(12):4820–7.

135. Chatterjee N, Walker GC. Mechanisms of DNA damage, repair, and mutagenesis. Environ Mol Mutagen. 2017;58(5):235–63.

136. Morgan MA, Lawrence TS. Molecular Pathways: Overcoming Radiation Resistance by Targeting DNA Damage Response Pathways. Clin Cancer Res Off J Am Assoc Cancer Res. 2015 Jul 1;21(13):2898–904.

137. Canman CE, Lim D-S, Cimprich KA, Taya Y, Tamai K, Sakaguchi K, et al. Activation of the ATM Kinase by Ionizing Radiation and Phosphorylation of p53. Science. 1998 Sep 11;281(5383):1677–9.

138. Rosenwald A, Chuang EY, Davis RE, Wiestner A, Alizadeh AA, Arthur DC, et al. Fludarabine treatment of patients with chronic lymphocytic leukemia induces a p53-dependent gene expression response. Blood. 2004 Sep 1;104(5):1428–34.

139. Ricci F, Tedeschi A, Morra E, Montillo M. Fludarabine in the treatment of chronic lymphocytic leukemia: a review. Ther Clin Risk Manag. 2009;5:187–207.

140. Hallek M, Fischer K, Fingerle-Rowson G, Fink A, Busch R, Mayer J, et al. Addition of rituximab to fludarabine and cyclophosphamide in patients with chronic lymphocytic leukaemia: a randomised, open-label, phase 3 trial. The Lancet. 2010 Oct 2;376(9747):1164–74.

141. Hallek M, Cheson BD, Catovsky D, Caligaris-Cappio F, Dighiero G, Döhner H, et al. iwCLL guidelines for diagnosis, indications for treatment, response assessment, and supportive management of CLL. Blood. 2018 Jun 21;131(25):2745–60.

142. Byrd JC, Furman RR, Coutre SE, Burger JA, Blum KA, Coleman M, et al. Three-year follow-up of treatment-naïve and previously treated patients with CLL and SLL receiving single-agent ibrutinib. Blood. 2015 Apr 16;125(16):2497–506.

143. Kovacs G, Robrecht S, Fink AM, Bahlo J, Cramer P, von Tresckow J, et al. Minimal Residual Disease Assessment Improves Prediction of Outcome in Patients With Chronic Lymphocytic Leukemia (CLL) Who Achieve Partial Response: Comprehensive Analysis of Two Phase III Studies of the German CLL Study Group. J Clin Oncol. 2016 Aug 29;34(31):3758–65.

144. Pettitt AR. Mechanism of action of purine analogues in chronic lymphocytic leukaemia. Br J Haematol. 2003;121(5):692–702.

145. Sandoval A, Consoli U, Plunkett W. Fludarabine-mediated inhibition of nucleotide excision repair induces apoptosis in quiescent human lymphocytes. Clin Cancer Res. 1996 Oct 1;2(10):1731–41.

146. Yamauchi T, Nowak BJ, Keating MJ, Plunkett W. DNA Repair Initiated in Chronic Lymphocytic Leukemia Lymphocytes by 4-Hydroperoxycyclophosphamide Is Inhibited by Fludarabine and Clofarabine. Clin Cancer Res. 2001 Nov 1;7(11):3580–9.

147. Niederle N, Megdenberg D, Balleisen L, Heit W, Knauf W, Weiß J, et al. Bendamustine compared to fludarabine as second-line treatment in chronic lymphocytic leukemia. Ann Hematol. 2013 May 1;92(5):653–60.

148. Eichhorst B, Fink A-M, Bahlo J, Busch R, Kovacs G, Maurer C, et al. First-line chemoimmunotherapy with bendamustine and rituximab versus fludarabine, cyclophosphamide, and rituximab in patients with advanced chronic lymphocytic leukaemia (CLL10): an international, open-label, randomised, phase 3, non-inferiority trial. Lancet Oncol. 2016 Jul 1;17(7):928–42.

149. Pan Z, Scheerens H, Li S-J, Schultz BE, Sprengeler PA, Burrill LC, et al. Discovery of Selective Irreversible Inhibitors for Bruton's Tyrosine Kinase. ChemMedChem. 2007 Jan 15;2(1):58–61.

150. Honigberg LA, Smith AM, Sirisawad M, Verner E, Loury D, Chang B, et al. The Bruton tyrosine kinase inhibitor PCI-32765 blocks B-cell activation and is efficacious in models of autoimmune disease and B-cell malignancy. Proc Natl Acad Sci U S A. 2010 Jul 20;107(29):13075–80.

151. Byrd JC, Furman RR, Coutre SE, Flinn IW, Burger JA, Blum K, et al. Ibrutinib Treatment for First-Line and Relapsed/Refractory Chronic Lymphocytic Leukemia: Final Analysis of the Pivotal Phase Ib/II PCYC-1102 Study. Clin Cancer Res. 2020 Aug 1;26(15):3918–27.

152. Burger JA, Tedeschi A, Barr PM, Robak T, Owen C, Ghia P, et al. Ibrutinib as Initial Therapy for Patients with Chronic Lymphocytic Leukemia. N Engl J Med. 2015 Dec 17;373(25):2425–37.

153. Byrd JC, Furman RR, Coutre S, Flinn IW, Burger JA, Blum KA, et al. The Bruton's Tyrosine Kinase (BTK) Inhibitor Ibrutinib (PCI-32765) Promotes High Response Rate, Durable Remissions, and Is Tolerable in Treatment Naïve (TN) and Relapsed or Refractory (RR) Chronic Lymphocytic Leukemia (CLL) or Small Lymphocytic Lymphoma (SLL) Patients Including Patients with High-Risk (HR) Disease: New and Updated Results of 116 Patients in a Phase Ib/II Study. Blood. 2012 Nov 16;120(21):189–189.

154. Woyach JA, Smucker K, Smith LL, Lozanski A, Zhong Y, Ruppert AS, et al. Prolonged lymphocytosis during ibrutinib therapy is associated with distinct molecular characteristics and does not indicate a suboptimal response to therapy. Blood. 2014 Mar 20;123(12):1810–7.

155. Chen S-S, Chang BY, Chang S, Tong T, Ham S, Sherry B, et al. BTK inhibition results in impaired CXCR4 chemokine receptor surface expression, signaling and function in chronic lymphocytic leukemia. Leukemia. 2016 Apr;30(4):833–43.

156. Brown JR, Byrd JC, Coutre SE, Benson DM, Flinn IW, Wagner-Johnston ND, et al. Idelalisib, an inhibitor of phosphatidylinositol 3-kinase p110δ, for relapsed/refractory chronic lymphocytic leukemia. Blood. 2014 May 29;123(22):3390–7.

157. Furman RR, Sharman JP, Coutre SE, Cheson BD, Pagel JM, Hillmen P, et al. Idelalisib and Rituximab in Relapsed Chronic Lymphocytic Leukemia. N Engl J Med. 2014 Mar 13;370(11):997–1007.

158. Jones JA, Robak T, Brown JR, Awan FT, Badoux X, Coutre S, et al. Efficacy and safety of idelalisib in combination with ofatumumab for previously treated chronic lymphocytic leukaemia: an open-label, randomised phase 3 trial. Lancet Haematol. 2017 Mar 1;4(3):e114–26.

159. Del Gaizo Moore V, Brown JR, Certo M, Love TM, Novina CD, Letai A. Chronic lymphocytic leukemia requires BCL2 to sequester prodeath BIM, explaining sensitivity to BCL2 antagonist ABT-737. J Clin Invest. 2007 Jan 2;117(1):112–21.

160. Souers AJ, Leverson JD, Boghaert ER, Ackler SL, Catron ND, Chen J, et al. ABT-199, a potent and selective BCL-2 inhibitor, achieves antitumor activity while sparing platelets. Nat Med. 2013 Feb;19(2):202–8.

161. Stilgenbauer S, Eichhorst B, Schetelig J, Coutre S, Seymour JF, Munir T, et al. Venetoclax in relapsed or refractory chronic lymphocytic leukaemia with 17p deletion: a multicentre, open-label, phase 2 study. Lancet Oncol. 2016 Jun 1;17(6):768–78.

162. Patel V, Balakrishnan K, Bibikova E, Ayres M, Keating MJ, Wierda WG, et al. Comparison of Acalabrutinib, A Selective Bruton Tyrosine Kinase Inhibitor, with Ibrutinib in Chronic Lymphocytic Leukemia Cells. Clin Cancer Res. 2017 Jul 15;23(14):3734–43.

163. Barf T, Covey T, Izumi R, Kar B van de, Gulrajani M, Lith B van, et al. Acalabrutinib (ACP-196): A Covalent Bruton Tyrosine Kinase Inhibitor with a Differentiated Selectivity and In Vivo Potency Profile. J Pharmacol Exp Ther. 2017 Nov 1;363(2):240–52.

164. Byrd JC, Harrington B, O'Brien S, Jones JA, Schuh A, Devereux S, et al. Acalabrutinib (ACP-196) in Relapsed Chronic Lymphocytic Leukemia. N Engl J Med. 2016 Jan 28;374(4):323–32.

165. Byrd JC, Wierda WG, Schuh A, Devereux S, Chaves JM, Brown JR, et al. Acalabrutinib monotherapy in patients with relapsed/refractory chronic lymphocytic leukemia: updated phase 2 results. Blood. 2020 Apr 9;135(15):1204–13.

166. Awan FT, Schuh A, Brown JR, Furman RR, Pagel JM, Hillmen P, et al. Acalabrutinib monotherapy in patients with chronic lymphocytic leukemia who are intolerant to ibrutinib. Blood Adv. 2019 May 14;3(9):1553–62.

167. Woyach JA, Blachly JS, Rogers KA, Bhat SA, Jianfar M, Lozanski G, et al. Acalabrutinib plus Obinutuzumab in Treatment-Naïve and Relapsed/Refractory Chronic Lymphocytic Leukemia. Cancer Discov. 2020 Mar 1;10(3):394–405.

168. Flinn IW, O'Brien S, Kahl B, Patel M, Oki Y, Foss FF, et al. Duvelisib, a novel oral dual inhibitor of PI3K-δ,γ, is clinically active in advanced hematologic malignancies. Blood. 2018 Feb 22;131(8):877–87.

169. Flinn IW, Hillmen P, Montillo M, Nagy Z, Illés Á, Etienne G, et al. The phase 3 DUO trial: duvelisib vs ofatumumab in relapsed and refractory CLL/SLL. Blood. 2018 Dec 6;132(23):2446–55.

170. Furman RR, Cheng S, Lu P, Setty M, Perez AR, Guo A, et al. Ibrutinib Resistance in Chronic Lymphocytic Leukemia. N Engl J Med. 2014 Jun 12;370(24):2352–4.

171. Woyach JA, Furman RR, Liu T-M, Ozer HG, Zapatka M, Ruppert AS, et al. Resistance Mechanisms for the Bruton's Tyrosine Kinase Inhibitor Ibrutinib. N Engl J Med. 2014 Jun 12;370(24):2286–94.

172. Liu T-M, Woyach JA, Zhong Y, Lozanski A, Lozanski G, Dong S, et al. Hypermorphic mutation of phospholipase C, γ2 acquired in ibrutinib-resistant CLL confers BTK independency upon B-cell receptor activation. Blood. 2015 Jul 2;126(1):61–8.

173. Woyach JA, Ruppert AS, Guinn D, Lehman A, Blachly JS, Lozanski A, et al. BTKC481S-Mediated Resistance to Ibrutinib in Chronic Lymphocytic Leukemia. J Clin Oncol. 2017 May 1;35(13):1437–43.

174. Ahn IE, Underbayev C, Albitar A, Herman SEM, Tian X, Maric I, et al. Clonal evolution leading to ibrutinib resistance in chronic lymphocytic leukemia. Blood. 2017 Mar 16;129(11):1469–79.

175. Burger JA, Landau DA, Taylor-Weiner A, Bozic I, Zhang H, Sarosiek K, et al. Clonal evolution in patients with chronic lymphocytic leukaemia developing resistance to BTK inhibition. Nat Commun. 2016 May 20;7:11589.

176. Kapoor I, Li Y, Sharma A, Zhu H, Bodo J, Xu W, et al. Resistance to BTK inhibition by ibrutinib can be overcome by preventing FOXO3a nuclear export and PI3K/AKT activation in B-cell lymphoid malignancies. Cell Death Dis [Internet]. 2019 Dec 4 [cited 2019 Dec 20];10(12). Available from: https://www.ncbi.nlm.nih.gov/pmc/articles/PMC6892912/

177. Gehrke I, Bouchard EDJ, Beiggi S, Poeppl AG, Johnston JB, Gibson SB, et al. On-Target Effect of FK866, a Nicotinamide Phosphoribosyl Transferase Inhibitor, by Apoptosis-Mediated Death in Chronic Lymphocytic Leukemia Cells. Clin Cancer Res. 2014 Sep 15;20(18):4861–72.

178. Johnston JB, Kabore AF, Strutinsky J, Hu X, Paul JT, Kropp DM, et al. Role of the TRAIL/APO2-L death receptors in chlorambucil- and fludarabine-induced apoptosis in chronic lymphocytic leukemia. Oncogene. 2003 Nov;22(51):8356–69.

179. Di Veroli GY, Fornari C, Wang D, Mollard S, Bramhall JL, Richards FM, et al. Combenefit: an interactive platform for the analysis and visualization of drug combinations. Bioinformatics. 2016 Sep 15;32(18):2866–8.

180. Loewe S. The problem of synergism and antagonism of combined drugs. Arzneimittelforschung. 1953 Jun;3(6):285–90.

181. ImageJ [Internet]. [cited 2020 Apr 2]. Available from: https://imagej.nih.gov/ij/

182. Chou T-C. Drug Combination Studies and Their Synergy Quantification Using the Chou-Talalay Method. Cancer Res. 2010 Jan 15;70(2):440–6.

183. Kost SEF, Saleh A, Mejia EM, Mostafizar M, Bouchard EDJ, Banerji V, et al. Transcriptional Modulation by Idelalisib Synergizes with Bendamustine in Chronic Lymphocytic Leukemia. Cancers [Internet]. 2019 Oct 9 [cited 2020 Jun 22];11(10). Available from: https://www.ncbi.nlm.nih.gov/pmc/articles/PMC6826782/

184. Morbach H, Schickel J-N, Cunningham-Rundles C, Conley ME, Reisli I, Franco JL, et al. CD19 controls TLR9 responses in human B cells. J Allergy Clin Immunol. 2016 Mar;137(3):889-898.e6.

185. Lu H, Huang H. FOXO1: A potential target for human diseases. Curr Drug Targets. 2011 Aug;12(9):1235–44.

186. Bruijn MJW de, Rip J, Ploeg EK van der, Greuningen LW van, Ta VTB, Kil LP, et al. Distinct and Overlapping Functions of TEC Kinase and BTK in B Cell Receptor Signaling. J Immunol. 2017 Apr 15;198(8):3058–68.

187. Talab F, Allen JC, Thompson V, Lin K, Slupsky JR. LCK Is an Important Mediator of B-Cell Receptor Signaling in Chronic Lymphocytic Leukemia Cells. Mol Cancer Res. 2013 May 1;11(5):541–54.

188. Fontán L, Melnick A. Molecular Pathways: Targeting MALT1 Paracaspase Activity in Lymphoma. Clin Cancer Res. 2013 Dec 15;19(24):6662–8.

189. Sen R. Control of B Lymphocyte Apoptosis by the Transcription Factor NF-κB. Immunity. 2006 Dec 1;25(6):871–83.

190. Gerondakis S, Siebenlist U. Roles of the NF-κB Pathway in Lymphocyte Development and Function. Cold Spring Harb Perspect Biol [Internet]. 2010 May [cited 2020 Jul 27];2(5). Available from: https://www.ncbi.nlm.nih.gov/pmc/articles/PMC2857169/

191. Roux PP, Richards SA, Blenis J. Phosphorylation of p90 Ribosomal S6 Kinase (RSK) Regulates Extracellular Signal-Regulated Kinase Docking and RSK Activity. Mol Cell Biol. 2003 Jul;23(14):4796–804.

192. Schouten GJ, Vertegaal AC, Whiteside ST, Israël A, Toebes M, Dorsman JC, et al. IkappaB alpha is a target for the mitogen-activated 90 kDa ribosomal S6 kinase. EMBO J. 1997 Jun 2;16(11):3133–44.

193. Dustin LB, Plas DR, Wong J, Hu YT, Soto C, Chan AC, et al. Expression of Dominant-Negative Src-Homology Domain 2-Containing Protein Tyrosine Phosphatase-1 Results in Increased Syk Tyrosine Kinase Activity and B Cell Activation. J Immunol. 1999 Mar 1;162(5):2717–24.

194. Chiang GG, Sefton BM. Specific Dephosphorylation of the Lck Tyrosine Protein Kinase at Tyr-394 by the SHP-1 Protein-tyrosine Phosphatase. J Biol Chem. 2001 Jun 22;276(25):23173–8.

195. Ueno H, Kondo E, Yamamoto-Honda R, Tobe K, Nakamoto T, Sasaki K, et al. Association of Insulin Receptor Substrate Proteins with Bcl-2 and Their Effects on Its Phosphorylation and Antiapoptotic Function. Mol Biol Cell. 2000 Feb;11(2):735–46.

196. Lee K, Heffington L, Jellusova J, Nam KT, Raybuck A, Cho SH, et al. Requirement for Rictor in homeostasis and function of mature B lymphoid cells. Blood. 2013 Oct 3;122(14):2369–79.

197. Brunet A, Park J, Tran H, Hu LS, Hemmings BA, Greenberg ME. Protein Kinase SGK Mediates Survival Signals by Phosphorylating the Forkhead Transcription Factor FKHRL1 (FOXO3a). Mol Cell Biol. 2001 Feb 1;21(3):952–65.

198. Wen AY, Sakamoto KM, Miller LS. The Role of the Transcription Factor CREB in Immune Function. J Immunol Baltim Md 1950. 2010 Dec 1;185(11):6413–9.

199. Blois JT, Mataraza JM, Mecklenbraüker I, Tarakhovsky A, Chiles TC. B Cell Receptor-induced cAMP-response Element-binding Protein Activation in B Lymphocytes Requires Novel Protein Kinase Cδ. J Biol Chem. 2004 Jul 16;279(29):30123–32.

200. Du K, Montminy M. CREB Is a Regulatory Target for the Protein Kinase Akt/PKB. J Biol Chem. 1998 Dec 4;273(49):32377–9.

201. Tan Y, Rouse J, Zhang A, Cariati S, Cohen P, Comb MJ. FGF and stress regulate CREB and ATF-1 via a pathway involving p38 MAP kinase and MAPKAP kinase-2. EMBO J. 1996 Sep 1;15(17):4629–42.

202. Wang J-M, Chao J-R, Chen W, Kuo M-L, Yen JJ-Y, Yang-Yen H-F. The Antiapoptotic Gene mcl-1 Is Up-Regulated by the Phosphatidylinositol 3-Kinase/Akt Signaling Pathway through a Transcription Factor Complex Containing CREB. Mol Cell Biol. 1999 Sep 1;19(9):6195–206.

203. Oakes SA, Candotti F, Johnston JA, Chen Y-Q, Ryan JJ, Taylor N, et al. Signaling via IL-2 and IL-4 in JAK3-Deficient Severe Combined Immunodeficiency Lymphocytes: JAK3-Dependent and Independent Pathways. Immunity. 1996 Dec 1;5(6):605–15.

204. Brugarolas J, Chandrasekaran C, Gordon JI, Beach D, Jacks T, Hannon GJ. Radiation-induced cell cycle arrest compromised by p21 deficiency. Nature. 1995 Oct;377(6549):552–7.

205. Barr AR, Cooper S, Heldt FS, Butera F, Stoy H, Mansfeld J, et al. DNA damage during S-phase mediates the proliferation-quiescence decision in the subsequent G1 via p21 expression. Nat Commun [Internet]. 2017 Mar 20 [cited 2020 Jul 28];8. Available from: https://www.ncbi.nlm.nih.gov/pmc/articles/PMC5364389/

206. Ferrer G, Bosch R, Hodgson K, Tejero R, Roué G, Colomer D, et al. B cell activation through CD40 and IL4R ligation modulates the response of chronic lymphocytic leukaemia cells to BAFF and APRIL. Br J Haematol. 2014;164(4):570–8.

207. Rozovski U, Wu JY, Harris DM, Liu Z, Li P, Hazan-Halevy I, et al. Stimulation of the B-cell receptor activates the JAK2/STAT3 signaling pathway in chronic lymphocytic leukemia cells. Blood. 2014 Jun 12;123(24):3797–802.

208. Severin F, Frezzato F, Visentin A, Martini V, Trimarco V, Carraro S, et al. In Chronic Lymphocytic Leukemia the JAK2/STAT3 Pathway Is Constitutively Activated and Its Inhibition Leads to CLL Cell Death Unaffected by the Protective Bone Marrow Microenvironment. Cancers. 2019 Dec;11(12):1939.

209. Montresor A, Toffali L, Rigo A, Ferrarini I, Vinante F, Laudanna C. CXCR4- and BCR-triggered integrin activation in B-cell chronic lymphocytic leukemia cells depends on JAK2-activated Bruton's tyrosine kinase. Oncotarget. 2018 Oct 1;9(80):35123–40.

210. Keegan AD, Zamoran J. Regulation of gene expression, growth, and cell survival by IL-4: Contribution of multiple signaling pathways. Cell Res. 1998 Mar;8(1):1–13.

211. Mingari MC, Gerosa F, Carra G, Accolla RS, Moretta A, Zubler RH, et al. Human interleukin-2 promotes proliferation of activated B cells via surface receptors similar to those of activated T cells. Nature. 1984 Dec;312(5995):641–3.

212. Arenas-Ramirez N, Woytschak J, Boyman O. Interleukin-2: Biology, Design and Application. Trends Immunol. 2015 Dec 1;36(12):763–77.

213. Furman RR, Asgary Z, Mascarenhas JO, Liou H-C, Schattner EJ. Modulation of NF-κB Activity and Apoptosis in Chronic Lymphocytic Leukemia B Cells. J Immunol. 2000 Feb 15;164(4):2200–6.

214. Elgueta R, Benson MJ, de Vries VC, Wasiuk A, Guo Y, Noelle RJ. Molecular mechanism and function of CD40/CD40L engagement in the immune system. Immunol Rev [Internet]. 2009 May [cited 2020 Jul 28];229(1). Available from: https://www.ncbi.nlm.nih.gov/pmc/articles/PMC3826168/

215. Burger JA. Nurture versus Nature: The Microenvironment in Chronic Lymphocytic Leukemia. Hematology. 2011 Dec 10;2011(1):96–103.

216. Landau DA, Sun C, Rosebrock D, Herman SEM, Fein J, Sivina M, et al. The evolutionary landscape of chronic lymphocytic leukemia treated with ibrutinib targeted therapy. Nat Commun [Internet]. 2017 Dec 19 [cited 2020 Jul 31];8. Available from: https://www.ncbi.nlm.nih.gov/pmc/articles/PMC5736707/

217. Palma M, Krstic A, Perez LP, Berglöf A, Meinke S, Wang Q, et al. Ibrutinib induces rapid down-regulation of inflammatory markers and altered transcription of chronic lymphocytic leukaemia-related genes in blood and lymph nodes. Br J Haematol. 2018;183(2):212–24.

218. Zarubin T, Han J. Activation and signaling of the p38 MAP kinase pathway. Cell Res. 2005 Jan;15(1):11–8.

219. Cuenda A, Rousseau S. p38 MAP-Kinases pathway regulation, function and role in human diseases. Biochim Biophys Acta BBA - Mol Cell Res. 2007 Aug 1;1773(8):1358–75.

220. Ringshausen I, Dechow T, Schneller F, Weick K, Oelsner M, Peschel C, et al. Constitutive activation of the MAPkinase p38 is critical for MMP-9 production and survival of B-CLL cells on bone marrow stromal cells. Leukemia. 2004 Dec;18(12):1964–70.

221. Zou X, Blank M. Targeting p38 MAP kinase signaling in cancer through post-translational modifications. Cancer Lett. 2017 Jan 1;384:19–26.

222. Simões AES, Rodrigues CMP, Borralho PM. The MEK5/ERK5 signalling pathway in cancer: a promising novel therapeutic target. Drug Discov Today. 2016 Oct 1;21(10):1654–63.

223. Nishimoto S, Nishida E. MAPK signalling: ERK5 versus ERK1/2. EMBO Rep. 2006 Aug;7(8):782–6.

224. Scheers E, Leclercq L, Jong J de, Bode N, Bockx M, Laenen A, et al. Absorption, Metabolism, and Excretion of Oral 14C Radiolabeled Ibrutinib: An Open-Label, Phase I, Single-Dose Study in Healthy Men. Drug Metab Dispos. 2015 Feb 1;43(2):289–97.

225. Hussaarts KGAM, Veerman GDM, Jansman FGA, van Gelder T, Mathijssen RHJ, van Leeuwen RWF. Clinically relevant drug interactions with multikinase inhibitors: a review. Ther Adv Med Oncol [Internet]. 2019 Jan 4 [cited 2020 Aug 14];11. Available from: https://www.ncbi.nlm.nih.gov/pmc/articles/PMC6322107/

226. Rothwarf DM, Zandi E, Natoli G, Karin M. IKK-γ is an essential regulatory subunit of the IκB kinase complex. Nature. 1998 Sep;395(6699):297–300.

227. Peterson TR, Laplante M, Thoreen CC, Sancak Y, Kang SA, Kuehl WM, et al. DEPTOR is an mTOR Inhibitor Whose Frequent Overexpression in Multiple Myeloma Cells Promotes their Survival. Cell. 2009 May 29;137(5):873–86.

228. Jabłońska E, Białopiotrowicz E, Szydłowski M, Prochorec-Sobieszek M, Juszczyński P, Szumera-Ciećkiewicz A. DEPTOR is a microRNA-155 target regulating migration and cytokine production in diffuse large B-cell lymphoma cells. Exp Hematol [Internet]. 2020 Jul 20 [cited 2020 Aug 14]; Available from: http://www.sciencedirect.com/science/article/pii/S0301472X20302708

229. Klein G, Lindahl T, Jondal M, Leibold W, Menézes J, Nilsson K, et al. Continuous Lymphoid Cell Lines with Characteristics of B Cells (Bone-Marrow-Derived), Lacking the Epstein-Barr Virus Genome and Derived from Three Human Lymphomas. Proc Natl Acad Sci U S A. 1974 Aug;71(8):3283–6.

230. Farrell PJ, Allan GJ, Shanahan F, Vousden KH, Crook T. p53 is frequently mutated in Burkitt's lymphoma cell lines. EMBO J. 1991 Oct;10(10):2879–87.

231. Molyneux EM, Rochford R, Griffin B, Newton R, Jackson G, Menon G, et al. Burkitt's lymphoma. The Lancet. 2012 Mar 31;379(9822):1234–44.

232. Liston DR, Davis M. Clinically Relevant Concentrations of Anticancer Drugs: A Guide for Nonclinical Studies. Clin Cancer Res. 2017 Jul 15;23(14):3489–98.

233. de Rooij MFM, Kuil A, Kater AP, Kersten MJ, Pals ST, Spaargaren M. Ibrutinib and idelalisib synergistically target BCR-controlled adhesion in MCL and CLL: a rationale for combination therapy. Blood. 2015 Apr 2;125(14):2306–9.

234. Niemann CU, Mora-Jensen HI, Dadashian EL, Krantz F, Covey T, Chen S-S, et al. Combined BTK and PI3Kδ inhibition with acalabrutinib and ACP-319 improves survival and tumor control in CLL mouse model. Clin Cancer Res Off J Am Assoc Cancer Res. 2017 Oct 1;23(19):5814–23.

235. Spriano F, Tarantelli C, Gaudio E, Gerlach MM, Priebe V, Cascione L, et al. Single and combined BTK and PI3Kδ inhibition with acalabrutinib and ACP-319 in pre-clinical models of aggressive lymphomas. Br J Haematol. 2019;187(5):595–601.

236. Chiron D, Liberto MD, Martin P, Huang X, Sharman J, Blecua P, et al. Cell-Cycle Reprogramming for PI3K Inhibition Overrides a Relapse-Specific C481S BTK Mutation Revealed by Longitudinal Functional Genomics in Mantle Cell Lymphoma. Cancer Discov. 2014 Sep 1;4(9):1022–35.

APPENDIX

Supplementary Table 1: Genes within the IL-4 pathway with reduced expression in IBR10^2 cells relative to BJABs.

Pathway	Overall Significance	Targets	Fold change	Brief description of function/roles
IL-4 signalling pathway	**2.44**	IRS1	**4.14**	IRS1 is an adapter protein and a substrate for the insulin receptor (INSR). IRS1 overexpression has been shown to enhance the anti-apoptotic function of bcl-2 and it also associates with bcl-XL[195]. IRS1 stimulation also activates the PI3K-AKT pathway[195].
		JAK3	**2.83**	JAK3 belongs to the JAK family of kinases. JAK3 has been shown to enhance IL-4 signalling in B-cells[203].
		IL4R	**2.44**	IL-4R encodes the IL-4 receptor, which when ligated in CLL cells, signals through the PI3K-AKT pathway[206]. IL-4 (along with CD40) stimulation has been shown to increase expression levels of the receptors of the pro-survival TNF superfamily members BAFF and APRIL in CLL cells[206]. This increase correlated with an increase in CLL cell viability.
		JAK2	**2.29**	JAK2 plays an important role in the JAK/STAT pathway, which is important to CLL cell survival. BCR ligation activates JAK3 and its downstream target STAT3; STAT3 is constitutively phosphorylated in CLL cells[207,208]. JAK inhibition has been shown to activate SHP-1 and boost ibrutinib's apoptotic activity in CLL-BMSC co-culture[208]. Finally, JAK2 has been shown to activate BTK and contribute to integrin activation in CLL cells, after CXCL12 treatment[209].
		IL2RG	**2.25**	IL2RG encodes the γ chain of the IL-2 receptor, which associates with IL-4R, upon IL-4 binding[210]. IL-2 signalling has been shown to promote B-cell proliferation and to signal through the PI3K-AKT, MAPK-ERK and JAK-STAT pathways[211,212].
		NFKB1	**1.68**	NFKB1 translation produces a DNA-binding subunit of the NF-kB complex (p105). The NF-kB pathway is an effector involved in BCR-mediated apoptosis in B-cells[189,190].
		PIK3CD	**1.62**	PIK3CD encodes the δ isoform of p110 PI3K. CLL cells signal through p110δ-AKT pathway upon BCR activation or IL-4/CD40L stimulation to promote survival[213,214].
		PTPN6	**1.51**	PTPN6 is also known as SHP-1, a phosphatase important to BCR pathway negative regulation[37]. In the absence of SHP-1 phosphatase activity, SYK was hyper-phosphorylated and hyperactive; therefore, SHP-1 is a negative regulator of SYK and therefore, BCR activation[193]. SHP-1 has also been shown to de-phosphorylate LCK[194].

Supplementary Table 2: Genes within the JAK-STAT pathway with reduced expression in IBR10[2] cells relative to BJABs.

Pathway	Overall Significance	Targets	Fold change
JAK/STAT pathway	**4.69**	TIMP1	**12**
		IRS1	**4.14**
		IL1RN	**2.33**
		JAK2	**2.29**
		FOXO1	**2.22**
		TEC	**2.11**
		ROCK2	**1.93**
		FOS	**1.9**
		PRKAA2	**1.9**
		PDE3B	**1.86**
		PRKAA1	**1.79**
		NFKB1	**1.68**
		RPS6KA1	**1.64**
		NOS3	**1.6**
		FLNA	**1.52**
		PTPN6	**1.51**

Abbreviations: PI3K (Phosphatidylinositol-3-kinase), AKT (Protein kinase B), ERK (extracellular signal-regulated kinase), BTK (Bruton's tyrosine kinase), CD40 (cluster of differentiation 40), IL-4 (interleukin-4), SYK (spleen tyrosine kinase), SHP-1 (src homology region 2 domain-containing phosphatase-1), IRS1 (insulin receptor substrate-1), bcl-1 (b-cell lymphoma 2), bcl-XL (b-cell lymphoma-extra large), serine/threonine-protein kinase-1), Mcl-1 (induced myeloid leukemia cell differentiation protein), MAPK (mitogen-activated protein kinase), JAK (Janus kinase), TNF (tumour necrosis factor), BAFF (B-cell activating factor) APRIL (a proliferation-inducing ligand),

Supplementary Table 3: Genes within the AXL pathway with reduced expression in IBR10^2 cells relative to BJABs.

Pathway	Overall Significance	Targets	Fold change
AXL pathway	**3.39**	TIMP1	**12**
		SNAI2	**4.26**
		TNF	**3.65**
		ANXA2	**3.07**
		CDKN1A	**2.79**
		PRKACA	**2.5**
		LTB	**2.44**
		SMO	**2.42**
		PPARG	**2.29**
		FOXO1	**2.22**
		ADGRE1	**1.78**
		GLI1	**1.66**
		ADAM11	**1.56**
		VIM	**1.52**
		CD274	**1.51**

Supplementary Table 4: Genes within the autophagy pathway with reduced expression in IBR10[2] cells relative to BJABs.

Pathway	Overall Significance	Targets	Fold change
Autophagy	**2.74**	PRKAA2	**1.9**
		PRKAA1	**1.79**
		ATK101	**1.63**
		PIK3C3	**1.57**
		ATG16L1	**1.55**
		UVRAG	**1.5**

Supplementary Table 5: Genes within the TWEAK (TNF-related weak inducer of apoptosis) pathway with reduced expression in IBR10^2 cells relative to BJABs.

Pathway	Overall Significance	Targets	Fold change
TWEAK signalling pathway	**2.57**	CCL5	**5.27**
		TRAF1	**3.91**
		TNF	**3.65**
		NFKB2	**2.87**
		RELB	**2.15**
		NFKB1	**1.68**
		CASP7	**1.57**

Supplementary Table 6: Genes within the MAPK pathway with reduced expression in IBR10[2] cells relative to BJABs.

Pathway	Overall Significance	Targets	Fold change
MAPK pathway	**2.36**	TNF	**3.65**
		DUSP6	**3.53**
		NFKB2	**2.87**
		MAP3K8	**2.54**
		PRKACA	**2.5**
		DUSP2	**2.33**
		RELB	**2.15**
		DUSP10	**2.02**
		FGF16	**1.97**
		HSPB1	**1.91**
		FOS	**1.9**
		NRKA1	**1.87**
		PTPN7	**1.81**
		DUSP16 (2)	**1.75**
		NFKB1	**1.68**
		NTRK2	**1.66**
		SRF	**1.65**
		JUND	**1.62**
		CACNG7	**1.61**
		PPM1B	**1.56**
		DUSP16	**1.56**
		FLNA	**1.52**

Supplementary Table 7: Transcriptome Analysis Console (TAC)-generated significant (>1.301) pathways upregulated in IBR10[2] cells relative to BJABs, with additional pathways provided.

Pathway number	Pathways	Overall Significance	Number of genes upregulated
1	Glycosaminoglycan metabolism	4.35	1
2	O-linked glycosylation	3.83	2
3	Felbamate metabolism	3.09	2
4	Deubiquitination	3.04	2
5	Splicing factor NOVA-regulated synaptic proteins	2.93	6
6	Cell cycle checkpoints	2.9	1
7	miR-targeted genes in lymphocytes	2.76	4
8	PKC-γcalcium signalling pathway in ataxia	2.49	4
9	Cell surface interactions at the vascular wall	2.41	1
10	Signalling by ROBO receptors	2.24	1
11	Class A/1 (Rhodopsin-like receptors)	2.06	5
12	TCF-dependent signalling in response to WNT	1.84	2
13	miR-targeted genes in epithelium	1.82	3
14	Olfactory bulb development and olfactory learning	1.73	3
15	Aflatoxin B1 metabolism	1.69	2
16	C-type lectin receptors (CLRs)	1.63	1
17	Complement cascade	1.63	1
18	Interleukin-1 family signalling	1.63	1
19	IL-18 signallling pathway	1.56	2
20	Acrylamide biotransformation and exposure biomarkers	1.54	1
21	Metabolism of dichloroethylene by CYP450	1.54	1
22	Colchicine metabolism pathway	1.54	1
23	Olfactory receptor activity	1.54	4
24	Nucleotide-binding oligomerization domain (NOD) pathway	1.54	4
25	Integrin cell surface interactions	1.48	1
26	miR-targeted genes in muscle cells	1.43	5
27	Mitotic G2-G2/M phases	1.43	2
28	Airway smooth muscle cell contraction	1.42	2

29	Intraflagellar transport proteins binding to dynein	1.39	3
30	Interferon gamma signalling	1.33	1
31	Cannabinoid receptor signalling	1.31	3
32	Signal transduction through IL1R	1.17	3
33	PTEN regulation	1.17	1
34	Integrin-mediated cell adhesion	1.16	6

Supplementary Table 8: Genes from all pathways identified in *supplementary table 7* above sorted according to fold change (BJAB – IBR10[2]).

Targets	Fold change	Pathway number
SEMA3A	-3.00	14
MAP2K6	-2.38	18, 32, 34
PTAFR	-2.28	11, 30
GNAQ	-2.25	8, 28
CEP250	-2.24	27
ITGA6	-2.11	34
DYNC2H1	-1.96	29
IKBKG	-1.91	24
GRIA2	-1.87	8, 26
OPRL1	-1.85	11
CARD8	-1.82	24
PRKACB	-1.80	31
MECOM	-1.79	33
ATP2B2	-1.77	8
ITGB7	-1.75	34
NPSR1	-1.74	11
CARD9	-1.74	16, 24
OR10P1	-1.73	23
AKR7A2	-1.71	15
IFT27	-1.71	29
MAP2K5	-1.71	34
LUM	-1.67	25
ZNF385A 2	-1.65	6
OR2A4	-1.65	23
USP34	-1.64	4, 12
GRIN1	-1.63	5, 14
NCDN	-1.63	5
TAB1	-1.62	32
ZNF385A 1	-1.60	6
TSPAN7	-1.60	9
CASP9	-1.60	24
CYP3A4	-1.59	3, 15, 22, 31
PLCB2	-1.59	8
NCF2	-1.59	19
POMGNT2	-1.58	2
CYP2E1	-1.58	3, 20, 21
CNR2	-1.58	31

C3AR1	-1.57	11, 17
FOXM1	-1.57	27
CHST4	-1.55	2
CSN3	-1.55	5
DAB1	-1.54	5
CAPG	-1.54	7, 13, 26
FFAR2	-1.54	11
MET	-1.54	7, 13, 26
CEMIP	-1.53	1
BPGM	-1.53	19
OR9G1	-1.53	23
OR51L1	-1.53	23
IFNB1	-1.53	32
NEO1	-1.52	5
MAPK7	-1.52	7, 26, 34
ITGAM	-1.52	34
STXBP2	-1.51	5
PGM1	-1.51	7, 13, 26
SLIT2	-1.51	10, 14
KAT5	-1.51	12
USP13	-1.50	4
MYLK	-1.50	28
IFT122	-1.50	29

Supplementary Table 9: An outline of the top 100 genes upregulated in IBR10^2 cells relative to BJABs, sorted based on fold change (BJAB – IBR10^2).

Gene	Fold change
FYB	-6.75
TNNI1	-6.36
HBD	-4.75
FOXI1	-3.96
HPGDS	-3.64
JAKMIP2	-3.51
MCTP1	-3.27
CKMT1A	-3.24
HEPACAM2	-3.13
SEMA3A	-3.00
HIST1H1B	-2.76
CHRNA6	-2.75
CLVS1	-2.74
LOC728485; CTD-2162K1	-2.67
TNFSF8	-2.59
FAM46C	-2.55
IGSF11	-2.50
MYBPH	-2.45
TBC1D9	-2.45
SERPINA9	-2.44
NRSN2	-2.41
MGLL	-2.41
GAREM1	-2.41
CNGA4	-2.39
MAP2K6	-2.38
BTBD8	-2.38
SLA	-2.36
HYPK	-2.35
FRRS1	-2.33
CCDC110	-2.32
MME	-2.32
ADGRG5	-2.31
MC4R	-2.31
KLF7	-2.31
TAT	-2.30
C10orf71	-2.30
PTAFR	-2.28
HEMGN	-2.28
BAZ2B	-2.27
CKMT1B; CKMT1A	-2.27
GNAQ	-2.25
ZMIZ1	-2.24
CEP250	-2.24
C10orf128	-2.23
TOMM40L; MIR5187	-2.23
TCP11L2	-2.18
P2RY8	-2.15
P2RY8	-2.15
PDE4B	-2.14
PRDM8	-2.14

Gene	Fold change
SLC1A1	-2.14
ASIC1	-2.13
PDZRN3	-2.13
ACTL9	-2.12
GPR135	-2.12
SLC2A5	-2.12
ITGA6	-2.11
TLCD2	-2.11
CLMN	-2.10
DYRK1B	-2.09
RAB41	-2.07
SDPR	-2.07
FAM167A	-2.06
CDC42SE2	-2.05
FAM205A	-2.05
TUBGCP3	-2.04
NBEA	-2.04
PSRC1	-2.02
NREP	-2.02
B3GNT5	-2.01
ARHGEF33	-2.01
EPB41L4A	-2.00
HIST1H4C	-2.00
TUBA3E	-1.99
ZNF862	-1.98
ADAM28	-1.98
TLE3	-1.97
SLCO1A2	-1.97
DYNC2H1	-1.96
SLCO5A1	-1.96
NIPSNAP3A; NIPSNAP3E	-1.95
LZTS1	-1.95
MPP2	-1.95
SIGLECL1	-1.94
PPP1R3A	-1.93
TCEB3B	-1.91
DEPTOR	-1.91
IKBKG	-1.91
RASL10B	-1.91
PPP1R1C	-1.90
LGR4	-1.90
MAPRE3	-1.90
dorsnarby; IGF2BP2	-1.90
CHN2	-1.90
WDR17	-1.90
SHPK; TRPV1	-1.89
FZD1	-1.88
ABHD3	-1.88
TMEM45B	-1.88
TNFSF10	-1.87